AN EXPERIMENTAL INVESTIGATION INTO THE EFFECTS OF HIGH THERMAL MASS ON BUILDING PERFORMANCE

A Thesis Submitted to
the Graduate School of Engineering and Sciences of
İzmir Institute of Technology
in Partial Fulfilment of the Requirements for the Degree of

MASTER OF SCIENCE

in Energy Engineering

by
Özgür KARATAŞ

August 2019
İZMİR

We approve the thesis of **Özgür KARATAŞ**

Examining Committee Members:

Prof. Dr. Tahsin BAŞARAN
Department of Architecture, İzmir Institute of Technology

Prof. Dr. Gülden GÖKÇEN AKKURT
Department of Energy Systems Engineering, İzmir Institute of Technology

Assoc. Prof. Dr. Alparslan TURGUT
Department of Mechanical Engineering, Dokuz Eylül University

20 August 2019

Prof. Dr. Tahsin BAŞARAN
Supervisor, Department of Architecture,
İzmir Institute of Technology

Assoc. Prof. Dr. M. Akif EZAN
Co-Supervisor, Department of Mechanical
Engineering, Dokuz Eylül University

Prof. Dr. Gülden GÖKÇEN AKKURT
Head of the Department of Energy Systems
Engineering

Prof. Dr. Aysun SOFUOĞLU
Dean of the Graduate School of
Engineering and Sciences

ACKNOWLEDGMENTS

It is my pleasure to acknowledge the roles of several individuals who were instrumental for the completion of my master's research.

First of all, I would like to express my deepest gratitude to my advisor, Prof. Tahsin Başaran, for his guidance, support, patience and encouragement during my thesis.

I would like to thank Nicolas Guillo and Helene Guillo for allowing me to use their home for the experiments, therefore making the experimental part of the thesis possible. During my various field visits, I always appreciated their hospitality.

I would like to thank to Bill Wilson and Yvonne Goldsmith

I would like to express my appreciation to Ozan Vardal, Yusuf Can Uz, Hasan Hüseyin Niğdeli and Sinan Yüksel for their friendship, support and contributions to my thesis.

I would like to thank to Serkan Emin for sharing his exceptional knowledge of numerical analysis.

I would like to thank to Geothermal Energy Research and Application Center for measuring the properties of the main material of the studied dwelling.

I would like to thank my partner Anina Kathrin Stauffacher for her encouragement to write my thesis.

Lastly, I offer sincere thanks to my family for their love, continuous counsel and unlimited patience throughout my education.

ABSTRACT

AN EXPERIMENTAL INVESTIGATION INTO THE EFFECTS OF HIGH TERMAL MASS ON BUILDING PERFORMANCE

The focus on energy efficiency in buildings has contributed to the increased interest in vernacular architecture using locally available materials. Monotype architecture has spread across Anatolia during last century despite builders having centuries of knowledge of vernacular dwelling. Climatic conditions are specific to geographical locations, therefore the architectural solutions respecting climatic conditions are also specific. Local construction materials are in harmony with the surroundings because they have previously been part of the current environment. The main aim of this thesis is to investigate and simulate the effects of high thermal mass on the thermal environment of cave dwellings. The case study was undertaken in a cave dwelling carved out of a fairy chimney in Ürgüp, Cappadocia. Data loggers were placed in the dwelling to observe the annual temperature and relative humidity fluctuations. Measurements showed that the interior temperature fluctuated around 18°C in January and 20°C in July, and the relative humidity fluctuated around 70% in January and 65% in July. These measurements showed that the interior conditions were thermally comfortable as a result of the high thermal mass of the cave dwelling. DesignBuilder software was used to simulate the thermal behaviour of the cave dwelling. The thermal conductivity, specific heat and density of the main material, volcanic tuff rock, were measured and defined in DesignBuilder. After defining all the inputs and boundary conditions, the numerical results obtained from the DesignBuilder provided thermal outputs which agreed with the experimental results.

ÖZET

YÜKSEK ISIL KÜTLENİN BİNA BAŞARIMI ÜZERİNE ETKİLERİNİN DENEYSEL İNCELENMESİ

Binalarda enerjinin etkin ve verimli kullanımının ön plana çıkması; geçmişten gelen sürdürülebilir yerel mimari birikimine ve yerel maleme kullanımına olan ilginin artmasına yol açmıştır. Anadoluda birçok yerel mimari örnekleri olmasına karşın son yüzyılda tek tip mimari yayılmıştır. İklim koşulları lokasyona özgüdür, iklim koşullarına karşı mimari çözümler de spesifiktir. Yerel malzemeler çevre ile uyumludur çünkü daha önce mevcut çevrenin bir parçası olmuştur. Bu tezin asıl amacı yüksek ısıl kütlenin konut ısıl ortamına olan etkilerini araştırmak ve simüle etmektir. Bu çalışma, Kapadokya Ürgüp'te peribacasından oyulmuş bir mağarada yapılmıştır. Veri kaydedicileri, yıl boyunca sıcaklık ve bağıl nem dalgalanmalarını gözlemlemek için konut içine yerleştirilir. Ölçümler Ocak ayı boyunca, iç sıcaklığın 18°C civarında dalgalandığı ve bağıl nemin %70 civarında değiştiğini göstermektedir. Temmuz ayında ise iç sıcaklık 20°C civarında ve bağıl nem %65 civarında dalgalanmaktadır. Bu sonuçlar, konutun yüksek ısıl kütlesi nedeniyle iç koşulların ısıl olarak konforlu olduğunu göstermektedir. DesignBuilder yazılımı mağara evini simüle etmek için kullanılmıştır. Konutun malzeme özellikleri ve sınır koşulları tanımlanmıştır. Ana malzeme olan volkanik tüf kayasının ısı iletkenliği, özgül ısısı ve yoğunluğu ölçülüp, DesignBuilder için tanımlanmıştır. Malzeme özellikleri ve sınır koşullarını tanımladıktan sonra, DesignBuilder'dan elde edilen sayısal sonuçlar, deneysel sonuçlar ile uyumlu çıkmıştır.

TABLE OF CONTENTS

LIST OF FIGURES

Figure **Page**

Figure **Page**

Figure **Page**

Figure **Page**

Figure **Page**

LIST OF TABLES

LIST OF ABBREVATIONS

EU	European Union
UN	United Nation
USA	United States of America
ACH	Air Change per Hour
MBE	Mean Bias Error
CV (RMSE)	Coefficient of Variation of Root Mean Square
CLO	Clothing
PAHS	Passive Annual Heat Storage
SBCI	Sustainable Buildings Climate Initiative

LIST OF NOMENCLATURE

Ω	Specific Humidity
Φ	Relative Humidity
c	Specific Heat Capacity
k	Thermal Conductivity
H	Heat Transfer Coefficient
A	Area
L	Thickness
T	Temperature [°C, K]
RH	Relative Humidity
Q	Amount of Net Heat Transfer
m	Mass
d	Density
V	Volume

CHAPTER 1

INTRODUCTION

During the last several decades, the world population and world economy has been growing, causing an increased demand on natural resources, both non-renewable and renewable. The built environment accounts for a large part of energy use (estimated to be about 40% of global energy use), energy-related greenhouse gas emissions (estimated to be approximately 30%), waste generation and use of natural resources. As a result, the building and construction sector is one of the most important areas of intervention and provides opportunities to limit environmental impact as well as contribute to the achievement of sustainable development goals [1]. In 2006, a partnership between the United Nations (UN) and the building sector called Sustainable Buildings and Climate Initiative (SBCI) was started to promote and support sustainable building practices on a global scale with a focus on energy efficiency and greenhouse gases emission reduction [2].

The focus on energy efficiency is contributing to an increased interest in vernacular architecture using locally available materials, which can minimize indirect resource and energy consumption through reduced transport. Cave dwellings using the existing geological environment are of specific interest when studying energy efficiency. They have previously been shown to moderate indoor air temperature through insulating and mass effect properties, providing protection from hot weather and/or increasingly hot climate [3]. In 1983, Hait [4] described the concept of Passive Annual Heat Storage (PAHS), saying “heat can be collected, stored and retrieved over the entire year, without using the energy robbing mechanical equipment”. Various earthen materials such as rocks and soils, contribute differently to energy efficiency due to their different thermal mass. Underground buildings have been shown to have great potential for sustainable development by increasing the natural plantation and minimizing the building energy consumption [5].

Observing modern-day architecture in Turkey, most buildings are similar and monotype. One reason for this monotype architecture is the widespread use of modern construction techniques and technologic materials. The materials used in construction

are all the same and do not necessarily reflect the local context, such as Eastern Anatolia or Western Anatolia, or use locally available materials. As a result, construction often does not satisfy the thermal comfort in those dwellings or are not energy efficient.

There are many examples of vernacular dwellings across Anatolia: Harran Houses in Şanlıurfa, Cave Dwellings in Cappadocia, Diyarbakır Houses in Diyarbakır, and Greek Houses in the Western Aegean region. These dwellings reflect the architecture construction techniques and building materials specific to the local region.

The aim of this study is to examine the specific case of a cave dwelling carved into a fairy chimney in Cappadocia, south of Ürgüp, to better understand its energy efficiency due to the high thermal mass of the volcanic rocks. The thermal behaviour of the cave dwelling is examined by comparing indoor and outdoor temperature and humidity measurements, and determining rock properties.

This study is described in five chapters;

In Chapter 2, the definition of fundamentals and literature survey are reviewed in terms of vernacular architecture, thermal efficiency of dwellings and 3D simulations of buildings.

In Chapter 3, the cave dwelling in Ürgüp is described with respect to its surroundings and thermophysical properties.

Chapter 4 covers the experimental set up and the methodology. The meteorology data of Ürgüp and the thermal properties of the tuff rock are analysed.

In Chapter 5 the boundary conditions are defined and the results of the 3D simulation of the cave dwelling modelled using Design Builder interface with Energy Plus are outlined.

In Chapter 6 the one year temperature and humidity measurements are evaluated in terms of thermal comfort. The effect of the high thermal mass is investigated. The output of the time dependent 3D simulation of the cave dwelling is compared with the actual measurements.

In the light of these findings, the results of the study are evaluated and some recommendations are given for future studies in the conclusion.

CHAPTER 2

DEFINITION OF TERMS AND LITERATURE REVIEW

2.1. Vernacular Architecture

Vernacular dwelling designs have developed over time. The designs vary based on climatic conditions, available materials, needs of society, and the economy[1]. Different societies have designed their own vernacular dwellings depending on their surroundings and available resources, continuously learning from past experiences. Since climatic conditions are specific to each location, so too are the architectural solutions. Local materials are in harmony with the surroundings because they are part of the immediate environment[6]. Therefore, transportation costs are very low, and building with local materials is sustainable [7].

2.2. Sustainability in Architecture

The concept of sustainability in architecture is based on a conscious approach to the natural environment, taking into consideration the efficiency and moderation in the use of design materials available. Sustainability's major criteria is to meet the needs of the current generation without compromising the future generations to meet their needs. The traditional architecture in Anatolia is based on a complex process where building masters match local environmental characteristics, such as materials, with the needs, expectations and values of the local people.

In the production process of traditional buildings in Cappadocia, building masters try to integrate the buildings into nature by using local materials. As a result, they have developed an ecological building tradition over the centuries. The indoor thermal comfort for occupants is primarily maintained by the thermal qualities of tuff stone; these properties are also useful for long term food storage [8].Underground buildings in general show great potentiality for sustainable development by increasing the natural plantation and minimizing the building energy consumption [5]. Sustainability concept meets the current generations need while not compromising from the needs of the future generations.

2.3. Thermal Mass

Thermal mass is the ability of materials to absorb, store and release energy. The thermal mass concept is very similar to a battery. During winter, the walls and roof of the dwellings (referring to the thermal mass of the building) absorb sunlight and store the heat during the day. During the night, the stored heat is released and causes the dwelling to stay warm. Thermal mass is stated as a passive thermal conditioning system causing an e.g. indoor temporal lag of outdoor temperature variations. Effectively designed use of thermal mass in buildings can make a difference in comfort and cooling/heating costs. Building material has an important role delaying heat transfer from the exterior to the interior. It slows down the heat transfer during the day and releases the heat, gained during the day, at night [9]. Compared to low thermal mass materials, high thermal mass materials allow time lag and reduce the effects of outdoor temperature swings [10]. High thermal mass materials require a lot of heat energy to change their temperature. Common examples of high density materials are ceramics, brick, rock and concrete. As seen in the formula below, c is a material-specific heat property - quantifying the amount of heat required to change the temperature of a mass unit of a substance by one degree - which explains the principle of material-dependency outlined in this paragraph. The basic formula describing the thermal mass concept is;

$$Q = m.c.\Delta T \tag{2.1}$$

2.4. Solar Passive Heating

Solar passive heating is basically the solar heat gain from the surroundings facing the equator (south facing in the northern hemisphere, north facing in the southern hemisphere). The simplest form of solar passive heating is obtaining sunlight through glass windows. Massive walls or floor is needed to absorb the solar heat gain to store during the day [11].

Dwellings with solar passive heating require appropriate shading for filtering or blocking sunlight during summer but allowing sunlight to enter during the winter.

Solar passive heating must be designed wisely because inappropriate applications may lead to thermal discomfort. The energy gained with solar passive

heating must be stored with massive walls or floor. If the dwelling has inadequate mass storage, it can be over heated. The mass need of the dwelling must be calculated based on a 24-hour cycle [11].

2.5. Natural Ventilation

Ventilation, using thermal buoyancy and wind, is one effective passive heat control system. Ventilation allows;

- Supplying fresh air, exhausting CO_2 and bad smells.
- Cooling down the interior temperature when the $T_o<T_i$.
- Cooling down the human body with heat dissipation from the skin [11].

Passive ventilation requires an inlet and outlet temperature difference and/or wind effect and the direction. The temperature difference between inlet and outlet enables airflow from inlet to outlet with stack-effect. This case only occurs when $T_o<T_i$. Passive ventilation regulates the interior temperature, supplies fresh air and exhausts stale air.

2.5.1.Stack-Effect Ventilation

Buoyancy difference is the key factor of stack effect. The temperature difference between indoor and outdoor enables the air movement. In cold climates, the higher temperature indoor air rises in the dwelling with buoyancy forces and creates pressure difference which allows to suck cold air through the lower openings [12]. In warm climates, in contrast to cold climates, the cold air creates positive pressure at the bottom and flings the cold air from the lower openings.

2.5.2.Wind Driven Ventilation

The wind pressure also has an additive effect on ventilation. Wind driven pressure is effected by the magnitude of the wind, the direction of the wind, the geometry of openings of the dwelling, the surrounding of the dwelling and the vegetation. Since the direction and the magnitude of the wind is not stable throughout the day and seasons, the distribution of the openings is important [13]. Having openings on different facades and different levels accordingly providing different pressures on openings with different wind patterns.

2.6. Quality of Indoor Space and Thermal Comfort Conditions

Quality of indoor space is affected by many parameters, the most important parameters are temperature, relative humidity and air flow.

Nicol et al. [14] explained in their book "Adaptive Thermal Comfort: Principles and Practice" that human's 'core temperature' must be stable at all times like all other mammals. Constant body temperature is maintained through blood circulation. Blood is pumped towards the skin to shed heat or away from skin to retain warmth, resulting in shivering, sweating, or goose bumps. The human body takes action when it is too cold or too hot to maintain stable 'core temperature'. These actions are all taken as a result of thermal discomfort.

ANSI/ASHRAE Standard 55-2010 [15] describes the thermal comfort as the satisfaction of mind with the thermal environment. The satisfaction varies from person to person and even for the same persons in different situations. That means there is no specific conditions for thermal comfort. Factors affecting thermal comfort include metabolic rate, clothing insulation, air temperature, radiant temperature, air speed and humidity.

Humans can sense changes in temperature relatively but not changes in relative humidity. However, relative humidity has effects on mucous membrane irritation of eyes and upper airways. Human bodies react to changes of relative humidity. A relative humidity range of 40-50% stabilizes the precorneal tear film and precludes irritations of the eyes. Similarly, nasal activities settle at this relative humidity range [16]. Indoor environment quality is highly dependent on thermal comfort.

2.7. Literature Review

Vernacular dwellings are disappearing and their associated construction techniques are being forgotten day by day. For centuries, different architectural styles were used by different communities. The exiguity of energy sources made researchers study ancient construction techniques and ancient buildings. In the literature, some studies investigated vernacular dwellings experimentally and as well as with the aid of computer software.

Ogoli [10] investigated the effects of thermal mass in Nairobi, Kenya, comparing timber walled test chambers and natural stoned test chambers under different ceiling

and roofing types. The experiment took place between January and March 1997, during the warm period. Measurements were taken in 10 minutes intervals in each of the test chambers. Dry-bulb temperature, wet-bulb temperature, mean-radiant temperature and humidity were measured for the comparison. Through these experiments, it was observed that thermal mass had an effect on interior temperatures. The temperatures in the high thermal mass stone buildings was shown to vary less because the thermal mass delayed transmission of heat to the interior.

Singh et al. [7] studied vernacular architecture examples in North-East India and investigated the relationships between bioclimatism, socio-economic status, cultural setup and sustainability. Singh et al. studied 14 vernacular dwellings, all more than 70 years old, located in three different North-East Indian climatic zones. It was observed that the common constraints during construction were bioclimatic conditions and locally available materials.

Tassiopoulou et al. [17] studied two different forms of traditional dwellings on mainland Greece and low-rainfall islands, representing five different climatic zones. The study used TAS° thermal analysis software with climatic data from 1977 to 1989 recorded in Athens. The authors modelled the traditional vernacular dwelling with traditional use, a traditional vernacular dwelling with modern use, and an insulated vernacular dwelling with modern use. Between the investigated model and the uses, the traditional use of the vernacular dwelling was the most energy efficient during winter time. This study showed that the traditional vernacular dwelling provides thermal comfort for both summer and winter, and the dwellings are well designed with respect to Greek climate.

Sözen and Gedik [18] studied traditional architecture in Diyarbakır Houses and indicated that Traditional Diyarbakır House's thick basalt walls ranging from 50cm to 80cm provided thermal comfort with low coefficient of heat transmission, about 0.5 W/mK. These walls decelerated the heat transfer during the day and night, thus the indoor temperatures remained stable.

Başaran [19] analysed the thermal performance of a typical Harran House and also evaluated the effect of thermal mass of the house and the solar chimney effect. It was shown that the Harran Houses are not only climate friendly designs but also environmentally friendly designs. The thick-walled structure of Harran Houses, varying from 50cm to 60cm, provided good insulation and the dome's chimney, which varied

from 20cm to 30cm, provided natural ventilation. Başaran recorded the temperature and relative humidity from several indoor and outdoor points between 15th of July at 20:46 and 19th of July at 05:08, possibly the hottest times of the year. The experiment showed that the indoor wall's surface temperature changed by only 2˚C while the outdoor temperature changed by 20˚C. The indoor relative humidity changed by only 10% while the outdoor relative humidity changed by 50%. The indoor temperature and humidity fluctuations versus time can be seen in Figure 2.1.

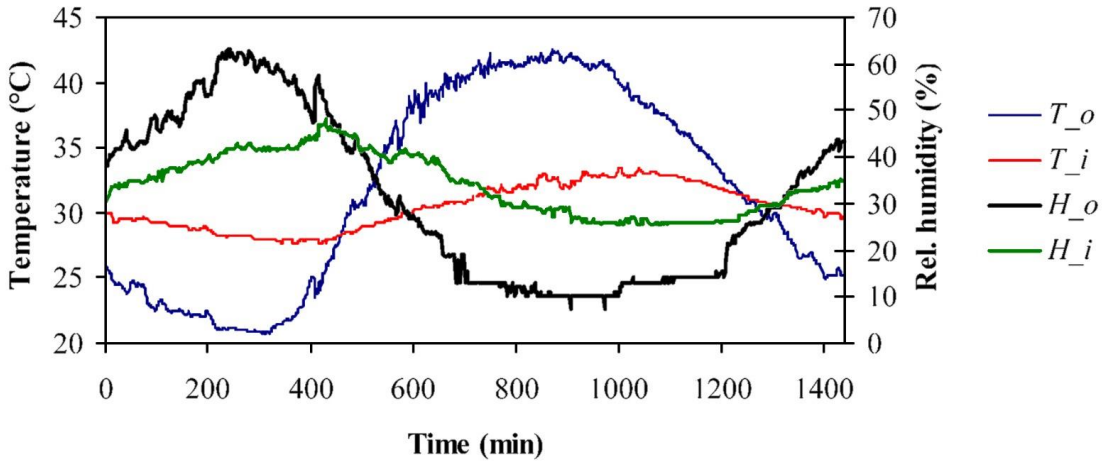

Figure 2.1. Temperature (indicated T) and relative humidity (indicated H) variations at the inside (indicated i) and outside (indicated o) of the domed houses, (Source: [20])

The experimental results showed that thermal comfort in the building was good even while the outdoor environment underwent extreme conditions. Başaran solved a 1D time dependent heat conduction equation by using the finite difference numerical model for finding temperature distribution through the wall. The results of 1D heat conduction solution showed the effect of both the thickness and the thermophysical properties of the walls. The thick walls and the building material were shown to clearly contribute positively to the indoor thermal comfort in the studied dwellings, especially during the hot summer. The Harran House was also modelled in a commercial software for the winter state as seen in Figure 2.2 [20]. The entrance of the dwelling was the inlet of the cold air and the chimneys of the dwelling was the outlet. An open pit fire was located at the entrance in order to increase the inlet air temperature. The inlet velocity and temperature of the cold air was assumed to be 0.25m/s and 5.8°C respectively, and

the open pit fire heat transfer rate was assumed to be 9kW. Convection heat transfer coefficient for the exterior surfaces was assumed at 20W/m^{2}K and the thermal conductivity of the building was assumed to be 0.975W/mK. With all these variables, the temperature and velocity distributions were produced by the software as seen in Figure 2.2.

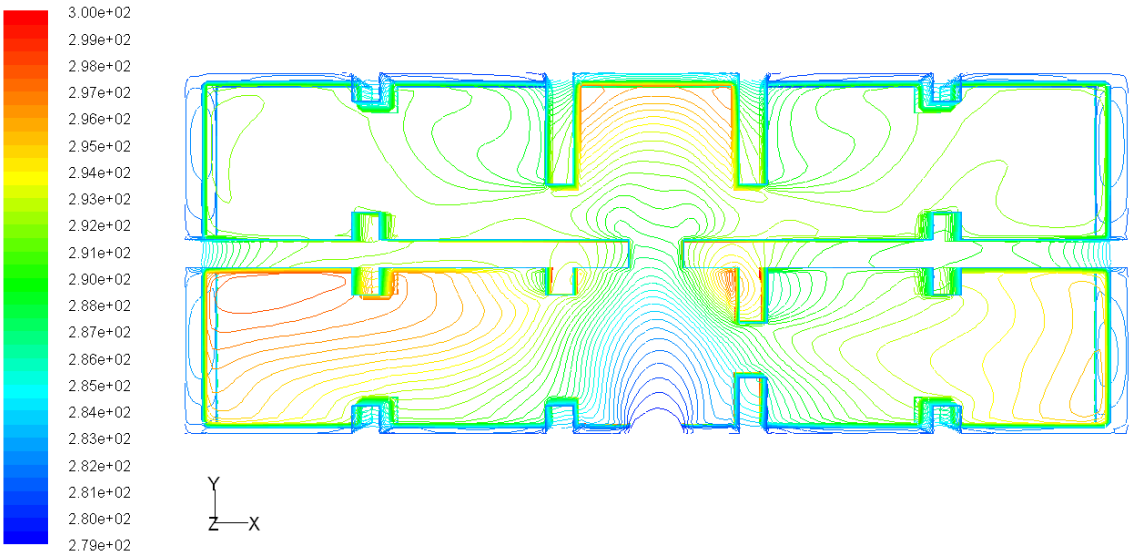

Figure 2.2. Temperature (K) distribution of the inside of the house at 1m high level, (Source: [20])

Aydan and Ulusay [21] studied mechanical characteristics of underground structures in Cappadocia. These included detailed investigations of Derinkuyu, Kaymaklı, and Özkonak underground cities. In this study, the temperature and humidity variations during a full day in March in Ürgüp and Ortahisar were monitored. Findings showed very little temperature and humidity fluctuations indoors while the outdoor temperatures changed dramatically. Findings also showed that the amplitude of humidity and temperature variations became smaller as the depth of the underground cities increased as seen in Figure 2.3.

Basaran and Kaya [22] studied an Ephesus House which was excavated by Hilke Thür. The house and surroundings were modelled using Gambit Software and Fluent code to analyse thermophysical properties based on measurements of the construction materials. The outside temperature and solar radiation data were obtained from Turkish Meteorology (DMI). The Ephesus houses were heated by open coal burners. In the model, the coal burners were also included as heat generators. With these parameters,

the temperature distribution of the dwelling was obtained in January and June (without burners). It was shown that during hottest summer and coldest winter times the dwelling had relatively high thermal comfort in the light of the numerical models.

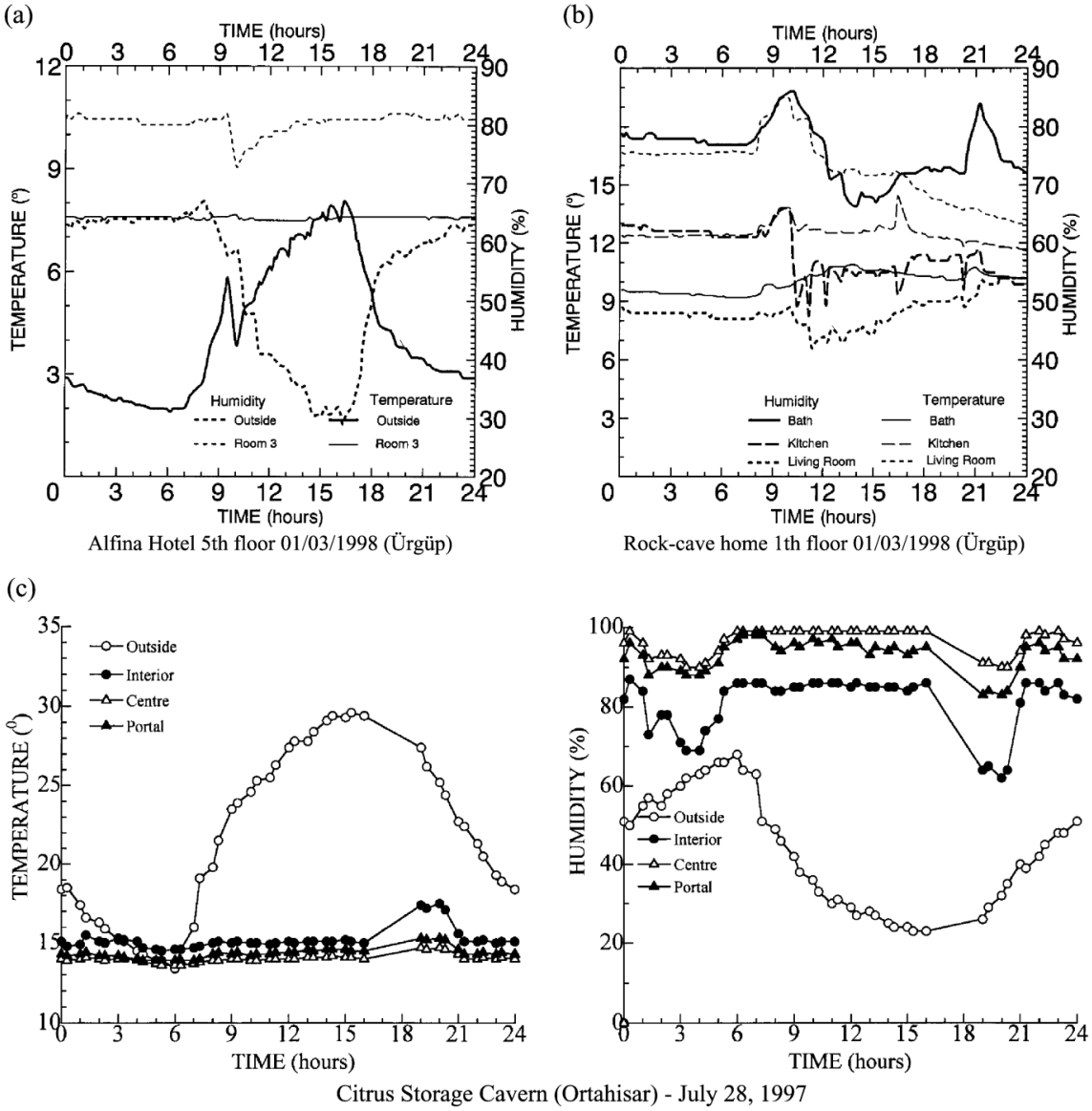

Figure 2.3. Variation of temperature and humidity in different modern rock settlements (a and b) and in a storage cavern (c) at the Cappadocia Region as documented by Aydan and Ulusay, (Source: [21])

Deng et al. [23] studied thermal mass effectiveness of external walls on the heating and cooling loads on a standard residence. The residence was modelled with EnergyPlus software. The model showed that there was no significant difference between high thermal mass and low thermal mass buildings from heating and cooling loads of buildings in HSCW (Hot Summer and Cold Winter) as seen on Figure 2.4.

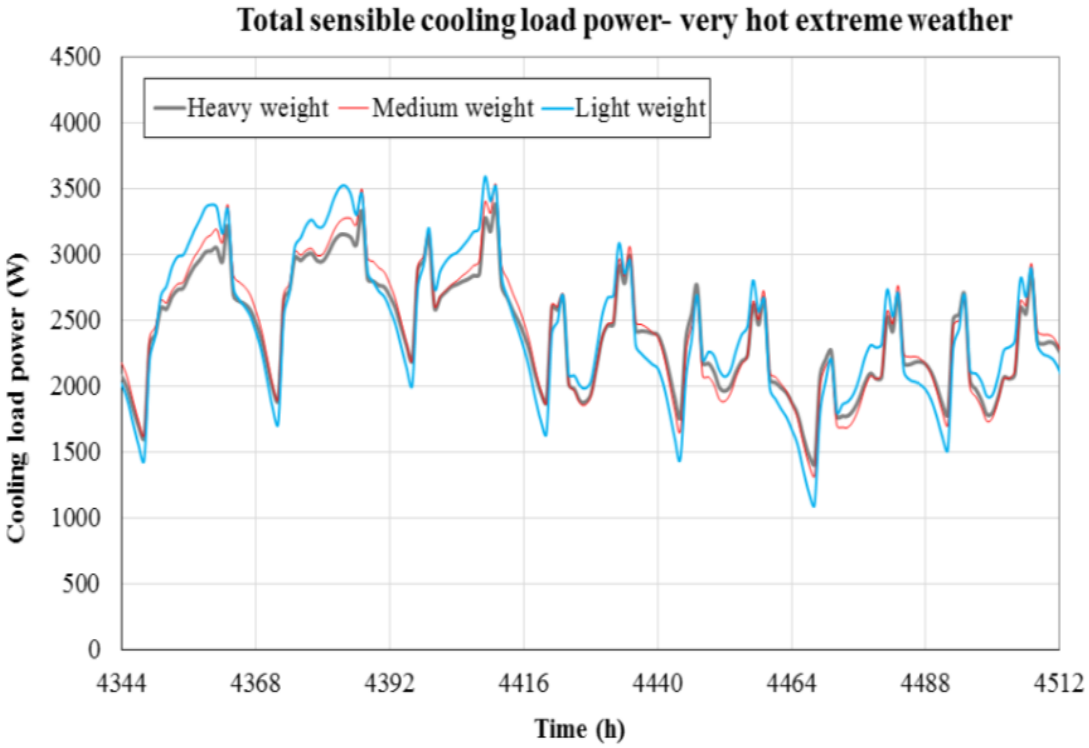

Figure 2.4. Total Sensible cooling load power in full time cooling pattern in Changsha Climate in a week of extreme hot weather (1st-7th July), (Source: [23])

On the other hand, under the same conditions it was shown that the high thermal mass building's thermal comfort was better. This is because the low and medium thermal mass buildings were over heated under summer conditions while the high thermal mass buildings regulated the indoor temperature better and reduced the complexity of thermal comfort as seen on Figure 2.5.

Turgay Coşkun investigated how to improve indoor climate of historic libraries and made experiments for the study in Necip Pasa Library in İzmir, Turkey. For the evaluations data loggers are placed for a whole year. DesignBuilder simulation program is used to simulate the library indoor conditions. The model is calibrated accordingly the ASHRAE Guideline 14. The manuscript zone temperature comparison of the measurements and the simulations is seen in Figure 2.6 [24]. The relative humidity comparison of the measurements and the simulations is seen in Figure 2.7.

The manuscript temperature and relative humidity MBE and CVRMSE values are within the accepted interval as seen in Table 2.1. However, the entrance zone relative humidity MBE is not in the accepted interval, which is not a critical zone in the library [24].

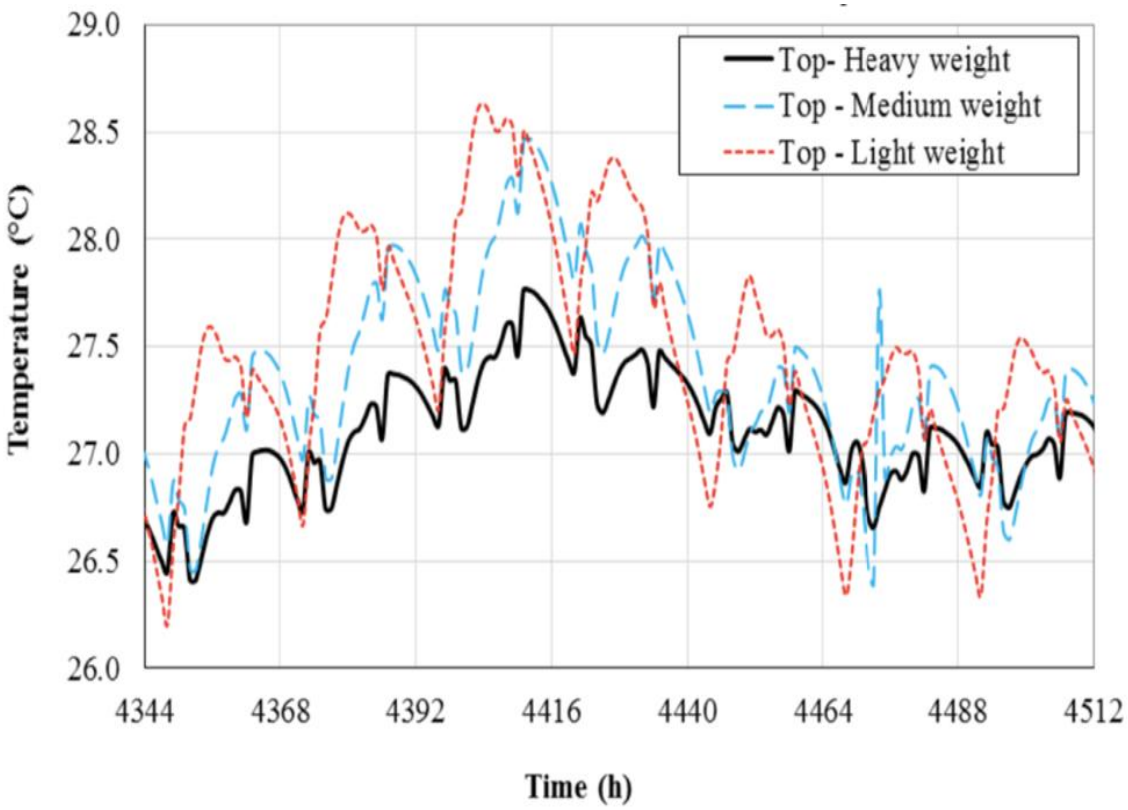

Figure 2.5. Operative temperature of room with a cooling temperature control band 26.1±1.0 °C under different thermal masses in Changsha Climate in a week of extreme hot weather (1st-7th July), (Source: [23])

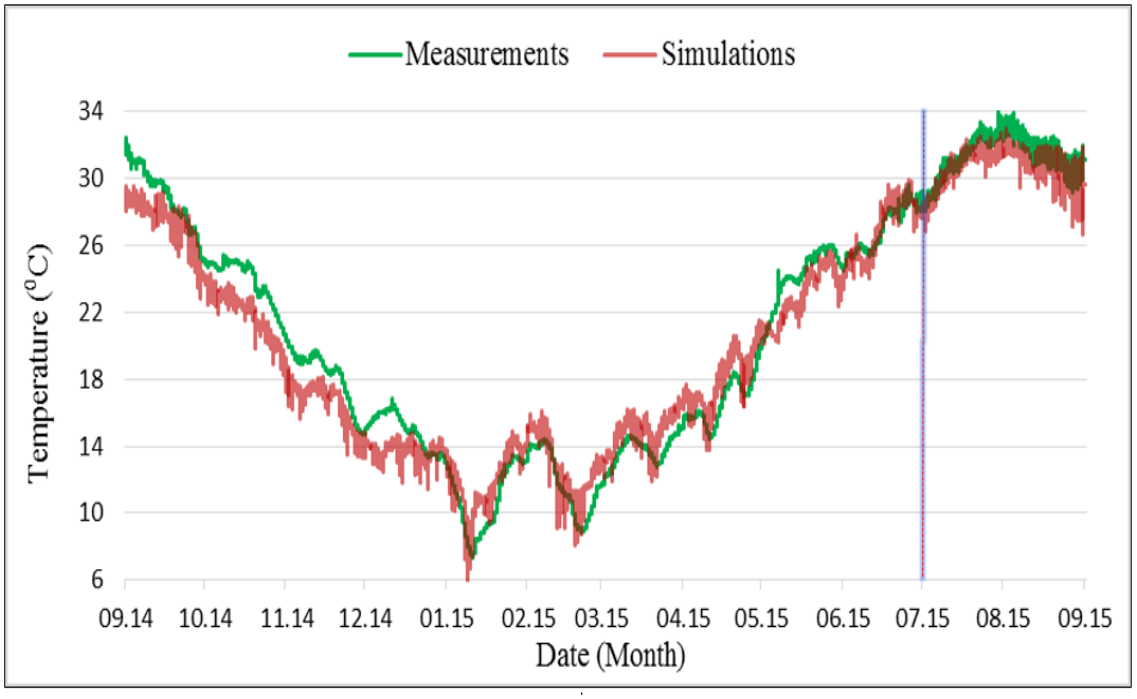

Figure 2.6. Measured and simulation temperature graph, (Source: [24])

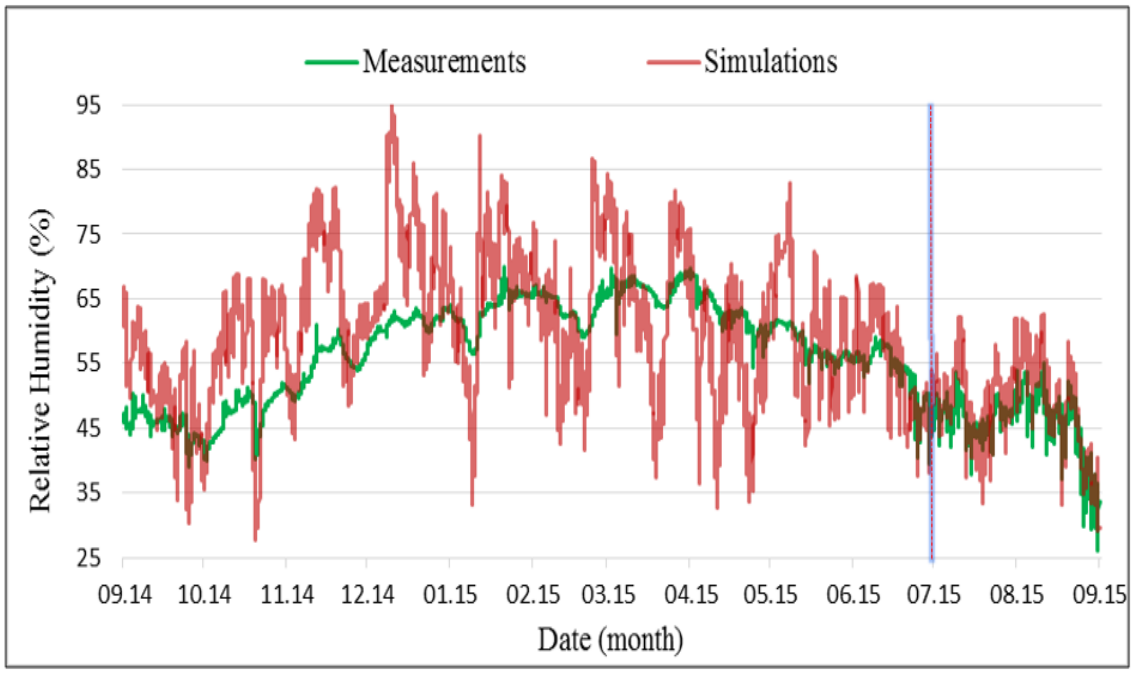

Figure 2.7. Relative humidity comparison of the measurements and the simulation graph, (Source: [24])

Table 2.1. Calculated error values for Simulation of the Library, (Source: [24])

	Temperature		Relative Humidity	
	MBE (%)	CV (RMSE) (%)	MBE (%)	CV (RMSE) (%)
Manuscript Zone	-1.25	7.71	5.02	17.7
Main Hall	-0.71	7.16	4.63	15.24
Entrance Zone	-6.58	12.5	14.52	22.04
ASHRAE 14 Standards, 2002	±10	30	±10	30

Solmaz Sakar and Sahin Güçhan [3] investigated two different types of construction techniques from foundations to roofs. In this study, it was mentioned that the vernacular dwellings have masonry walls or rock-cut walls. Different types of masonry walls were encountered during the study. Double sided masonry walls had

gaps in the middle and wall thickness that varied from 40cm to 85cm. Single sided masonry walls varied from 18cm to 30cm in thickness. Rock-cut walls were mostly carved in fairy chimneys, people shaped rocks to different dimensions according to the space they needed. It was also observed that people carved fireplaces, niches and furniture out of rocks. This study concluded that the Cappadocia geological structures affected the construction techniques in the region and the local materials were compatible with the extreme continental climate. The interior of the dwelling was cool during summer and warm during the winter.

In light of the above summarized papers and research already conducted, this study focuses on the experimental investigation into the effects of high thermal mass on building performance in a vernacular dwelling located in a fairy chimney south of Ürgüp town. Being located in an area of extremes with cold winters and hot summers, thermal efficiency of historic vernacular constructions is an important feature of architectural design considerations. This study aims to provide research data for future evidence-based decision making when constructing housing facilities in Cappadocia, Turkey.

CHAPTER 3

CONTEXT OF STUDIED CAVE DWELLING

3.1. Geographical Location of Cave Dwelling

Cappadocia is located in Central Anatolia and features a unique landscape characterized by mushroom-like rock structures called “fairy chimneys”. Göreme National Park and the Rock Sites of Cappadocia, added to the UNESCO World Heritage List in 1985, covers the region between the cities of Nevşehir, Ürgüp and Avanos. Sites include Karain, Karlık, Yeşilöz, Soğanlı and the subterranean cities of Kaymaklı and Derinkuyu. The density of Cappadocia’s rock-hewn cells, churches, troglodyte villages and subterranean cities make it one of the world's most striking and largest cave-dwelling complexes - dating back to the remains of a traditional human habitat of the 4th century. Additionally, the unique beauty of the decor of the Christian sanctuaries makes Cappadocia one of the leading examples of the post-iconoclastic Byzantine art period. [25]

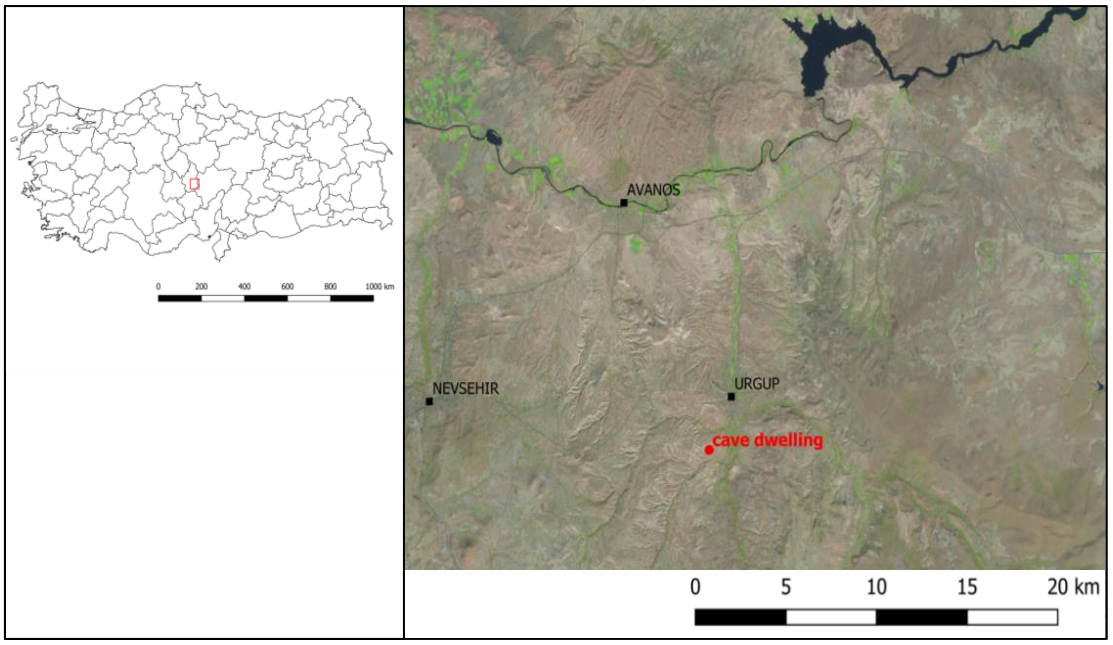

Figure 3.1. Location of cave dwelling at N 38.608 / E 34.900 south of Ürgüp shown on satellite image [26] with main town locations [27]; area of satellite image shown on inlet map of Turkey [27] on the left.

The studied cave dwelling is located in Ürgüp, Nevsehir, Cappadocia as seen in Figure 3.1. The dwelling, which is dug into a fairy chimney, is isolated from other cave dwellings. The location is south of Ürgüp town at N 38.608 / E 34.900 at an altitude of 1065m.

3.2. Geological Setting and Formation of Fairy Chimney

Le Pennec et al. [28] studied the Central Anatolian Volcanic Plateau in which the fairy chimneys are formed. Upper Miocene–Holocene ignimbrites (a pyroclastic flow deposit composed of very poorly sorted mixture of volcanic ash, or tuff when lithified, pumice and rock fragments), volcanic ash deposits and lava flows intercalated with fluvio-lacustrine sediments form the Central Anatolian Volcanic Plateau, covering around 20,000 km^2. The fairy chimneys are composed of differentially eroding ignimbrites often alternating with fluvio-lacustrine sediments.

Sarikaya et al. [29] determined the erosion rates at three different evolutionary stages of fairy chimneys as seen in Figure 3.2.

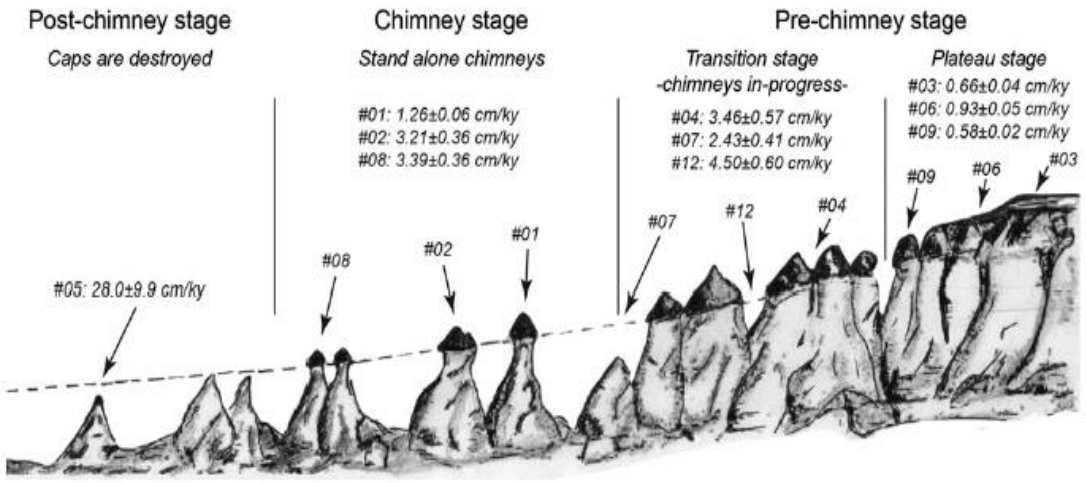

Figure 3.2. Sketch showing the most commonly observed formation mechanism of the fairy chimneys and results - of schematically located samples - showing determined erosion rates. Intercalated ignimbrite layers have different hardness and resistance to erosion; while soft and unwelded volcanic rocks (necks) are easy to erode, hard and welded ones (caps) are resistant to erosion, (Source: [29])

The evolution starts with gently sloping plateaus, which later differentially erode due to the variable physical characteristics of different ignimbrite layers. Plateaus

are dissected – often starting from cooling fractures – to form fairy chimneys. Because of the occasional presence of soft layers, such as lacustrine deposits and/or air fall deposits between the harder ignimbrite flows, chimney caps are formed in the overlying resistant ignimbrites. For a limited time the caps protect the fairy chimneys from erosion, giving rise to the development of the mushroom-like morphology. However, when the hard cap is eroded away, a sharp-pointed chimney is formed, and eventually the remaining cone is quickly destroyed by ongoing erosion.

3.3. Climatic Condition

The continental climate has significant effect on the development of fairy chimneys [3]. Central Anatolia summers are hot and dry and the winters are cold and wet. The average summer temperature is 19 °C, the average winter temperature is 0 °C and the average annual total precipitation is 421mm at Nevşehir Meteorological Station, at 1260m altitude [3]. The highest regional temperatures occur in July and August[21]. Precipitation peaks during winter and spring, and is lowest in the summer. The temperature drops under 0 °C between 87 and 107 days per year and the prevailing wind direction is NE-SW 1.8-2.3 m/s [3]. The dramatic temperature difference between summer and winter can be seen in Figure 3.3 and Figure 3.4.

Figure 3.3. Winter time photo is taken in Cappadocia Region on 16.01.2017

Figure 3.4. Summer time photo is taken in Cappadocia Region on 15.06.2016

3.4. Structural Characteristics and Use of the Cave Dwelling

The cave dwelling is made out of tuff with very thick walls. It is carved inside a fairy chimney range as seen in Figure 3.5.

Figure 3.5 Photo of the dwelling from east facade

On the north and south sides the fairy chimney is joined to the range. The west wall of the dwelling is about 5m thick. The east wall is the thinner part of the dwelling at about 2m thick. The door is made of wood, there are no windows or pillars within the dwelling as shown in Figure 3.6. The age of the cave dwelling is not known precisely. The cave dwelling was used as a barn by the past owners until the present owners converted the barn into a dwelling.

Figure 3.6. Photo of the dwellings interior

The cave dwelling is currently used as residential housing for a family of two adults and one child, a French couple and their son. They are running a ranch at the same area, they have horses, goats, geese, cats, dogs and a donkey. The owners have been earning their living with horseback touring since 2003. Their living is very modest and environmentally friendly. Their life is very self-sustainable, they produce their own milk, cheese and meat. In addition, they use part of their land to grow vegetables for their own needs. The family living in the dwelling is fully integrated into the Central Anatolian culture, speaking the local language and respecting the nature and the local culture.

The cave dwelling is located on the upper part of the property, right next to where horses kept in the open. The cave dwelling is a one room accommodation with an open kitchen and shower, both with a household connection of water. The toilet is located outside. The dwelling is inhabited year around except during short holidays.

During the winter months, the dwelling is heating with a wood-burning stove whilst during summer there is no cooling inside the dwelling.

In winter, the wood stove is utilized between approximately 18:00 and 23:00 burning only one bucket of hard wood. The indoor temperature starts dropping in the afternoon and rises again after 18:00 with the wood stove activity.

In summer, the entrance door is kept open during the day. That's why the infiltration is high during the summer.

CHAPTER 4

METHODOLOGY

In this study, temperature and relative humidity measurements are conducted in the studied cave dwelling in Ürgüp. Thermal conductivity, specific heat and density measurements are conducted at the Izmir Institute of Technology Laboratory.

4.1. Indoor Experimental Set-up

Measurements were made over a period of one year starting in June 2015 and ending in June 2016. Two Trotec BL-30 data loggers as seen in Figure 4.1, data loggers were used to record interior temperature and interior humidity of the cave dwelling. The temperature and relative humidity accuracies of Trotec BL-30 are listed in Table 4.1 and Table 4.2.

Figure 4.1. Trotec BL-30 Data logger, (Source [29])

Table 4.1. Temperature measurement accuracy table, (Source:[30])

Temperature	Measurement range	-40°C to +70°C
	Accuracy (-40°C to -10°C and +40°C to +70 °C)	± 2,0°C
	Accuracy (-10°C to +40°C)	± 1,0°C

Table 4.2. Relative humidity measurement accuracy table, (Source:[30])

Humidity	Measurement range	0 to 100%
	Accuracy (0 -20 and 80-100%)	± 5,0%
	Accuracy (20- 40 and 60-80%)	± 3,5%
	Accuracy (40 - 60%)	± 3,0 %

Device 1 (Serial number: 12089459) was placed in the centre of the living space at a height of 1.30m from the ground as seen in the Figure 4.2. Device 2 (Serial number: 140117893) was placed on the opposite side of the living space at a height of 1.30m as seen in Figure 4.2 and Figure 4.3.

Figure 4.2. The location of the data logger (the red and yellow circle symbolizes the data logger)

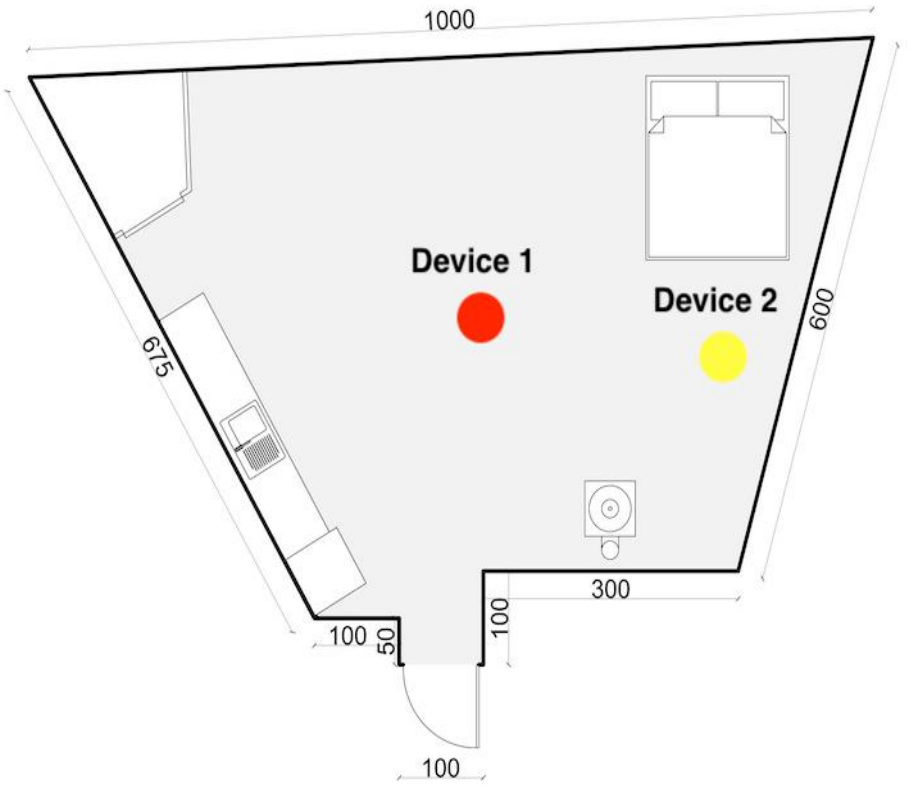

Figure 4.3. Locations of the devices

The Figure 4.2 photo was taken two years after the experiment, for this reason the order of the living space was changed. The measurements were taken every 20 minutes for 12 months. The measured results of the both devices were very similar. Device 1 data is evaluated, displayed and compared with simulation results in Chapter 6. The outliers and the missing intervals are replaced with the Device 2 data.

The data loggers were purchased shortly before the experiment took place. The data loggers are sold factory-calibrated. After the experiment, the data loggers calibrated by Chamber of Mechanical Engineers Calibration Laboratory. The temperature calibration results can be seen in Table 4.3.

Table 4.3. Device 1 temperature calibration results

Reference Value °C	Measured Value °C	Correction °C	Uncertainty °C
15,0	14,9	-0,1	0,5
20,0	19,7	-0,3	0,5
30,0	29,7	-0,3	0,5

The measured temperature results are calibrated with the equation in Figure 4.4. The relative humidity calibration results can be seen in Table 4.4. The measured relative humidity results are calibrated with the equation in Figure 4.5.

Table 4.4. Device 1 Relative humidity calibration results

Reference Value %RH	Measured Value %RH	Correction %RH	Uncertainty %RH
29.2	32.8	3.6	2.0
48.6	52.0	3.4	2.0
66.8	68.5	1.7	2.0

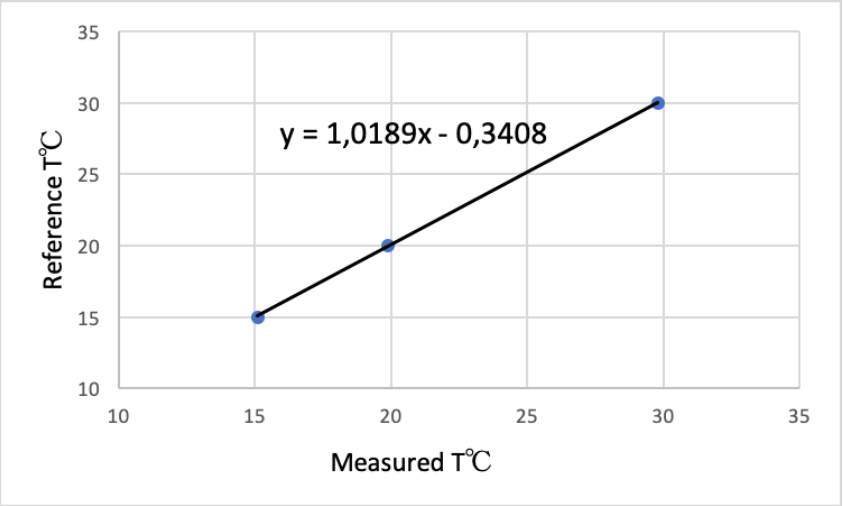

Figure 4.4. Temperature correction function

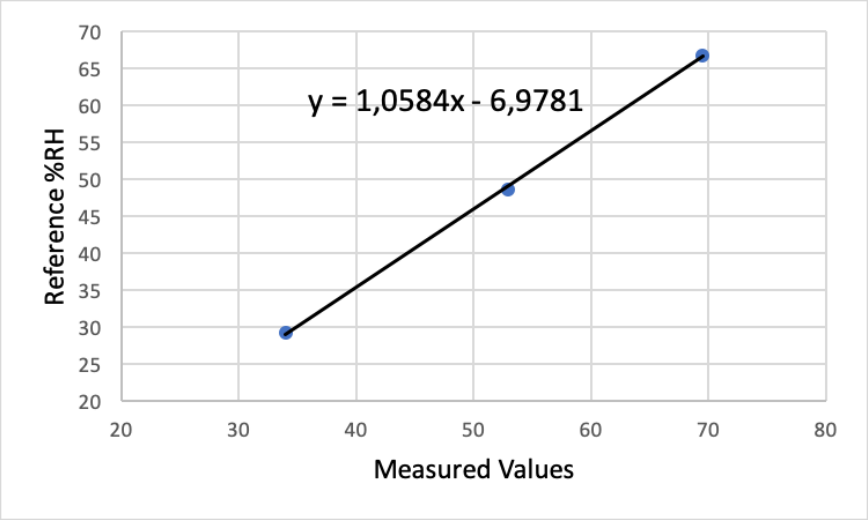

Figure 4.5. Relative humidity calibration function

4.2. Outdoor Climate Data

Hourly outdoor climatic data of temperature and relative humidity for 2015 and 2016 was collected from the Ürgüp Meteorology Station. Missing values were estimated through interpolation so that average results were not affected. As seen in Table 4.5 and Table 4.6, The monthly maximum, minimum outdoor temperature and relative humidity are extremely different for the years 2015 and 2016.

Table 4.5. Max-Min temperature and relative humidity values of the year 2015 [32]

Year	Month	Max T (℃)	Max RH (%)	Min T (℃)	Min RH (%)
2015	January	14.5	95.0	-20.5	25.0
	February	18.3	94.0	-15.0	16.0
	March	21.0	95.0	-6.4	15.0
	April	31.6	93.0	1.5	11.0
	May	28.7	94.0	6.8	23.0
	June	28.7	94.0	6.8	23.0
	July	36.3	950	7.3	10.0
	August	35.9	96.0	7.1	17.0
	September	35.1	91.0	5.8	9.0
	October	25.5	97.0	-0.3	21.0
	November	18.5	97.0	-6.8	14.0
	December	9.2	97.0	-10.9	35.0

Table 4.6. Max-Min temperature and relative humidity values of the year 2016 [32]

Year	Month	Max T (℃)	Max RH (%)	Min T (℃)	Min RH (%)
2016	January	15.5	98.0	-22.0	32.0
	February	21.1	97.0	-11.5	21.0
	March	24.0	97.0	-8.3	11.0
	April	28.2	95.0	-3.2	13.0
	May	27.2	97.0	1.6	18.0
	June	34.8	96.0	3.4	14.0
	July	37.7	92.0	8.6	5.0
	August	36.8	92.0	10.4	11.0
	September	33.1	97.0	-0.6	14.0
	October	29.8	96.0	-4.6	9.0
	November	23.8	95.8	-10.4	6.0
	December	11.1	97.0	-18.9	26.0

4.3. Thermal Conductivity of Tuff

For the simulation in DesignBuilder, the thermal conductivity of the main material of the cave dwelling was needed. A KEM QTM 500 probe was used to measure the thermal conductivity. The KEM QTM 500 probe has a single heater and a thermocouple. To calculate the thermal conductivity, constant electricity is given to the heater, then the temperature of the wire increases exponentially [31]. The limitations of QTM 500 is seen in Table 4.7.

Table 4.7. KEM QTM 500 Specifications (Source: [31])

Type and model name	QTM-500 Quick Thermal Conductivity Meter
Measuring method	Hot Wire method
Measuring range	0.023 to 12W/mK
Precision	±5% reading value per reference plate
Reproducibility	±3% reading value per reference plate
Temperature	- 10 to 200℃ (Thermal bath is necessary for measurement at different room temperature)
Measuring time	Standard 60sec (specimen must be in temperature equilibrium)
Sensor	PD-11 Box Probe Constantan heater wire and chromel-alumel thermocouple
Heater current precision	±0.1% of setup value
Minimum sample size	Approx. 100(W)×50(L)×20(Thickness) (mm)

The basic principle of QTM 500 is determining the thermal conductivity from the alteration of the logarithmic graphic line as seen in Figure 4.6.

Due to the tuff rock's nature, its properties may vary depending upon where the samples are taken. Two samples were taken from the fairy chimney under investigation. The thermal conductivity was measured with the KEM QTM 500 thermal conductivity meter as seen on Figure 4.7.

$$\lambda = \frac{q \cdot \ln(t_2/t_1)}{4\pi(T_2 - T_1)}$$

λ ; thermal conductivity of sample		[W/mK]
q ; generated heat per unit length of sample/time		[W/m]
t_1, t_2 ; measured time length		[sec]
T_1, T_2 : Temperature at t_1, t_2		[K]

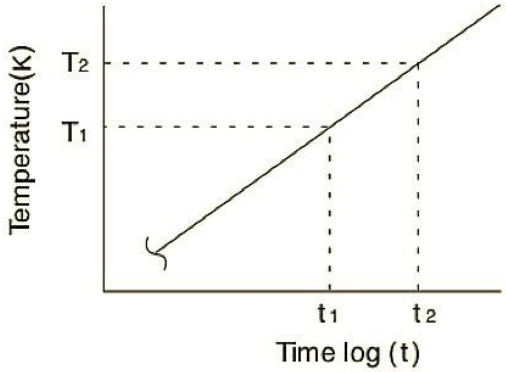

Figure 4.6. KEM QTM 500 Principle of thermal conductivity calculation, (Source: [31])

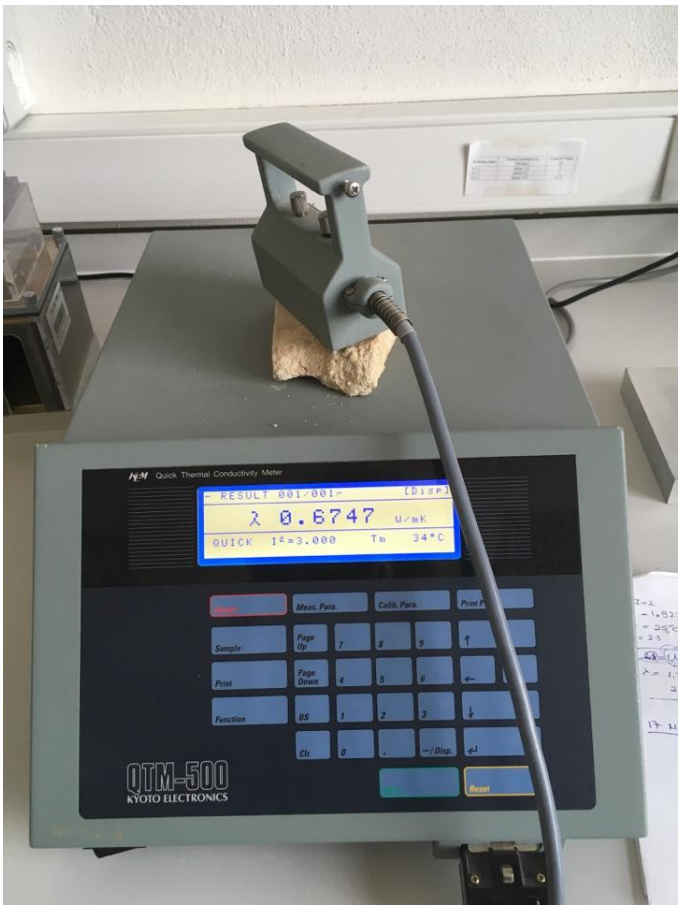

Figure 4.7. Thermal conductivity measurement with KEM QTM 500.

The samples were cut into 3cm*11cm*6cm pieces which were larger than the probe's size. Three measurements were taken from each sample to obtain the closest value to the average tuff rock thermal conductivity. The measurements, average and the standard deviation of the thermal conductivity measurements can be seen on Table 4.8.

Table 4.8. Thermal Conductivity measurements of the tuff rock sample

	k_1	k_2	k_3	k_4	k_5	k_6	$k_{average}$	Std. Dev.
Thermal Conductivity	0.9089 W/mK	0.8372 W/mK	0.7281 W/mK	0.6805 W/mK	0.6747 W/mK	0.6450 W/mK	0.7457 W/mK	0.1046

The thermal conductivity measurement range is wide as seen Figure 4.8. First measurement could be taken as an outlier. However, tuff rock has a heterogeneous compound and that measurement could stand for important percentage of the measurements. That's why first measurement also included to the average thermal conductivity calculations.

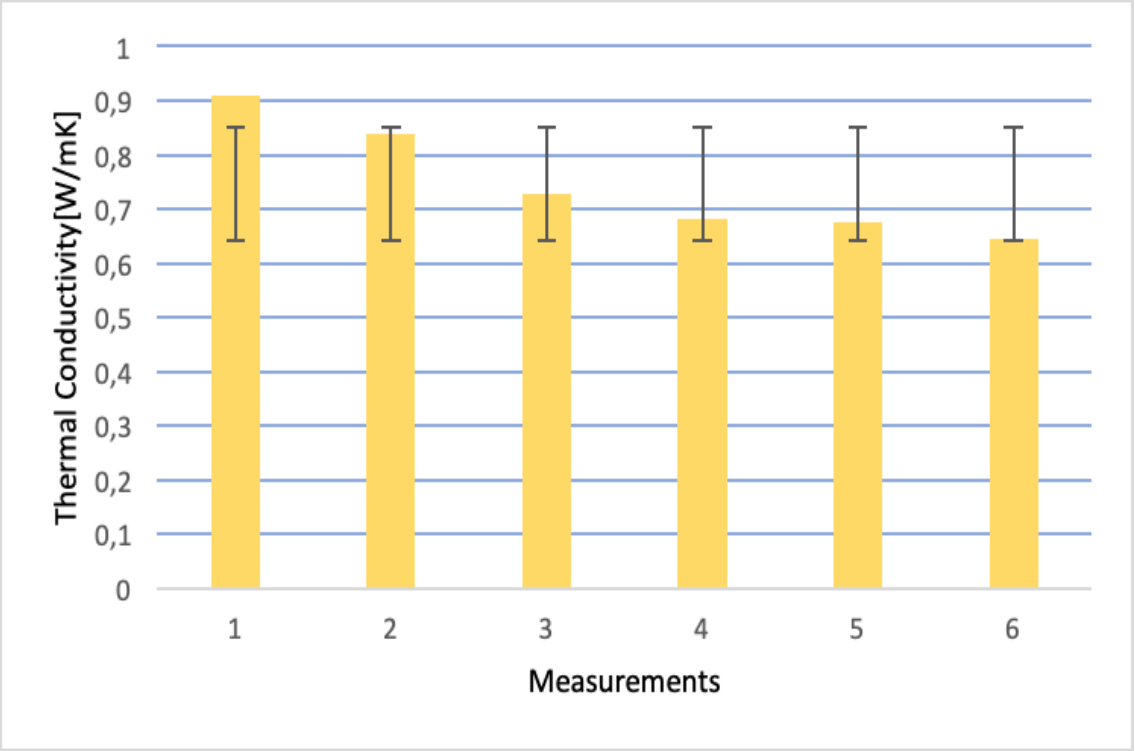

Figure 4.8. Thermal conductivity measurements with standard deviation error bar

4.4. Specific Heat of Tuff

For the simulation on the DesignBuilder, the specific heat of the main material of the dwelling was measured with TA Instruments DSC Q10 as seen in Figure 4.9.

Figure 4.9. TA Instruments DSC Q10 while measuring the specific heat of the tuff sample

Specific heat is a function of temperature as seen in Figure 4.10. The specific heat at 20°C which is 1690.7J/kg K was entered into DesignBuilder.

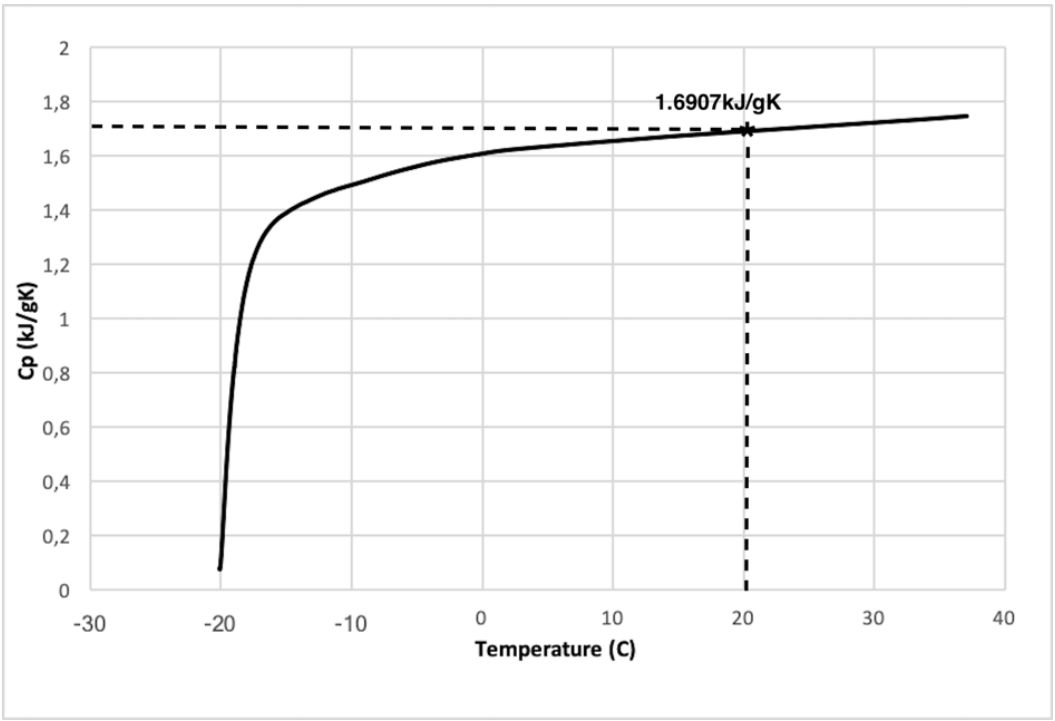

Figure 4.10. The temperature function of the specific heat.

4.5. Density of Tuff

For the simulation on the DesignBuilder, the density of the main material of the dwelling was measured with the Sartorius CP Model CPA224S. First the weight of the water and the vessel was tared as seen in Figure 4.11. Then the weight of the tuff sample was measured as 3.8195g shown in Figure 4.12. The weight of the rock under the buoyancy of water was measured at 1.5220g shown in Figure 4.13. Finally, the weight of the soaked the tuff was measure at 4.3655g as seen in Figure 4.14. The density of the tuff sample is calculated below. The water density is assumed to be 1g/ml. The density of the tuff rock is calculated as d_{tuff}=1.3430g/ml with the aid of the equation below.

$$d = m/V \tag{4.1}$$

Figure 4.11. The tared scale

Figure 4.12. The weight of the tuff sample

Figure 4.13. The weight of the tuff sample under the buoyancy

Figure 4.14. The weight of the soaked tuff sample.

CHAPTER 5

METHODOLOGY

As mentioned in Chapter 1, the building and construction sector has one of the biggest impact on the environment. Energy efficiency has become one of the most important criteria for designing buildings. Like applying vernacular architecture designs to their buildings with hundreds of years' experience behind the logic; using the computer simulations is becoming essential. The computer simulations are a key to identifying weak links in design and finding solutions.

DesignBuilder is a user-friendly computer simulation program which uses the American Energy Society's Energy Plus software in the background [35]. In this study DesignBuilder is used to simulate the studied dwelling and compare the simulation to the actual experimental findings.

5.1. Specification of the Cave Dwelling

The cave dwelling's built year is not known and the building techniques in the past was with mechanical hand tools. Thus, the interior geometry is not as smooth as that of a standard dwelling. Figure 5.1 shows the dimensions of the interior walls which were assumed to be straight.

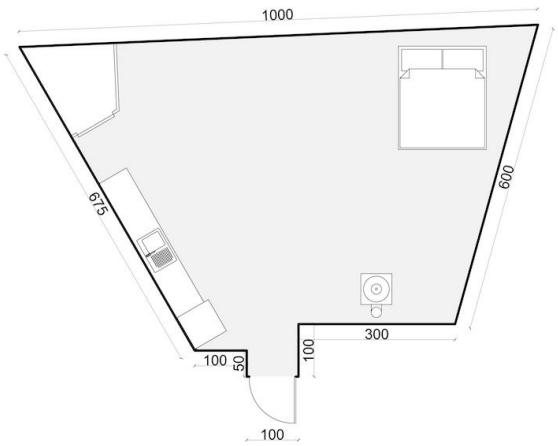

Figure 5.1. Interior plan of the cave dwelling (dimensions in cm)

The actual ceiling height ranged from 2.0m to 2.4m and was assumed to be 2.2m for the DesignBuilder simulation. The interior space was measured with a laser meter and a compass. The exterior of the dwelling was modelled as seen in Figure 5.2.

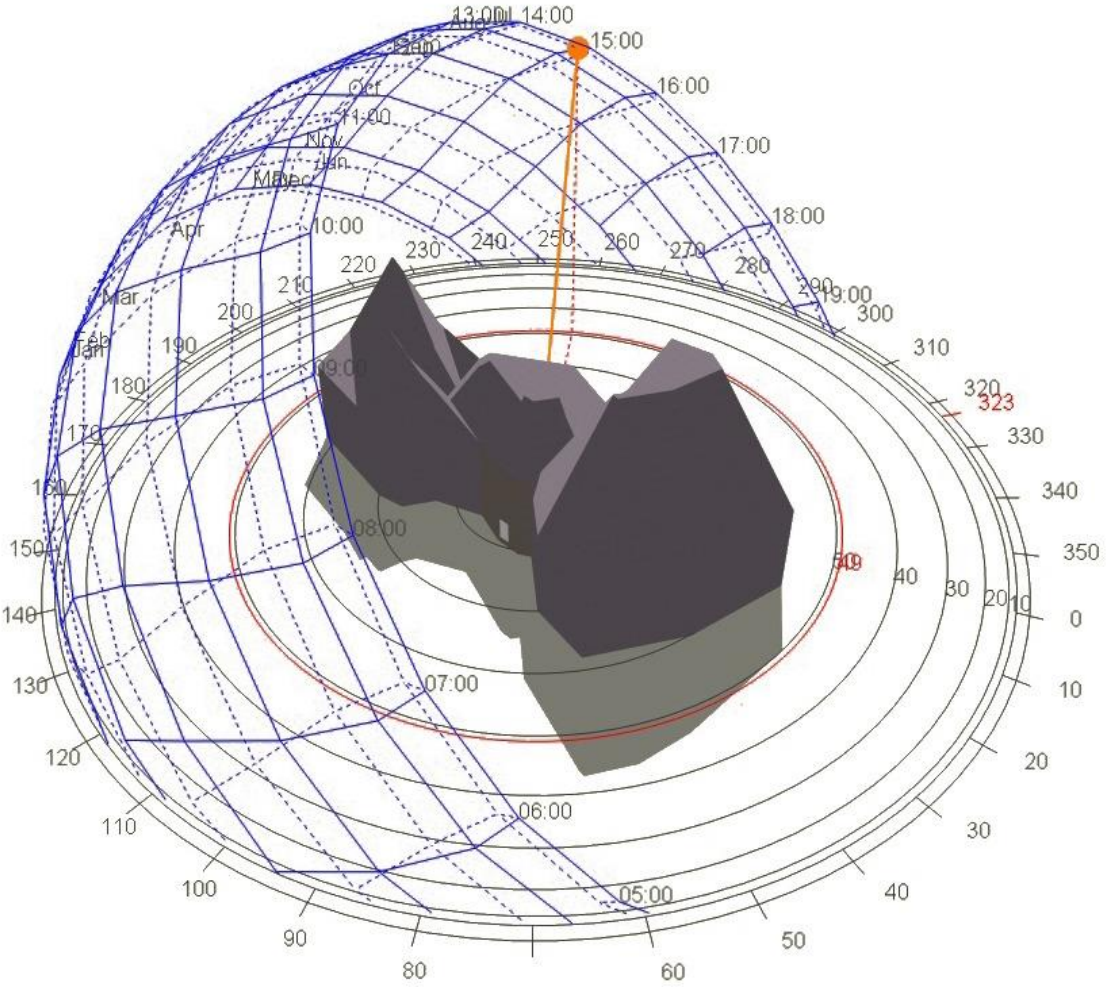

Figure 5.2. The 3D model of the cave dwelling and the solar radiation pattern

With those measurements, the total area of the cave dwelling was calculated to be 46,9m^2, and the total volume of the cave dwelling was calculated at 103,2m^3.

The cave dwelling has no windows, the only openings are the door and the chimney. The door of the dwelling is facing the East and made out of double layer glass.

The top view of the fairy chimney range sketch is drawn with AutoCAD program with using the drone picture of the top view. The interior part is attached from the door reference point. All the facades and the section views are seen in Figure 5.3.

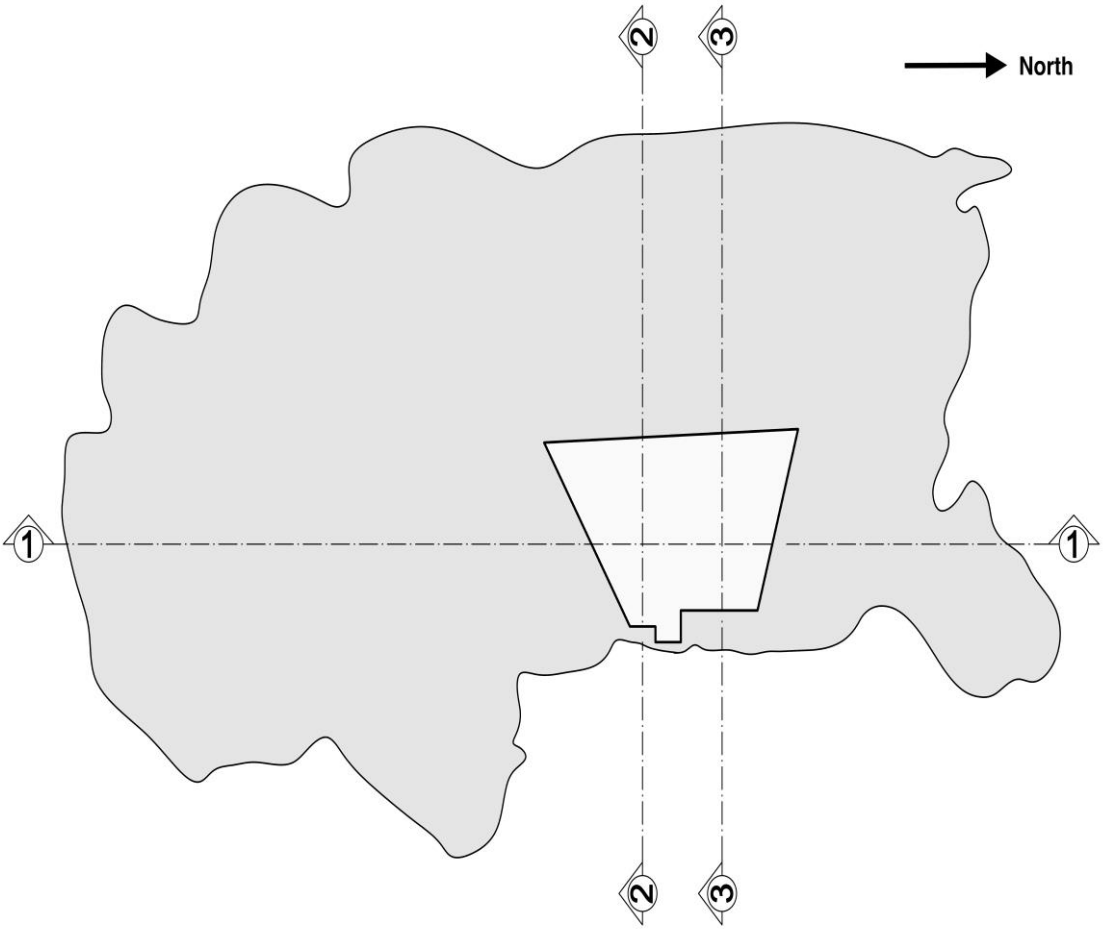

Figure 5.3. Cave dwelling top view in the fairy chimney range

The north, west and south walls of the dwelling were assumed to be adiabatic because the north and south walls merged with neighbouring fairy chimneys as seen in Figure 5.4.

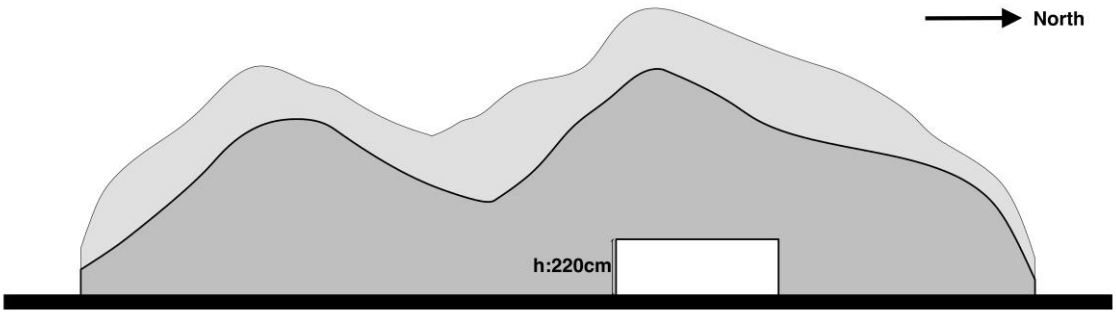

Figure 5.4. Section 1, the view from the East side of the dwelling

The East facade walls of the cave dwelling are in different thicknesses. As seen in Figure 5.5 the 2.2m^2 part of the wall has 0.4m thickness which is the thinnest wall of the cave dwelling.

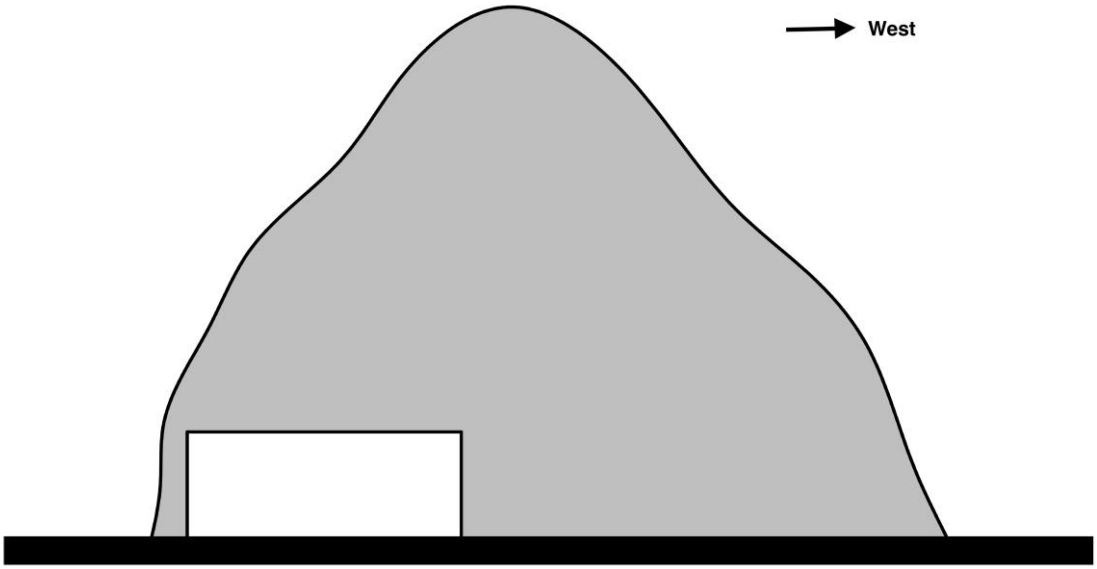

Figure 5.5. Cave dwelling Section 3, thinnest part of the East facade.

The other part of the East facade of the dwelling is seen in Figure 5.7 which is 1m thick.

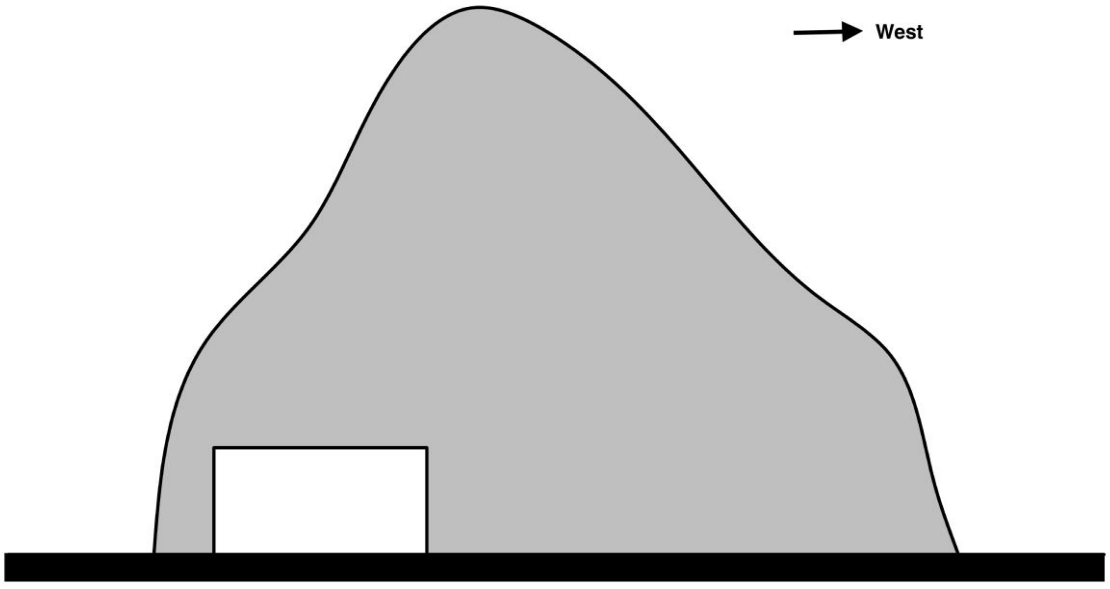

Figure 5.6. Cave dwelling Section 3, thicker part of the East facade wall.

The west wall is more than 8m thickness and half way under the ground, that's why it is also assumed that it is adiabatic.

The specific heat of the tuff rock was entered as 1.6907kJ/gK at 20 °C, the density of the tuff rock was entered in DesignBuilder as 1.3430g/ml

The thermal conductivity measurements of the tuff rock are in a wide range. The average thermal conductivity was entered in DesignBuilder as 0.7457 W/mK. However, in the calibration of the simulation the MBE and CV(RMSE) are calculated for different values as well.

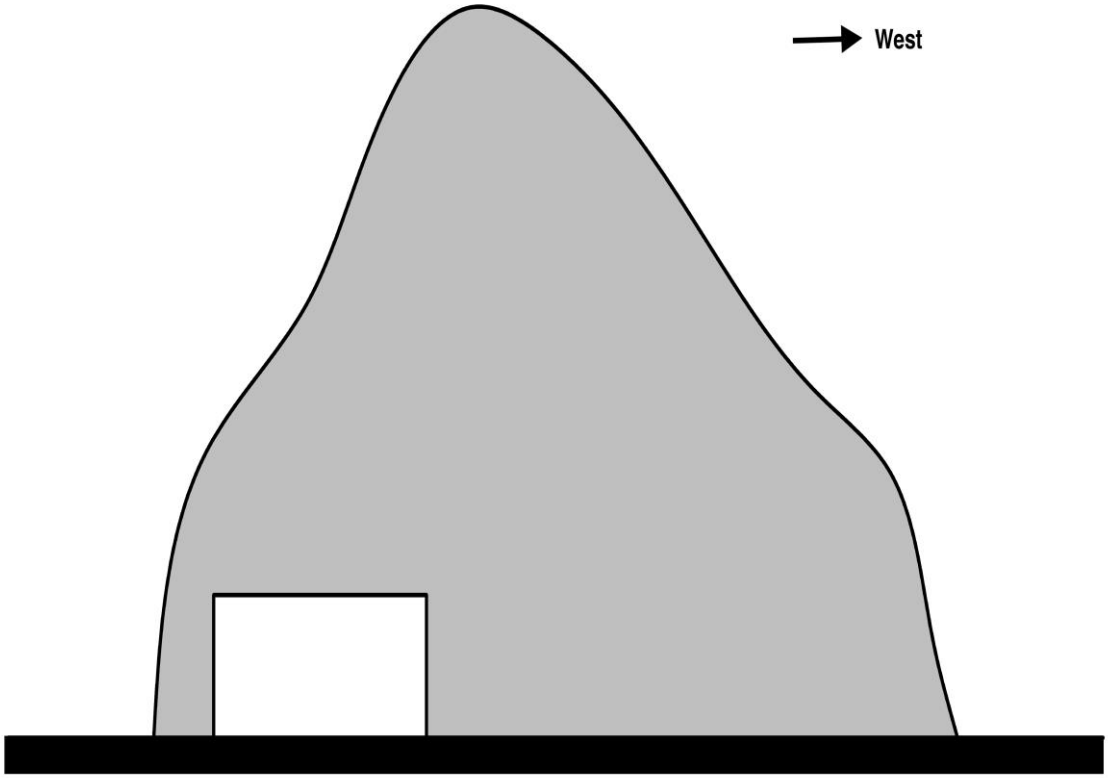

Figure 5.7. Cave dwelling Section 3, thicker part of the East facade wall.

5.2. Heating and cooking and shower activities of the cave dwelling

Heat gain from the household and electronic devices entered Designbuilder as 0.334kWh for each hour of the year. The detailed generated heat gain from the devices can be seen on Table 5.1.

Table 5.1. Heat generation from household and electronics [38],[39],[40]

Devices	Power of device	Hours of use per day	Daily Gain
Lightening	100W	8h	800Wh
Refrigerator	-	-	1233Wh
Washing machine	-	-	471Wh
Dishwasher	-	-	707Wh
Oven	2400W	1h	2400Wh
Others	100W	24h	2400Wh
Total			8011Wh

All year round, the occupants have their breakfast inside the dwelling; during the day, the dwelling is empty until sunset. After sunset, the occupants return to the dwelling to cook dinner. The gas cooker is on between 07:00 to 08:00 and 18:00 to 19:00. Six bottles of propane gas are consumed during a year, amounting to 72kg of propane. For 1kg of propane the net heat gain is 13.6kWh [42]. The daily net heat gain from the propane stove entered DesignBuilder is 2.68kWh.

Table 5.2. The schedule of wood consumption.

Time Interval	January 1st January 31st	February 1st April 30th	May 1st September 30th	October 1st November 15th	November 16th December 31st
Amount of Fuel	8kg wood	6kg wood	No heating	6kg wood	8kg wood
Daily Heat Gain	20.544kWh	15.408kWh	0.0kWh	15.408kWh	20.544kWh
Hourly Heat Gain	2.568kWh	1.926kWh	0.0kWh	1.926kWh	2.568kWh

During the winter, the occupants heat the dwelling with a wood stove. Hard woods are used as fuel, the net heat gain is assumed to be 4.28kWh per 1kg of wood and the efficiency of the wood stove is assumed to be 60%[37].

Wood stove activity is generally between 18:00 to 24:00 for six hours. The amount of hard wood is varied between months and the amount of the wood consumption can be seen on Table 5.2.

5.3. Occupancy Schedule

The occupants are busy with the farm during the day. Their schedule starts with the sunrise as farm animals do and finishes with the sunset. Between 8:00 and 18:00 occupants are outside. Three people entered as occupants between 18:00 to 08:00 for 14 hours in DesignBuilder for the entire year.

5.4. Infiltration

The dwelling has only two openings which are the door and the chimney. There is no mechanical ventilation, but there is natural ventilation. During the experiment, infiltration measurements were not taken. The infiltration of the cave dwelling is dependent upon the temperature differences between the dwelling and the outdoors, wind, wind direction and wood stove activity. Any measurements taken would not have been representative of the site's environment.

During winter the door is almost always closed. Since the occupants work during the day, the dwelling is empty. At night, the temperature difference between the indoors and outdoors is extreme so it is impossible to keep the door open. The average air/fuel ratio is 12kg of air per 1kg of wood for an efficient burning [36]. Therefore, even the door is closed most of the time of the day, wood stove activity is the proof of the leakages into the dwelling. The door has leakages and the cold air enters from the door and supplies O_2 to make burning process possible as seen in Figure 5.8.

During summer period, between 1st of May to September 30th the door is wide open all day long but the fly net stays shut. This makes the summer infiltration value higher. Since the air flow through the door is not measured three different infiltration scenarios assumed and the infiltration values for winter and summer are shown on Table 5.3. The infiltration periods are chosen accordingly the wood stove fuel consumption

period. The fall and spring infiltration values assumed the average of the winter and the summer values.

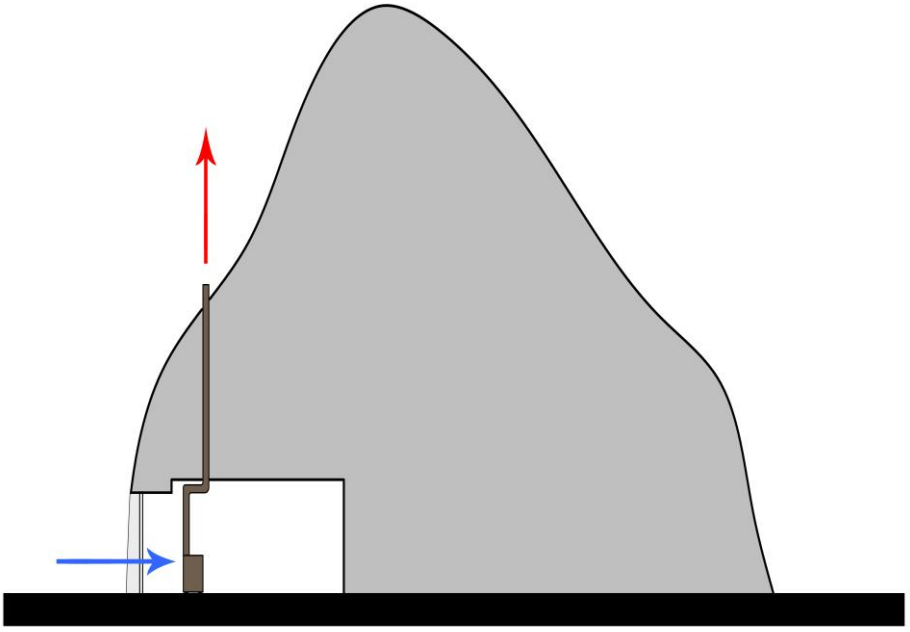

Figure 5.8. The ventilation direction of the dwelling whole year around

Table 5.3. Infiltration values entered to DesignBuilder.

Time Interval	January 1st to January 31st	February 1st to April 30th	May 1st to September 30th	October 1st to November 15th	November 16th to December 31st
Scenario 1	0.25 ACH	0.75 ACH	1.25 ACH	0.75 ACH	0.25 ACH
Scenario 2	0.5 ACH	1.0 ACH	1.5 ACH	1.0 ACH	0.5 ACH
Scenario 3	1.0 ACH	1.5 ACH	2.0 ACH	1.5 ACH	1.0 ACH

5.5. Climatic Conditions

Ürgüp State Meteorology Station temperature, relative humidity and wind data between June 2015 and June 2016 is used for the outdoor boundary conditions. The

excel data is converted with Elements software to Energy Plus weather format. Ürgüp Station doesn't have solar radiation measurements that is why for solar radiation Erkilet Weather Station data is used. Erkilet Weather Station is in Kayseri Airport, located at N37.78 / E35.48, altitude 1056m [32]. The location of the cave dwelling is N38.60 / E34.90, altitude 1065m. The air distance between the weather station and the cave dwelling is 54km and the altitude difference is 9m.

5.6. Calibration of the DesignBuilder Model

Calibration is an important procedure after modelling to have a reliable design. ASHRAE 14 guideline 14-2002: Measurement Energy and Demand Savings, calibration method is followed to calibrate the DesignBuilder model.

ASHRAE 14 guideline 14-2002 suggests to calculate and check two different statistical indicators, one of them is Mean Bias Error and the other is Coefficient of Variation of Root Mean Square [33]. MBE is the average forecast error which represents the systematic error of the simulation [34]. CV(RMSE) indicates the uncertainty in the simulation while comparing the simulation results and the measured results. MBE and CV(RMSE) functions are used to calibrate the model.

$$MBE = \frac{\sum_{i=1}^{N_i}(M_i - S_i)}{\sum_{i=1}^{N_i} M_i} \tag{5.1}$$

$$CV(RMSE) = \frac{\sqrt{\frac{\sum_{i=1}^{N_i} M_i - S_i{}^2}{N_i}}}{\frac{1}{N_i}\sum_{i=1}^{N_i} M_i} \tag{5.2}$$

According to ASHRAE Guideline 14, obtained MBE value must be within ±10% and the CV(RMSE) value must be within ±30%.

The cave dwelling interior construction dimensions are measured with the aid of laser meter, tape measure on site. The outer boundaries of the dwelling are obtained with the aid of drone photos and reference points. The construction of the simulation

model is based on these measurements. After running the simulation, first simulation results are obtained and the calibration procedure started. The uncertainty of the data loggers is taken into consideration with ±1.0˚C for temperature and ±3.5% for relative humidity. The simulation is carried out 47 times to reach the final results. During the calibration the thermal properties of the tuff, heating schedules, infiltration schedules, the geometry of the dwelling are updated and listed below;

- Different thermal conductivity values within the standard deviation of the thermal conductivity measurements of the tuff rock are entered the simulation to observe the effect. However, the average thermal conductivity (0.7457W/mK) is entered in the final calculations since the mean value is the most representative.
- The heating schedule of the dwelling is updated with respect to interview with the occupants and analyse the actual measurements.
- The fuel consumption of the wood stove is updated accordingly the seasons with respect to interview with the occupants and analyse the actual measurements.
- The infiltration schedules of the dwelling are updated with respect to heating activities schedule.
- The occupants were on holiday and the caretaker was living in the dwelling during October and February. The schedule of the caretaker is unknown that's why the October and February months are not taken into consideration for calibration process.

Hourly measurements and the simulation results are used for the MBE and CV(RMSE) calculations. On Table 5.4 for different thermal conductivity values the MBE and CV(RMSE) are displayed for both temperature and relative humidity. The temperature MBE and CV(RMSE) are within the ASHRAE Guideline 14 limits. However, the relative humidity error values are both out of scope for each scenario. The complex characteristics of the tuff rock precludes to simulate the relative humidity fluctuations. The temperature and humidity results will be discussed in Chapter 6 in detailed.

Before the calibration of the DesignBuilder model, the actual measurements are calibrated accordingly the calibration report of the Chamber of the Mechanical Engineers.

Table 5.4. Calibration results of the DesignBuilder Simulation for different thermal conductivity values

	Temperature		Relative Humidity	
	MBE (%)	CV (RMSE) (%)	MBE (%)	CV (RMSE) (%)
Scenario 1 (k=0.6400 W/mK)	-7.27	12.21	43.28	46.73
Scenario 1 (k=0.7457 W/mK)	-6.15	11.17	43.13	46.59
Scenario 1 (k=0.8400 W/mK)	-5.06	10.32	42.91	46.43
Scenario 2 (k=0.6400 W/mK)	-3.85	9.57	43.30	46.84
Scenario 2 (k=0.7457 W/mK)	-2.85	8.76	42.98	46.56
Scenario 2 (k=0.8400 W/mK)	-2.75	8.67	42.97	46.55
Scenario 3 (k=0.6400 W/mK)	0.17	7.79	41.81	45.54
Scenario 3 (k=0.7457 W/mK)	1.03	7.58	41.43	45.20
Scenario 3 (k=0.8400 W/mK)	1.12	7.48	41.40	45.18
ASHRAE 14 Standards, 2002	±10	30	±10	30

According to ASHRAE Guideline 14, the DesignBuilder model's temperature MBE and CV(RMSE) error values are both within the accepted zone but the relative humidity's MBE and CV(RMSE) error values are both out of accepted zone. The study carried and based on Scenario 3 with k=0.7457W/mK in Chapter 6.

CHAPTER 6

RESULTS AND DISCUSSIONS

As mentioned in Chapter 3 the summer and the winter, day and night outdoor temperature and relative humidity fluctuations are extremely high. By contrast with the extreme outdoor temperature and relative humidity the indoor measurements are very consistent as seen in Table 6.1.

Table 6.1.Max-Min temperature and relative humidity values of the dwelling's interior during the experiment [32].

Year	Month	Max T_i (℃)	Max T_o (℃)	Min T_i (℃)	Min T_o (℃)	Max RH_i (%)	Max RH_o (%)	Min RH_i (%)	Min RH_o (%)
2015	June	22.0	28.7	16.9	6.8	93.9	94.0	64.3	23.0
	July	25.0	36.3	16.9	7.3	84.7	95.0	36.4	10.0
	August	25.3	35.9	19.1	7.1	75.3	96.0	44.7	17.0
	September	25.1	35.1	19.1	5.8	70.8	91.0	29.6	9.0
	October	24.1	25.5	17.1	-0.3	82.8	97.0	31.8	21.0
	November	23.2	18.5	15.5	-6.8	95.4	97.0	34.8	14.0
	December	23.2	9.2	14.3	-10.9	76.0	97.0	33.5	35.0
2016	January	21.7	15.5	14.3	-22.0	83.6	98.0	36.7	32.0
	February	20.8	21.1	14.2	-11.5	84.1	97.0	42.9	21.0
	March	22.0	24.0	14.3	-8.3	80.5	97.0	37.2	11.0
	April	22.7	28.2	16.0	-3.2	82.0	95.0	33.5	13.0
	May	21.1	27.2	15.9	1.6	88.4	97.0	42.4	18.0
	June	21.7	34.8	17.0	3.4	83.7	96.0	47.2	14.0

The temperature and relative humidity variations between the dates of 15.06.2015 and 15.06.2016 are shown in Figure 6.1 and Figure 6.2. As it is clearly seen from both

graphs, while the outdoor temperature and relative humidity fluctuates widely, the measured indoor temperature and relative humidity remains very consistent.

The Scenario 3 results are displayed in Figure 6.1 and Figure 6.2. The temperature results of the DesignBuilder simulation is consistent and according to ASHRAE Guideline 14, it is in calibration interval. The relative humidity results of the DesignBuilder simulation is not in the calibration interval and the simulation results are lower than measurements during whole winter period.

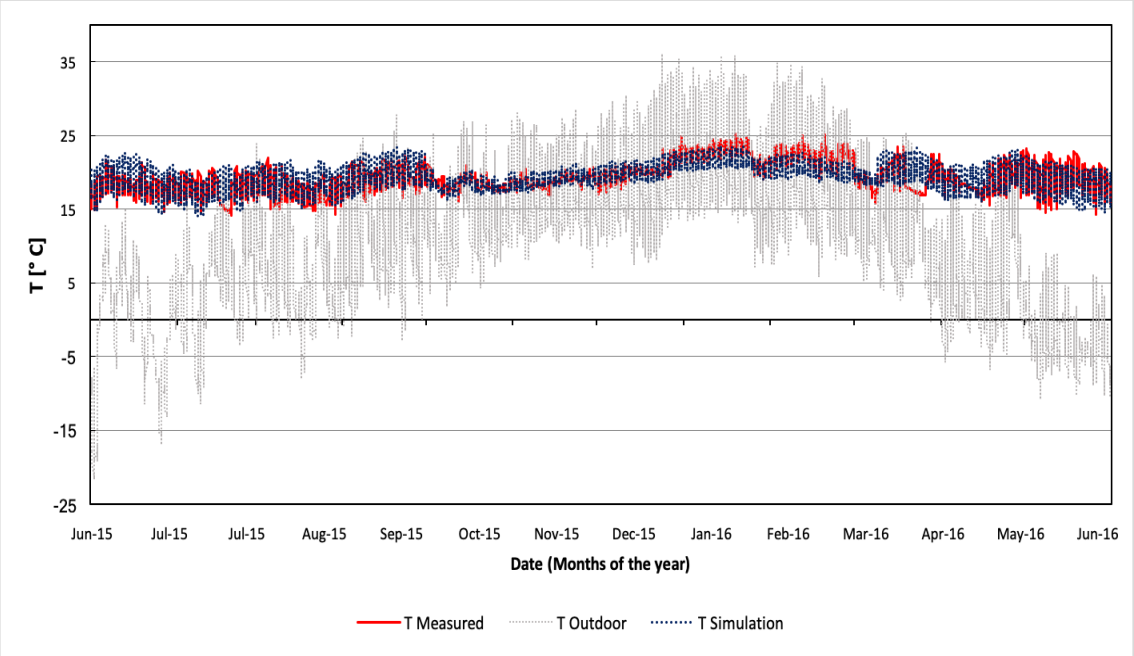

Figure 6.1. Annually measured and simulation temperature distribution in the cave dwelling and outdoor temperature.

The tuff rock has a porous characteristic, the rock soaks the humidity and emits the humidity whole year around. During winter, fall and spring the occupants boil water on top of the stove almost at all times. These keeps the cave dwelling humid under extreme dry conditions. The moisture diffusivity of the tuff rock and entrance of the simulated zone are complicated the modelling. As a result of those the humidity simulation results are lower than the actual measurements as seen in Figure 6.2. During summer the simulation relative humidity results are more similar to the actual measurements since there is no wood stove activity or boiling water on top of the wood stove.

The measured and simulation results are compared seasonally in detailed in following sections.

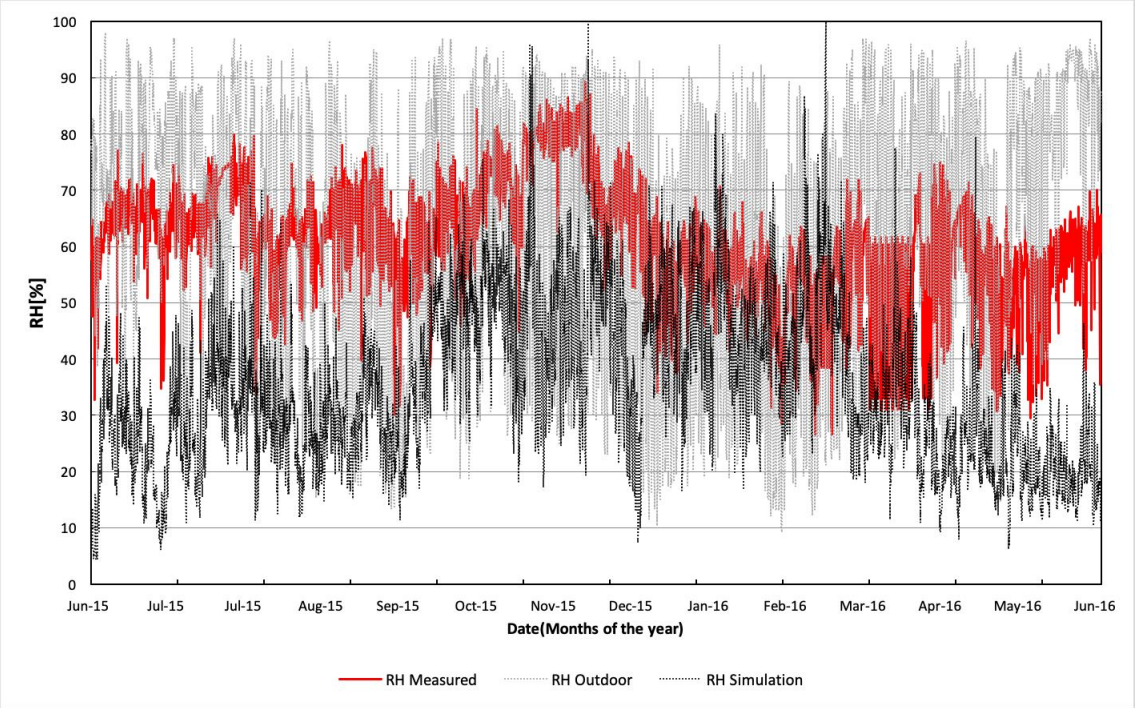

Figure 6.2 Annually measured and simulation relative humidity distribution in the cave dwelling and outdoor.

6.1. Summer Period

Figure 6.3 clearly shows the measured daily average temperature and measured relative humidity of the dwelling was very stable during July 2015. From sunrise at 06:00 the interior temperature began to increase, reaching a peak at 17:00 to 21°C and after 17:00 the interior temperature started decreasing. While the outdoor temperature fluctuated between 40°C and 10°C the indoor temperature is changed less than 2°C thanks to thermal mass effect of the cave dwelling. The simulation temperature results are also under mass effect and very similar to the measured temperature. The measured relative humidity is higher than the outdoor relative humidity by 20% and the measured relative humidity behaved similar to the outdoor relative humidity. The simulation relative humidity results are fluctuated much more widely compare to measured relative humidity. The rest of the summer months, June and August daily average graphs can be seen in Figure A 1 and Figure A 2.

Measured and simulated temperatures are very similar as seen in Figure 6.4 for whole July month. The indoor temperature fluctuations are caused by the high infiltration since the door is opened at all times and the hot air leakages from the

chimney with the stack effect. The rest of the summer months, June and August monthly temperature variations graphs can be seen in Figure A 3, Figure A 4.

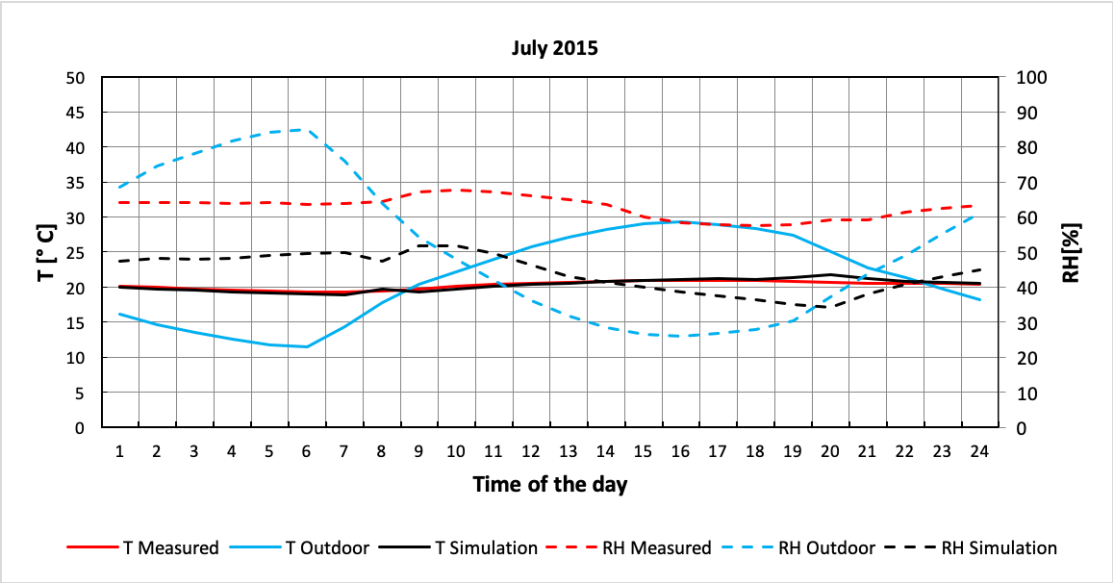

Figure 6.3. Daily Average of July 2015 [32]

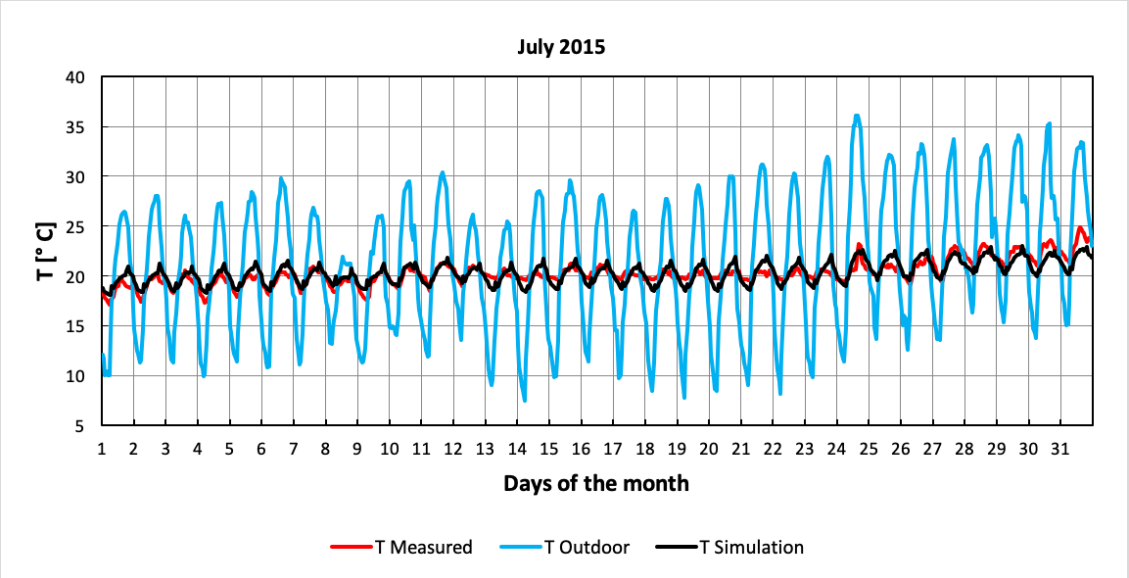

Figure 6.4. Measured, simulated interior and outdoor temperatures versus day of the month graph, July 2015

During July month measured relative humidity is fluctuated within %20 while the outdoor fluctuated within %60 as seen in Figure 6.5. The reason for that could be the porous characteristics of the tuff rock. The simulation results are mostly behaved

similar to the outdoor relative humidity but in a narrower interval. The rest of the summer months, June and August monthly relative humidity variations graph can be seen in Figure A 5 and Figure A 6.

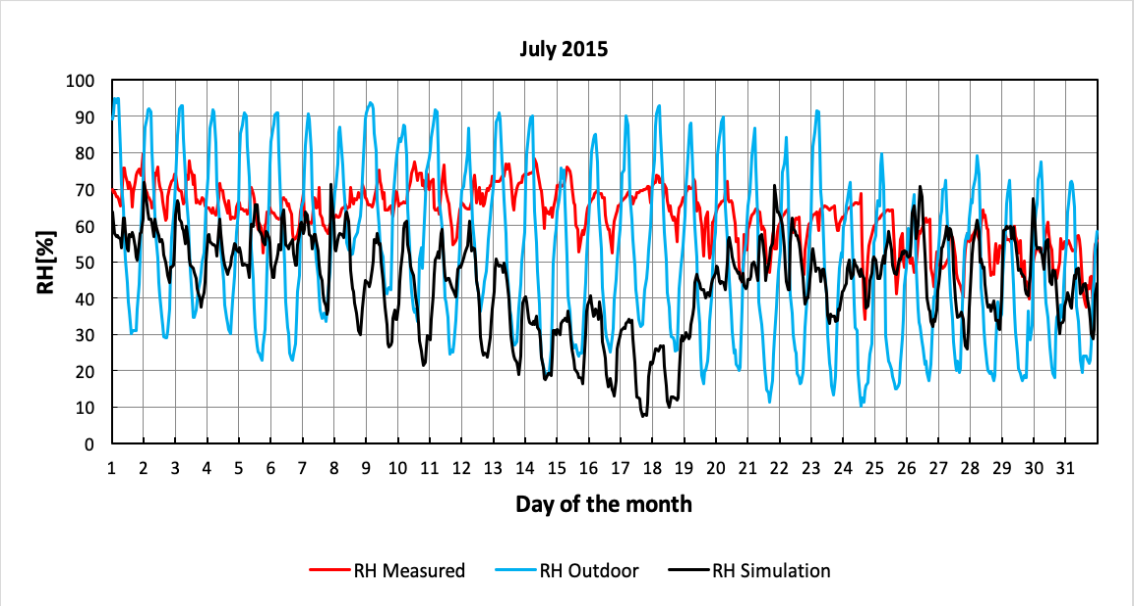

Figure 6.5. Measured, simulated indoor and outdoor relative humidity versus day of the month, July 2015

The interior relative humidity fluctuated within 20% while the outdoor relative humidity fluctuates within 60%. The interior average relative humidity mostly ranges between 60% and 80% which is close to a comfortable condition [15]. As seen on Figure 6.6 in July, indoor temperature is around 2ºC colder than the thermal comfort zone according to ASHRAE 55 with 0.75 clo, 1.0 metabolic rate (seating and sedentary activity) under 0.20m/s air velocity with ±0.5 PMV. According to the interview with the occupants during summer after hot days, the low temperature of the cave dwelling is appreciated and occupants felt comfortable with the interior thermal conditions. The rest of the summer months, June and August temperature humidity distribution charts can be seen in Figure A 7 and Figure A 8.

6.2. Fall period

November month is chosen to discuss since in October occupants were not at home instead dwelling was cared by caretaker and the schedule of the caretaker is unknown.

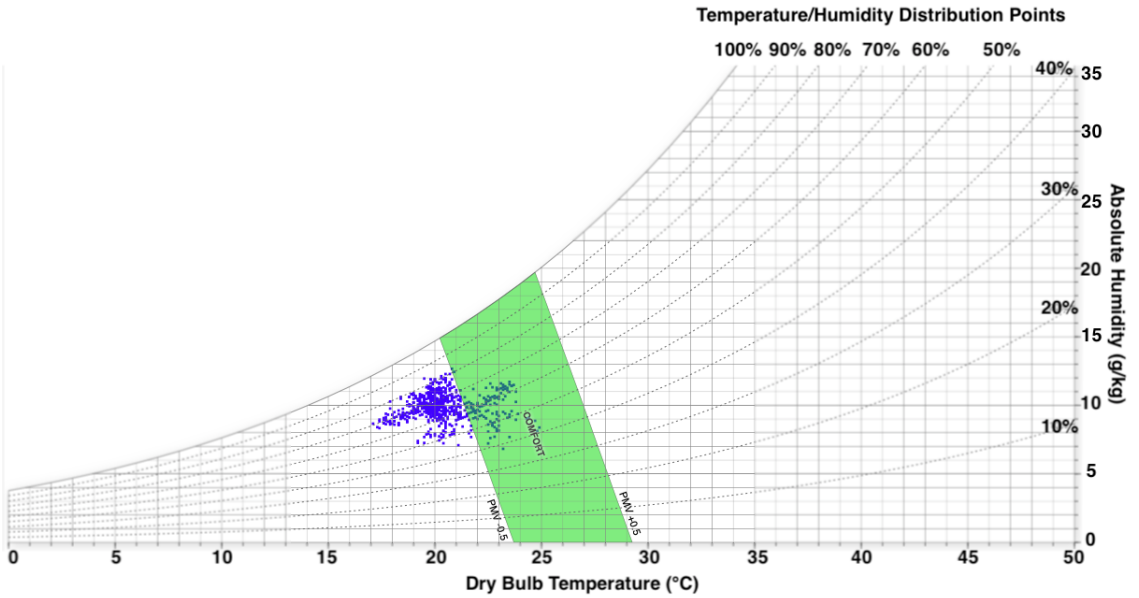

Figure 6.6. Hourly temperature, humidity distribution on psychrometric chart, July 2015 [33], (Source: [43])

During November, the wood stove was actively in use, after 18:00 the occupants started the fire and the indoor temperature rises as seen in Figure 6.7. At first part of the November month the wood stove fuel consumption was 6kg of hard wood and after 15th of November the fuel consumption increased to 8kg of hard wood. The infiltration value was 1.5ACH during the first part of the November month and after 15th of November, the infiltration value decreased to 1.0ACH. After the end of stove fire, thermal mass effect kept the indoor warm till the next day night, the temperature only fluctuated by 2°C while the outdoor fluctuated by 15°C. The interior relative humidity is very stable compare the 50% outdoor fluctuation. During the dry outdoor conditions, the tuff rock emits humid and keeps the indoor conditions stable. The rest of the fall months, September and October months daily average graphs can be seen in Figure A 11 and Figure A 12.

Measured and simulated temperatures are very similar as seen in Figure 6.8. The occupants were on holiday and the dwelling is empty between 8th and 18th of November 2015 as seen in Figure 6.8, for this period there was no activity defined on simulation. Thanks to high thermal mass the indoor temperature was settled around 17°C. After 18th of November occupants are arrived and the wood stove fuel consumption increased. September and October monthly temperature variations graphs can be seen in Figure A 11 and Figure A 12.

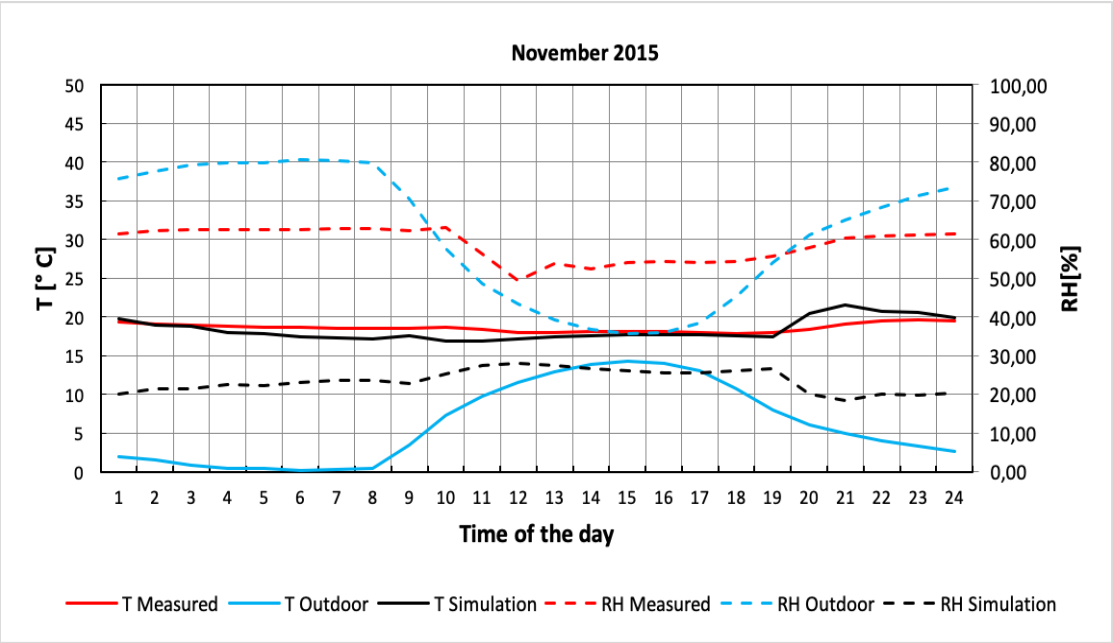

Figure 6.7. Daily Average of November 2015 [32]

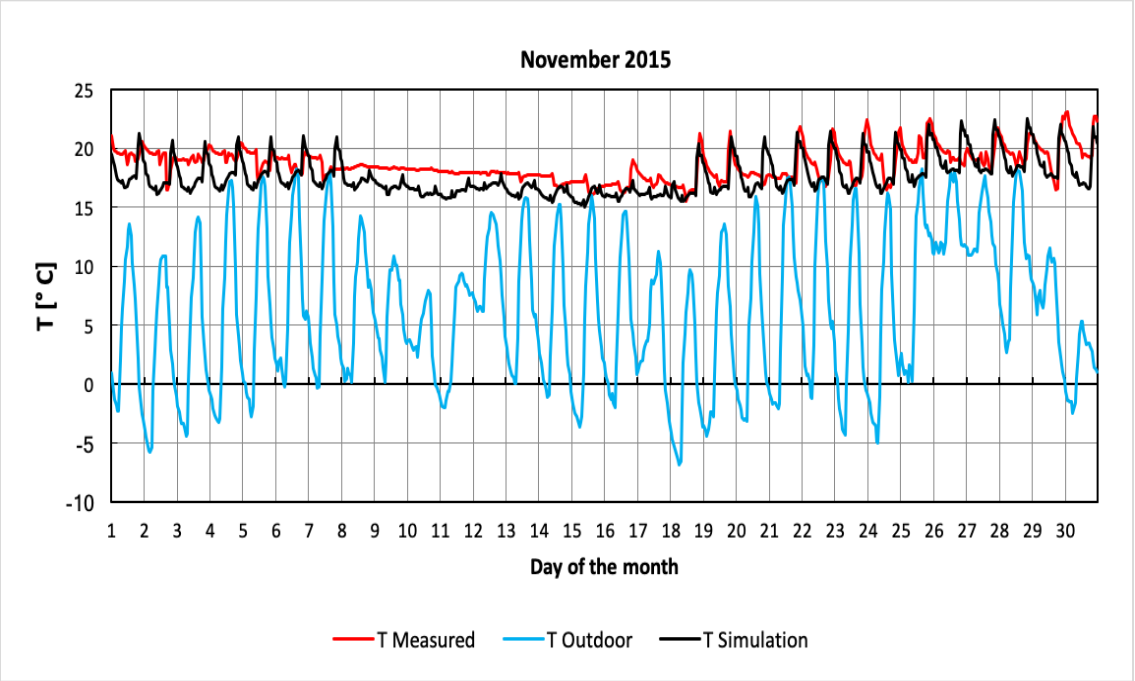

Figure 6.8.Measured, simulated interior and outdoor temperatures versus day of the month graph, November 2015

The measured relative humidity fluctuated within 20% while the outdoor fluctuated within 50%. The wood stove activity decreased the indoor humidity. The period between 8th and 18th of November while the occupants are on holiday the relative

humidity was very stable and after 18th of November when the wood stove fuel consumption increased the indoor relative humidity decreased as seen in Figure 6.9. September and October monthly relative humidity variations graphs can be seen in Figure A 13 and Figure A 14.

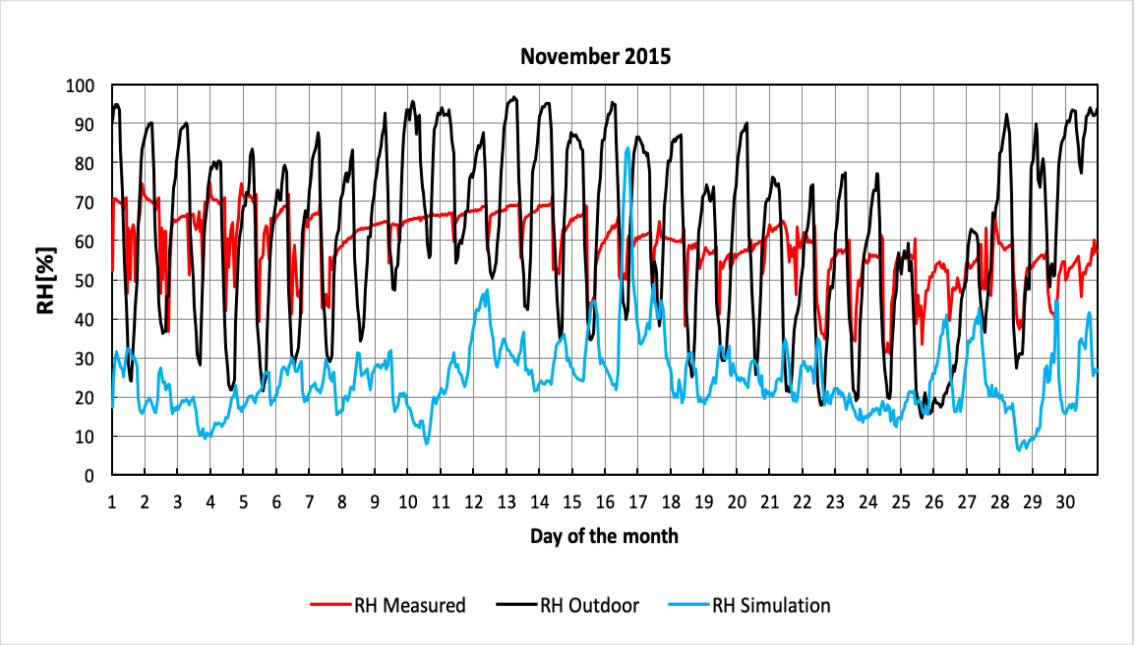

Figure 6.9.Measured, simulated indoor and outdoor relative humidity versus day of the month, November 2015

As seen on Figure 6.10 important percentage of the November month was within the thermal comfort zone according to ASHRAE 55 with 0.85 clo, 1.0 metabolic rate (seating and sedentary activity) under 0.15m/s air velocity with ±0.5 PMV. The holiday period measurements are highly effecting the results and they are out of the comfort zone. According to occupants during fall the interior of the cave dwelling was comfortable. The rest of the fall months temperature humidity distribution charts can be seen in Figure A 15, Figure A 16.

6.3. Winter Period

Under extreme winter conditions indoor winter conditions the indoor temperature was very stable and around 18ºC. As it can be seen on Figure 6.11 at 18:00 the wood stove activity started and after 24:00 the indoor temperature slowly dropped

by 2ºC thanks to the thermal mass of the cave dwelling. December and February months daily average graphs can be seen in Figure A 17 and Figure A 18.

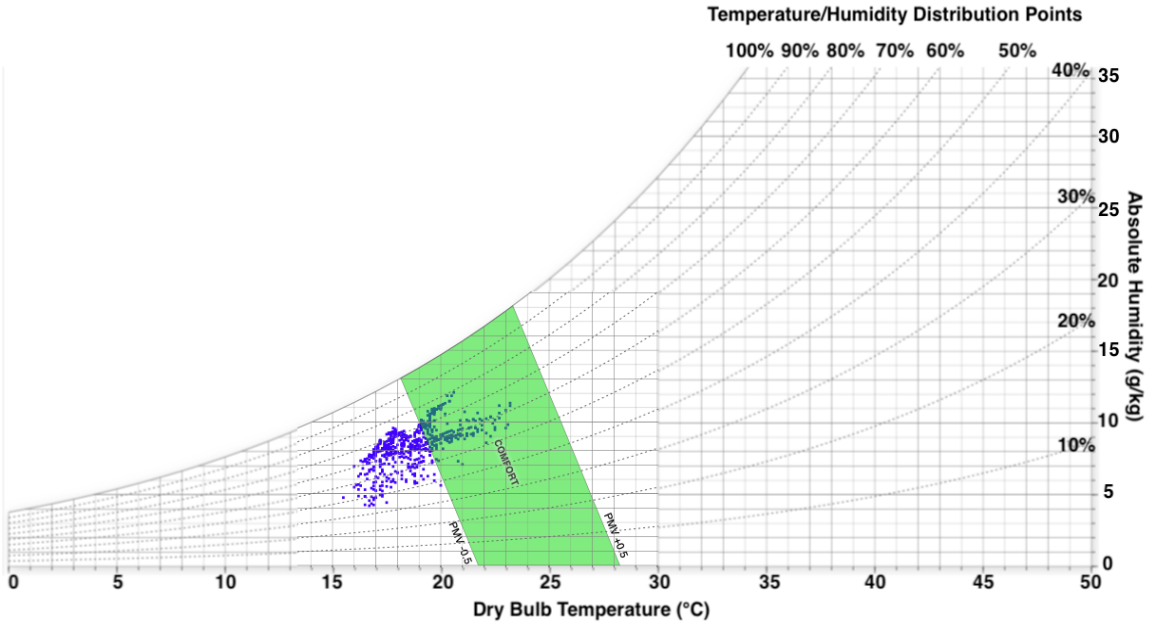

Figure 6.10 Hourly temperature, humidity distribution on psychrometric chart, November 2015 [33], (Source: [43])

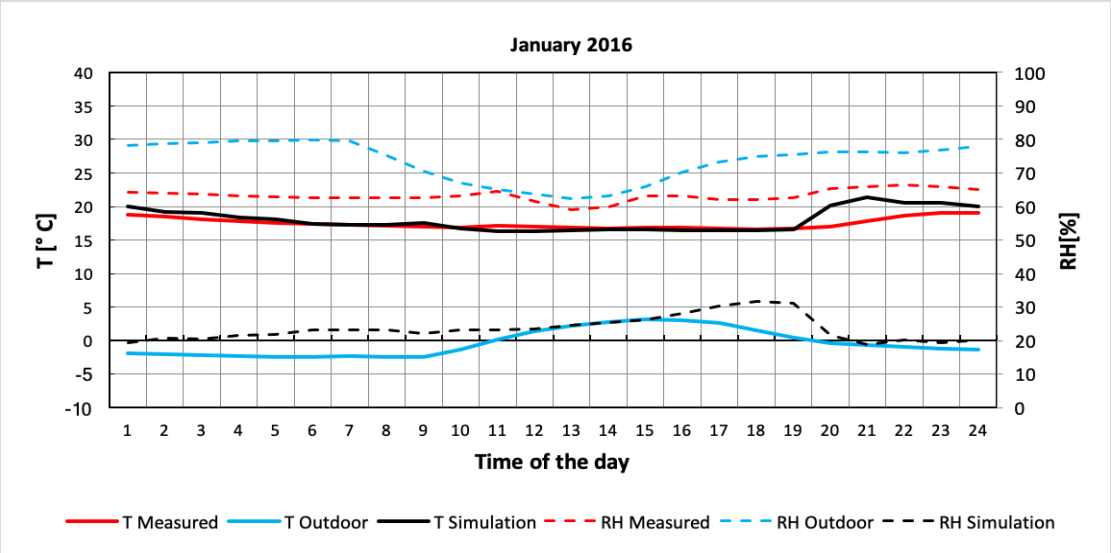

Figure 6.11 Daily Average of January 2016 [32]

While the daily outdoor maximum and minimum temperature difference was 15 ºC, the indoor temperature difference was around 2ºC as seen in Figure 6.12. The measured and simulated indoor temperature results were very similar. During whole month, the occupants were heating the dwelling every day regularly, as a result of this

the simulation results are very similar. December and February monthly temperature variations graphs can be seen in Figure A 19 and Figure A 20.

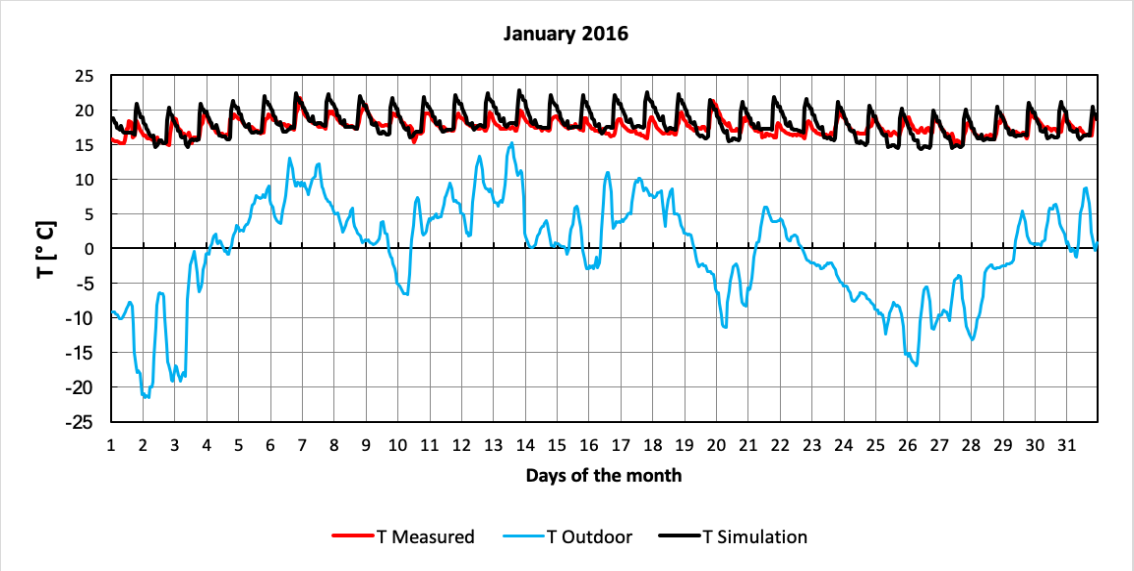

Figure 6.12 Measured, simulated interior and outdoor temperatures versus day of the month graph, January 2016

While the outdoor relative humidity is fluctuated between 90% and 50% relative humidity the indoor relative humidity fluctuated between 60% and 70% as seen in Figure 6.13. The simulation relative humidity values are very low compare to the actual measurements. The reason for that is the wood stove activity, the porous characteristic of the tuff and the boiling water on top of wood stove. December and February monthly relative humidity variations graphs can be seen in Figure A 21 and Figure A 22.

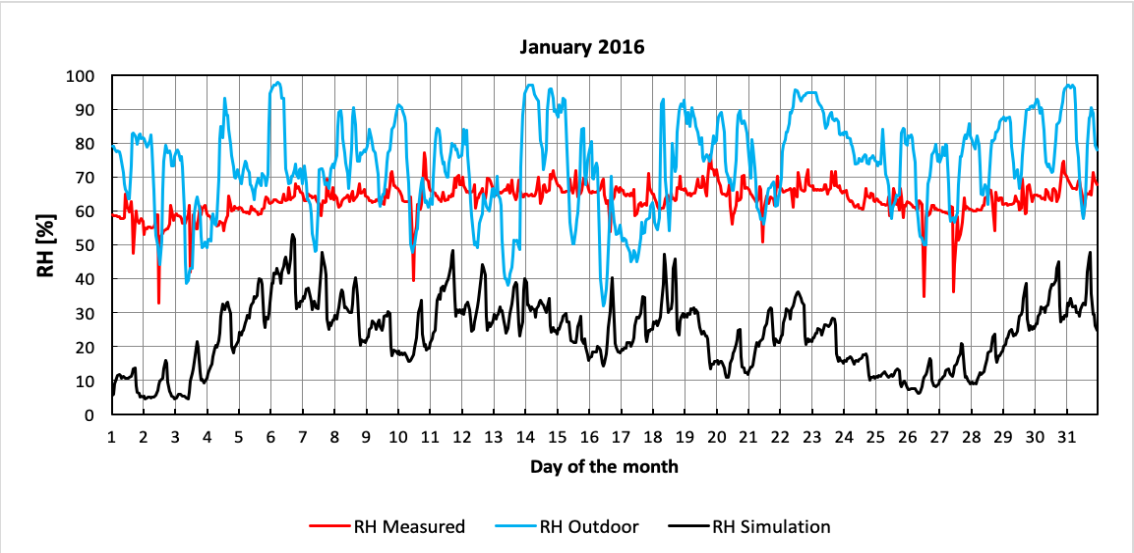

Figure 6.13 Measured, simulated indoor and outdoor relative humidity versus day of the month, January 2016

As seen on Figure 6.14 important percentage of the January month is within the thermal comfort zone according to ASHRAE 55 with 1.0 clo, 1.0 metabolic rate (seating and sedentary activity) under 0.10m/s air velocity with ±0.5 PMV. According to occupants some days in winter were very cold in the dwelling. Other than those days the dwelling was comfortable. The rest of the winter months temperature humidity distribution charts can be seen in Figure A 23, Figure A 24.

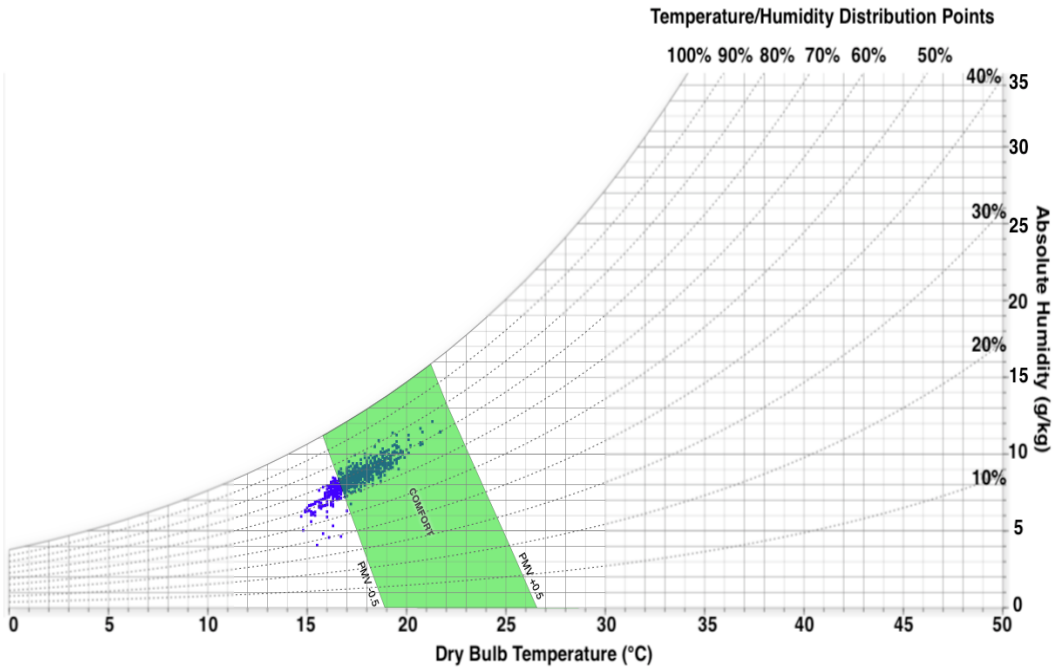

Figure 6.14. Hourly temperature, humidity distribution on psychrometric chart, January 2016 [33], (Source: [43])

6.4. Spring Period

As seen in Figure 6.15 the wood stove activity is started around 19:00 and lasted after midnight. The amount of the heat gained from the wood stove is decreased compare to winter. March and May months daily average graphs can be seen in Figure A 25 and Figure A 26.

While the daily outdoor maximum and minimum temperature difference was 15 ºC, the indoor temperature difference was around 2ºC as seen in Figure 6.16. The measured and simulated temperature results are very similar as seen in However, with the increase of the outdoor temperature in the end of the month the wood stove activity was irregular. March and May monthly temperature variations graphs can be seen in Figure A 27 and Figure A 28.

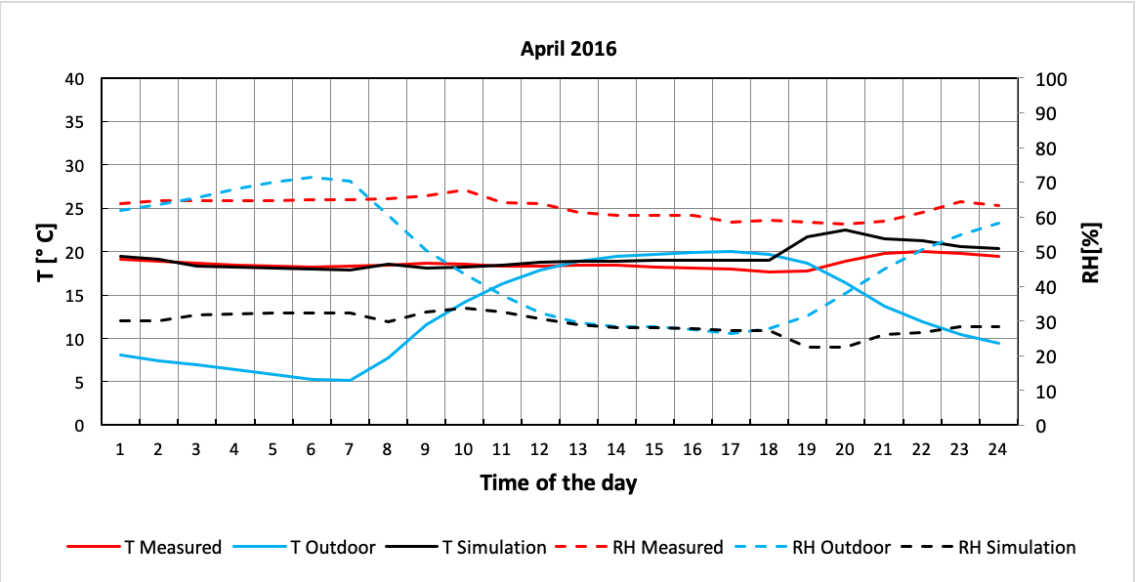

Figure 6.15. Daily Average of January 2016 [32]

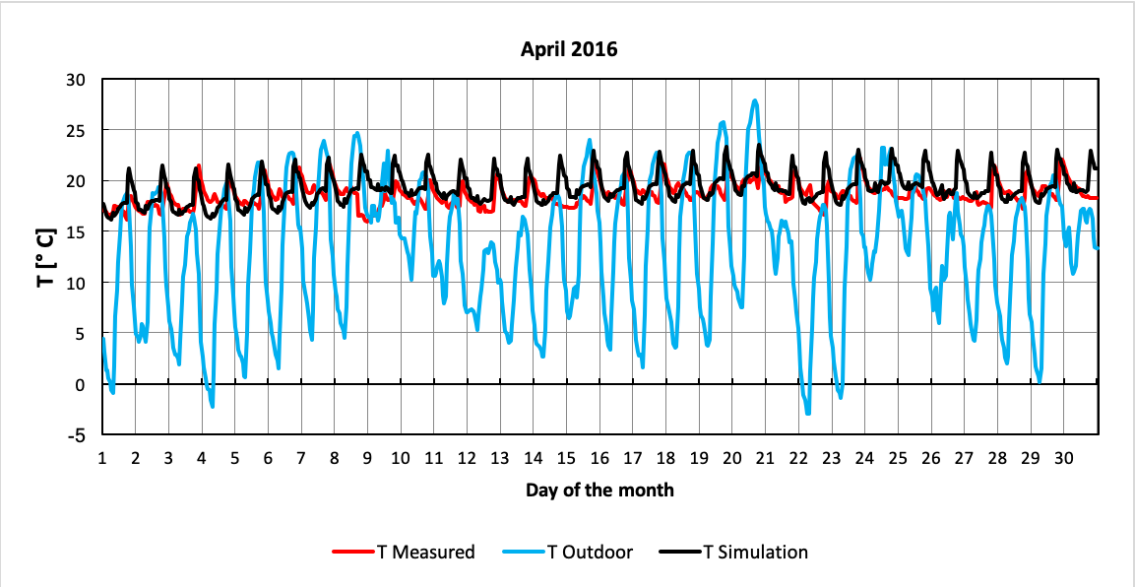

Figure 6.16. Measured, simulated interior and outdoor temperatures versus day of the month graph, April 2016

The indoor relative humidity is mainly fluctuated between 50% and 70% while the outdoor fluctuated between 20% and %80 as seen in Figure 6.17. The porous characteristics of the tuff kept the indoor humid while the outdoor was dry. The simulation results are much lower than the outdoor relative humidity because of the wood stove activity. March and May monthly relative humidity variations graphs can be seen in Figure A 29 and Figure A 30.

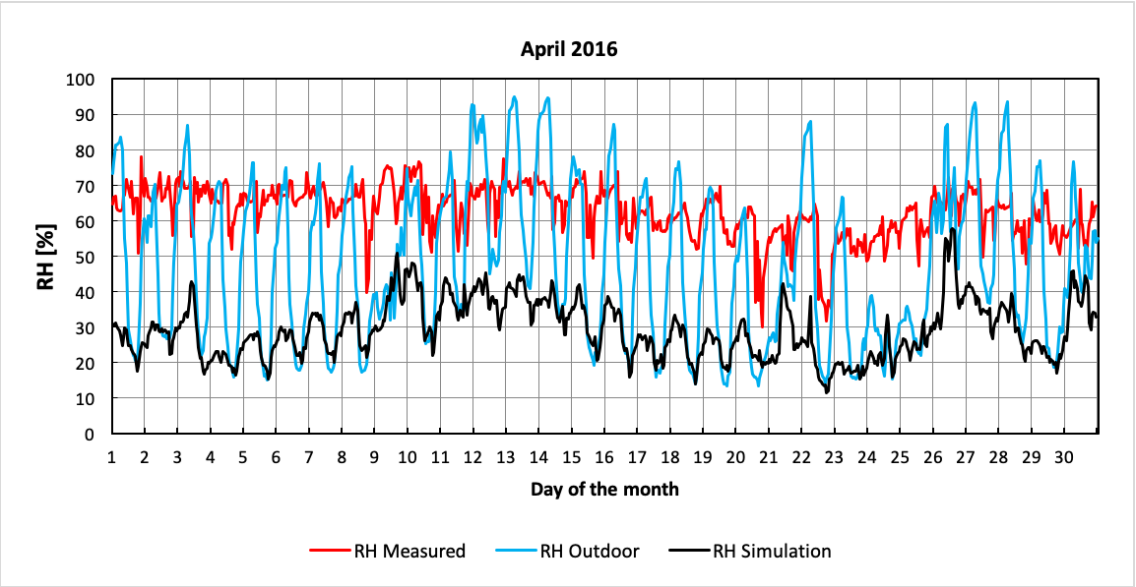

Figure 6.17. Measured, simulated interior and outdoor relative humidity versus day of the month graph, January 2016

As seen on Figure 6.18 important percentage of the April month is within the thermal comfort zone according to ASHRAE 55 with 0.85 clo, 1.0 metabolic rate (seating and sedentary activity) under 0.15m/s air velocity with ±0.5 PMV. According to occupants during spring the interior of the cave dwelling was comfortable. The rest of the spring months temperature humidity distribution charts can be seen in Figure A 31, Figure A 32.

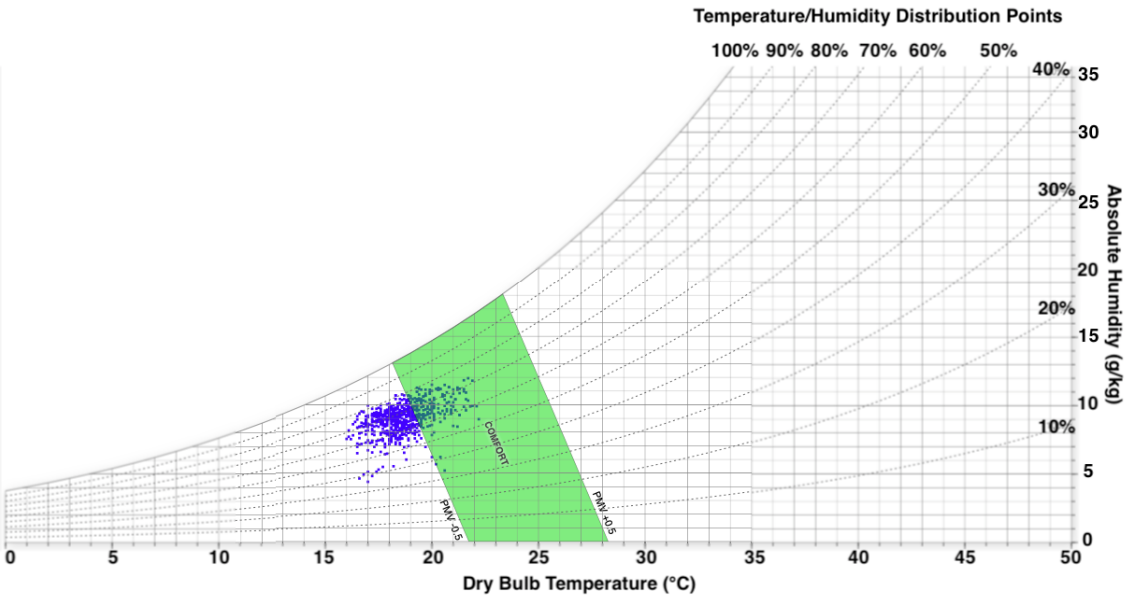

Figure 6.18.Hourly temperature, humidity distribution on psychrometric chart, April 2016 [33], (Source: [43])

CHAPTER 7

CONCLUSIONS

The main objective of this research is to monitor and simulate the thermal analysis of a Cappadocian cave dwelling carved into a fairy chimney. The research started with placing the data loggers into the cave dwelling to observe the interior temperature and relative humidity fluctuations. The measurements took place between June 2015 and June 2016. Data were collected in 20 seconds intervals. Climate data from State Meteorology was collected to investigate the effects of climate on the interior conditions during the same measurement period. The analysis indicated that interior of the cave dwelling was thermally comfortable even while extreme summer and winter weather conditions existed outside, owing to the thermal mass properties of the fairy chimney.

The second part of the research consisted of a thermal analysis of the cave dwelling using a computer simulation. Boundary conditions and limitations of the cave dwelling were defined. The thermal conductivity, specific heat and density of the main material, volcanic tuff rock, were measured. These parameters were entered into the simulation model. Then the calibration of the simulation process took place. The temperature result of the simulation is within the calibration limits. However, the relative humidity result of the simulation is not calibrated. The porous characteristics of the tuff material regulates and stabilizes the indoor humidity under extreme outdoor conditions and wood stove activity. The simulation results are highly effected from the wood stove activity while the measured results are effected from the boiling water on top of the wood stove and the porous characteristics of the tuff rock. When the wood stove is active it is observed that the simulation results are fluctuated at the lowest boundaries of the outdoor relative humidity.

The analysis shows that the massive rock-cut walls delay the heat transfer. In summer, the cave dwelling gains heat very slowly owing to the thermal mass and in winter the massive structure slowly loses the heat gained during the summer. The thermal behaviour of the dwelling is a more seasonal pattern than a daily pattern because the daily temperature differences are not able to change the cave dwelling's core temperature. The massive structure of the cave dwelling has an important role in

providing high thermal comfort since the internal temperature and relative humidity are very consistent during the year. The dwelling's thermal conditions are satisfactory to the occupants. During the coldest days, average fuel consumption by the wood stove is only 8kg per day, a very small amount considering the dramatic temperature changes during the day.

During site visits, it is observed that Cappadocia attracts people from all over the world with its unique landscape and ancient cultures. The organic animal breeding and agriculture are widespread across Cappadocia. Many of those people abandoned their ordinary lifestyle and moved to Cappadocia to live simple, healthy and sustainable lifestyle.

Future activities can further the work of this thesis. Another data logger can be placed at the exterior of the cave dwelling to improve the outdoor climate data by filling in missing data. The solar radiation data can be evaluated. The characteristics of the tuff rock can be analysed in detailed and understood to better simulate the relative humidity fluctuations. An extended thermal analysis of the simulation can be done by using a 3D virtual model such as ANSYS Fluent or COMSOL Multiphysics modelling software.

CHAPTER 8

REFERENCES

[1] UN Environment. "Sustainable Buildings". [Online]. Available: https://www.unenvironment.org/explore-topics/resource-efficiency/what-we-do/cities/sustainable-buildings [Accessed: March 9, 2019].

[2] UN Environment. "City activities". [Online]. Available: https://www.unenvironment.org/explore-topics/resource-efficiency/what-we-do/cities/city-activities [Accessed: March 9, 2019].

[3] F. Solmaz Sakar and N. Sahin Güçhan, "A unique example of vernacular construction in Anatolia: The construction technique in traditional Cappadocia houses", *9th International Conference on Structural Analysis of Historical Constructions*, 2014.

[4] J.N. Hait, "Passive Annual Heat Storage: Improving the Design of Earth Shelters", *USA Rocky Mountain Research Centre*, 1983.

[5] S.A. Alkaff, S.C. Sim, MN. Ervina Efzan, "A review of underground building towards thermal energy efficiency and sustainable development", *Renewable and Sustainable Energy Review*, vol. 60, 2016, 692 – 713

[6] N. Engin, N. Vural, M.R. Sumerkan, "Climatic effect in the formation of vernacular houses in the Eastern Black Sea region", *Building and Environment*, vol. 42, 2007, 960 – 969

[7] M. K. Singh, S. Mahaptra, S.K: Atreya, "Bioclimatism and vernacular architecture of north-east India", *Building and Environment*, vol. 44, 2009, 878-888

[8] Ö. Karakul, "Discovering the ecological principles of traditional architecture: Cappadocia Region", *Sustainable Housing 2016*, Proceedings of the International Conference on Sustainable Housing Planning, Management and Usability, 2016, 67 – 73

[9] A. Gagliano, F. Patania, F. Nocera, C. Signorello, "Assesment of the thermal performance of massive buildings", *Energy and Buildings*, vol. 72, 2014, 361-370.

[10] D.M. Ogoli, "Predicting indoor temperatures in closed buildings with high thermal mass", *Energy and Buildings*, vol. 25, 2003, 851 – 862.

[11] S.V. Szokolay, "Introduction to Architectural Science: The basis of sustainable design", chapter 1, Elsevier Science, 2004.

[12] Stefano Cammelli, Sergey Mijorski, "Stack effect in high-rise buildings", I*nternational Journal of High-Rise Buildings, vol.5, 2016.*

[13] Manuel Correia Guedes, "Sustainable Architecture in Africa", *Sustainability Energy and Architecture, 2013, 421-503.*

[14] F. Nicol, M. Humphreys, S. Roaf, "Adaptive Thermal Comfort: Principles and Practice", chapter 1, Routledge, 2012.

[15] ANSI/ASHRAE Standard 55-2010. [Online]. Available: http://arco-hvac.ir/wp-content/uploads/2015/11/ASHRAE-55-2010.pdf [Accessed: February 25, 2019].

[16] P. Wolkoff, S.K. Kjaergaard, "The dichotomy of relative humidity on indoor air quality", *Environment International*, vol. 33, 2007, 850 – 857.

[17] T. Tassiopoulou, P.C. Grindley, S.D. Porbert, "Thermal Behaviour of an Eighteenth-Century Athenian Dwelling", *Applied Energy*, vol. 53, 1996, 383 – 398.

[18] M.S. Sözen and G.Z. Gedik, "Evaluation of traditional architecture in terms of building physics: Old Diyarbakır houses", *Building and Environment*, vol. 42, 2007, 1810 – 1816.

[19] T. Başaran, "Thermal Analysis of the Domed Vernacular Houses of Harran, Turkey", *Indoor and Built Environment*, vol. 20, 2001, 5:543-554.

[20] T. Başaran, "A traditional example from Anatolia for energy efficient sustainable buildings: thermal analysis of domed houses of Harran" *10th Rehva World Congress, Sustainable Energy in Buildings, 2010.*

[21] Ö. Aydan, R. Ulusay. "Geotechnical and geoenvironmental characteristics of man-made underground structures in Cappadocia, Turkey", *Engineering Geology*, vol. 69, 2003, 245 – 272.

[22] T. Başaran and S. Kaya, "Efes'teki Peristil Bir Evin Isıl Davranışı" *International Ecological Architecture and Planning Symposium*, 2009.

[23] Jie Deng, Runming Yao, Wei Yu, Qiulei Zhang, Baizhan Li, "Effectiveness of the thermal mass of external walls on residential buildings for part-time part-space heating and cooling using the state-space method", *Energy and Buildings*, 2019.

[24] Turgay Coşkun, "Modelling Indoor Climate of Historic Libraries for Preventive Conservation of Paper Based Collections", Master's Thesis, Izmir Institute of Technology, Izmir, 2016.

[25] UNESCO United Nations Educational, Scientific and Cultural Organization. "Göreme National Park and the Rock Sites of Cappadocia". [Online]. Available: https://whc.unesco.org/en/list/357/ [Accessed: February 23, 2019].

[26] Copernicus Sentinel 2a data, "L1C_T36SXH_A017178_20181006T082824", processed by ESA. [Online]. Available: https://earthexplorer.usgs.gov/ [Accessed: March 10, 2019].

[27] General Command of Mapping Turkey, "Administrative Divisions dataset", [Online]. Available: https://data.humdata.org/dataset/turkey-administrative-boundaries-levels-0-1-2 [Accessed: March 10, 2019].

[28] J.-L. Le Pennec, J.-L. Bourdier, J.-L. Froger, A. Temel, G. Camus, A. Gourgaud, "Neogene ignimbrites of the Nevsehir Plateau (Central Turkey), stratigraphy, distribution and source constraints", Journal of Volcanology and Geothermal Research, vol. 63, 1994, 59–87.

[29] M.A. Sarikaya, A. Ciner, M. Zreda, "Fairy chimney erosion rates on Cappadocia ignimbrites, Turkey: Insights from cosmogenic nuclides", *Geomorphology*, vol. 234, 2015, 182 – 191.

[30] Trotec "BL30 Operating Manual". [Online]. Available: https://uk.trotec.com/fileadmin/downloads/Messgeraete/Klima/BL30/TRO-TR-BA-BL30-HS-002-INT-web.pdf [Accessed: February 24, 2019].

[31] Kyoto "QTM 500 Operating Manual". [Online]. Available: http://www.kyoto-kem.com/en/pdf/catalog/QTM-500.pdf

[32] State Meterological Station, Records for Weather Data, Turkey, Ürgüp, 2015-2016.

[33] ASHRAE Guideline 14, "Measurement of Energy and Demand Savings", 2002

[34] Takeyoshi Kato, "Integration of Disturbuted Energy Resources in Power Systems", 2016.

[35] R. See, P. Haves, P. Sreekanthan, J. O'Donnell, M. Basarkar, K. Settlemyre, "Development of a user interface for the EnergyPlus whole building energy simulation program", *Proceedings of the 12th International IBPSA Conference*, Sydney, 2011.

[36] Rick Curkeet, "Wood Combustion Basics". [Online]. Available: https://is.muni.cz/el/1423/podzim2013/MEB423/um/Wood_Lesson_02.pdf [Accessed: August 2,2019].

[37] Frank Wuttke, Sebastian Bauer, Marcelo Sanchez, "Energy Geotechnics: *Proceedings of the 1st international conference on Energy Geotechnics, ICEGT*, Kiel, Germany, 2016.

[38] Vestel Beyaz Eşya, "Vestel CM 7610 Teknik Bilgiler", Available: https://www.vestel.com.tr/vestel-cm-7610-camasir-makinesi [Accessed August 2, 2019].

[39] Vestel Beyaz Eşya, Vestel BM 511 Teknik Bilgiler", https://www.vestel.com.tr/vestel-bm-511-bulasik-makinesi [Accessed August 2, 2019].

[40] Vestel Beyaz Eşya, "Vestel NFY 620 Teknik Bilgiler" https://www.vestel.com.tr/vestel-akilli-nfy620-p [Accessed August 2, 2019].

[41] Vestel Beyaz Eşya, "Vestel TLS 80 Teknik Bilgiler" https://www.vestel.com.tr/vestel-tls80-m-mekanik-termosifon [Accessed August 2, 2019].

[42] LPG gas conversions. [Online]. Available: https://www.elgas.com.au/blog/389-lpg-conversions-kg-litres-mj-kwh-and-m3

[43] Psychrometric Chart. [Online]. Available: https://drajmarsh.bitbucket.io/psychro-chart2d.html

APPENDIX A

MONTHLY VARIATIONS IN THE CAVE DWELLING

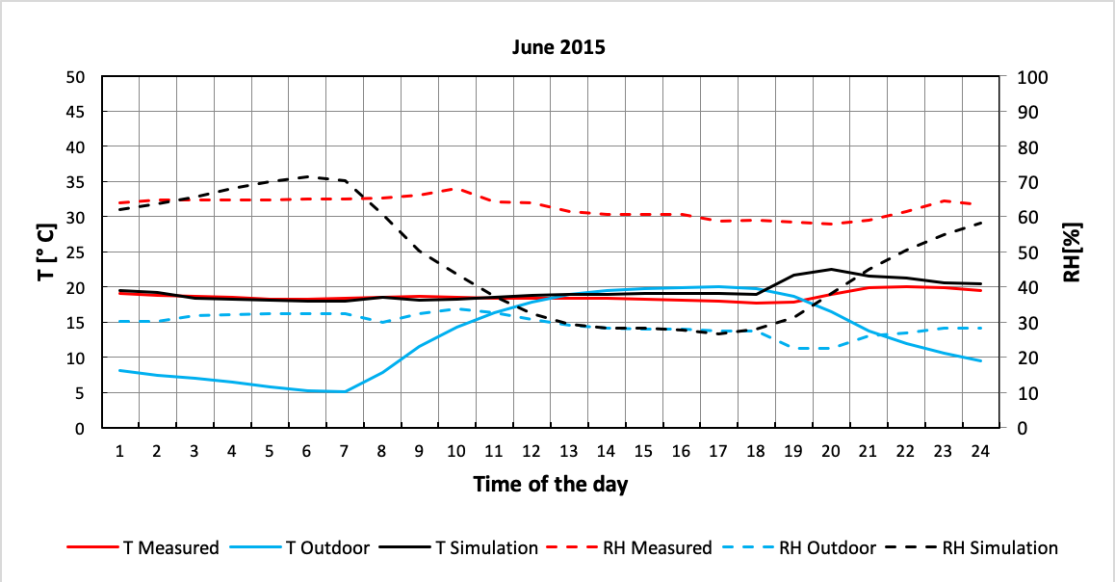

Figure A 1. Daily average of June 2015 [32]

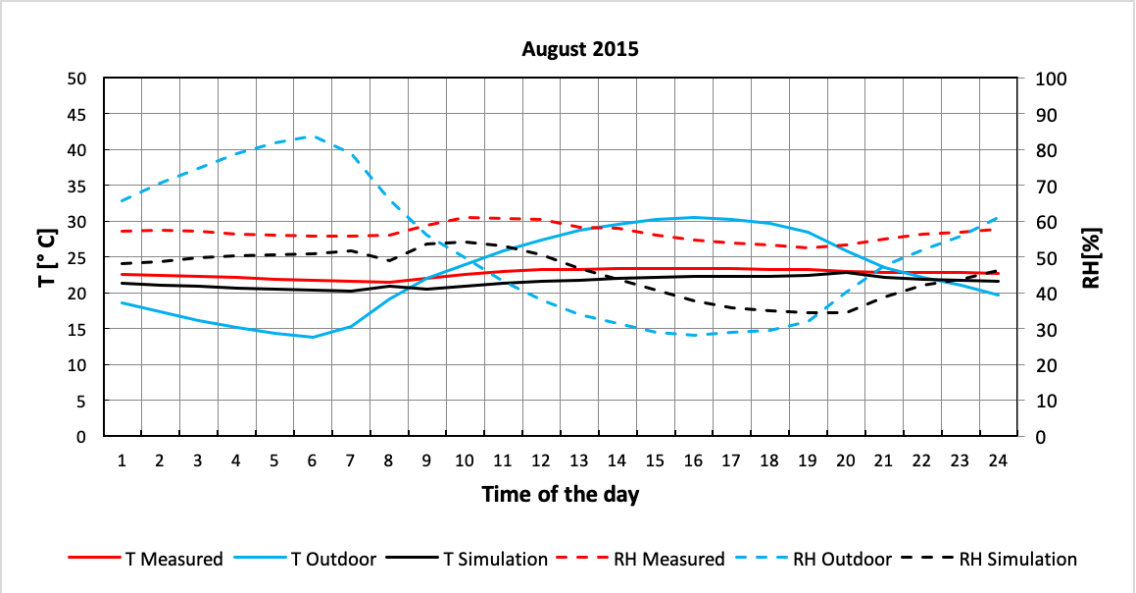

Figure A 2. Daily average of August 2015 [32]

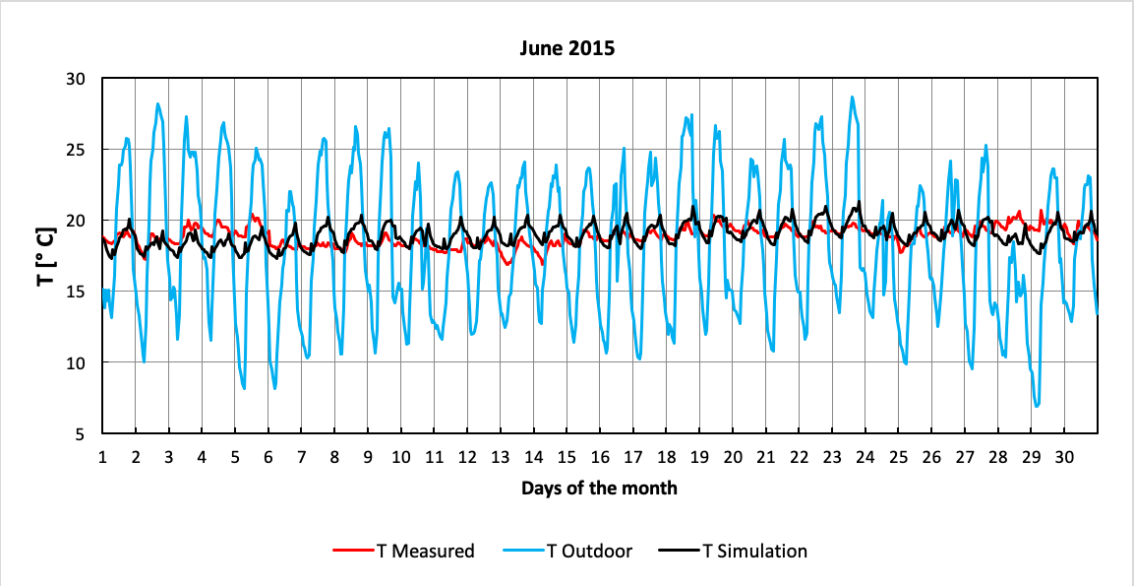

Figure A 3. Measured, simulated interior and outdoor temperatures versus day of the month graph, June 2015

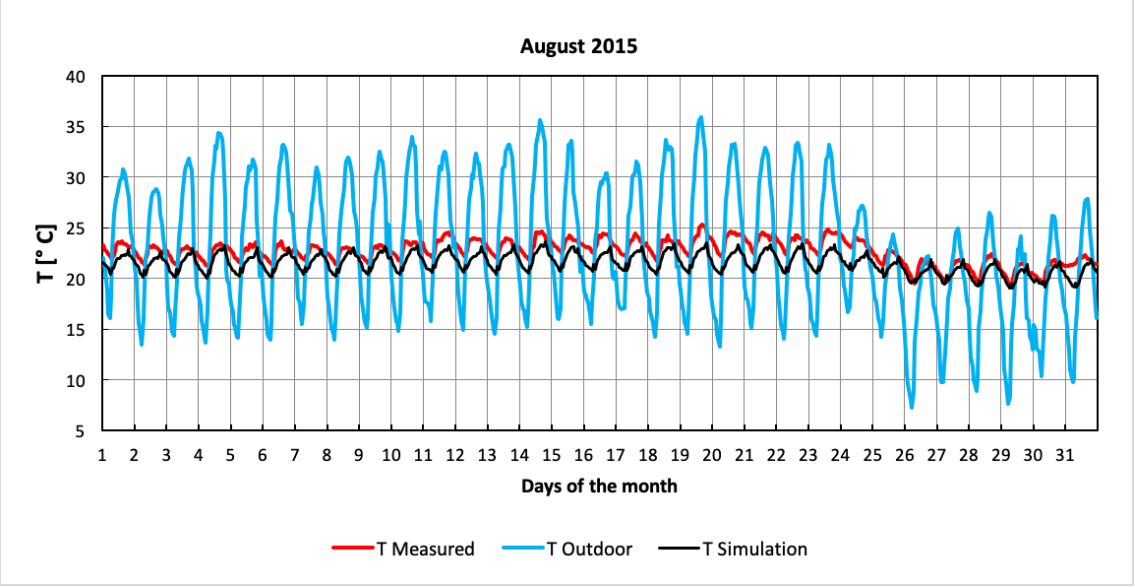

Figure A 4. Measured, simulated interior and outdoor temperatures versus day of the month graph, August 2015

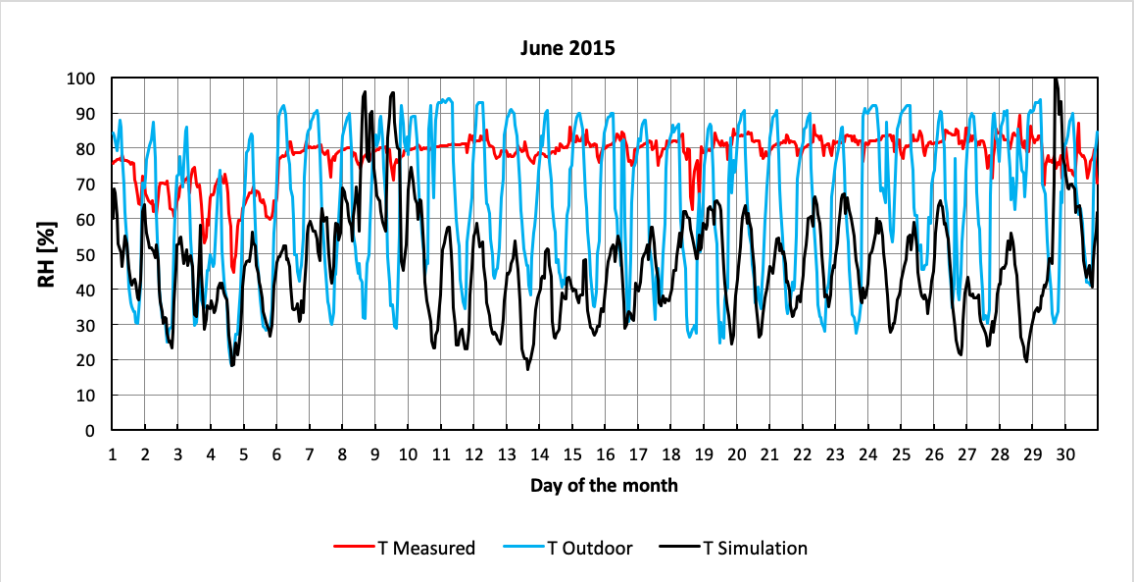

Figure A 5. Measured, simulated interior and outdoor relative humidity versus day of the month graph, June 2015

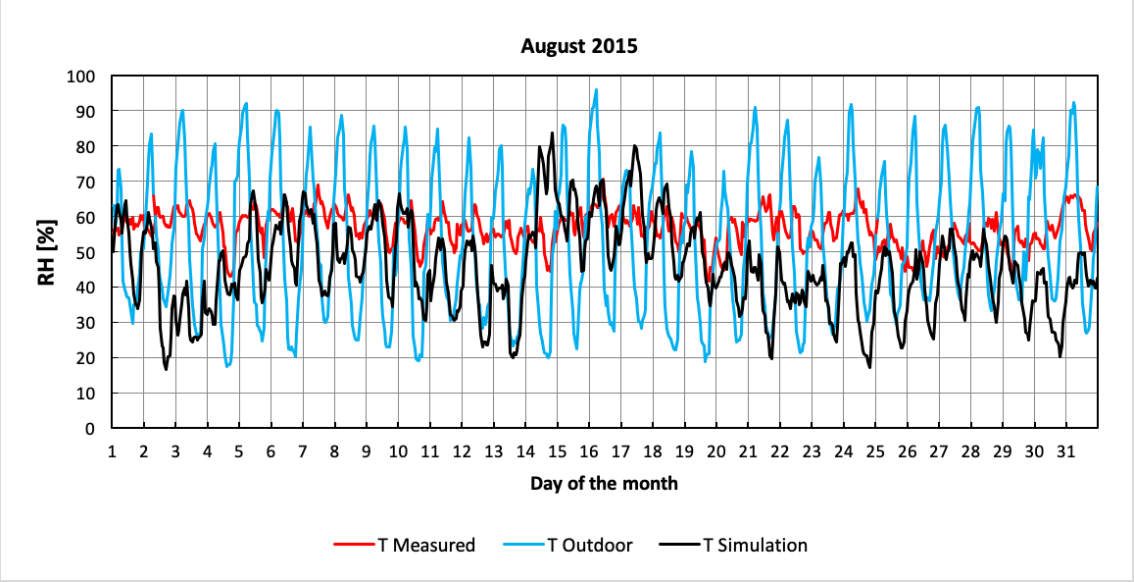

Figure A 6. Measured, simulated interior and outdoor relative humidity versus day of the month graph, August 2015

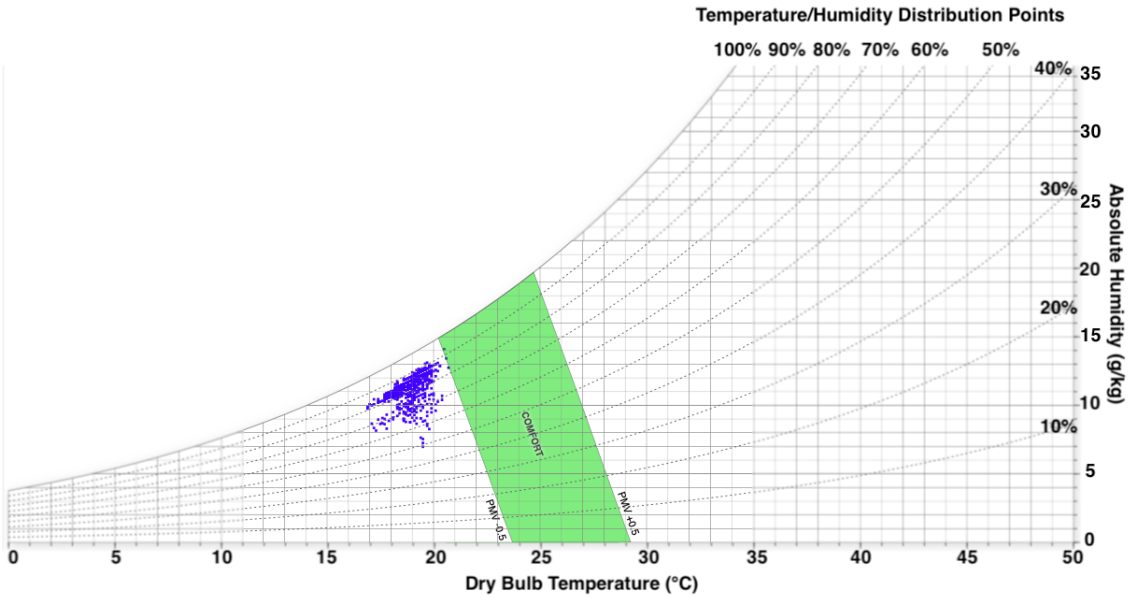

Figure A 7. Hourly temperature, humidity distribution on psychrometric chart, June 2015 [33], (Source: [43])

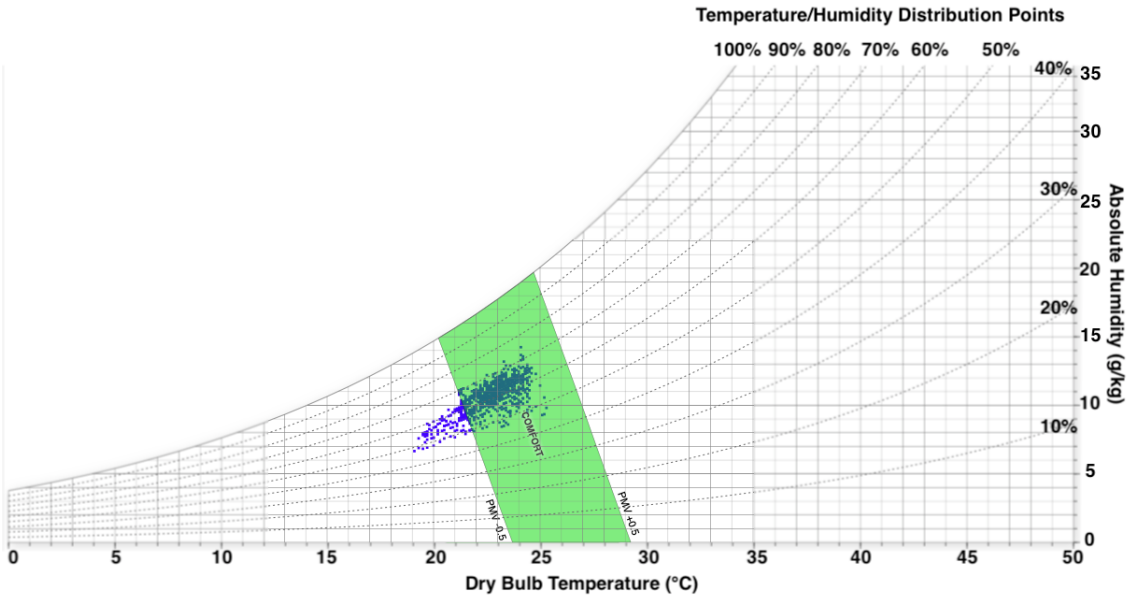

Figure A 8. Hourly temperature, humidity distribution on psychrometric chart, August 2015 [33], (Source: [43])

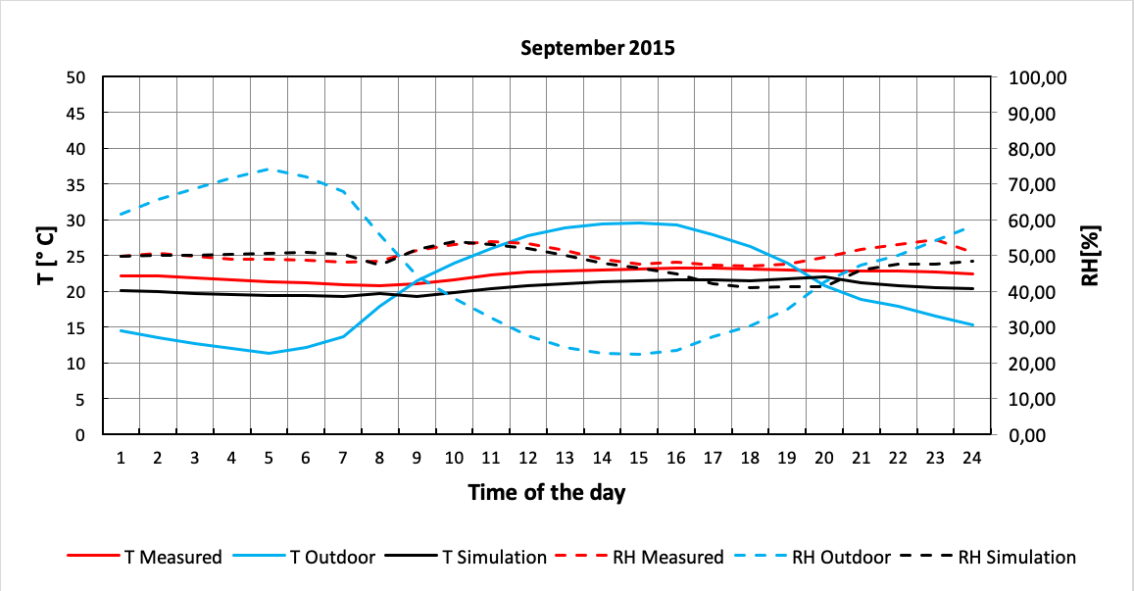

Figure A 9. Daily average of September 2015 [32]

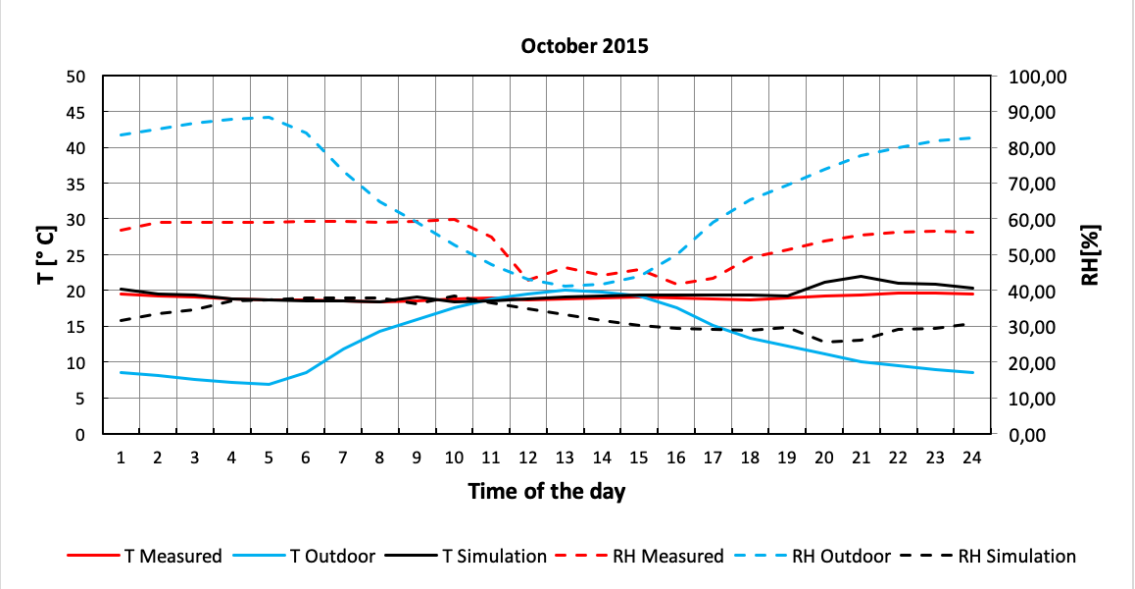

Figure A 10. Daily average of October 2015 [32]

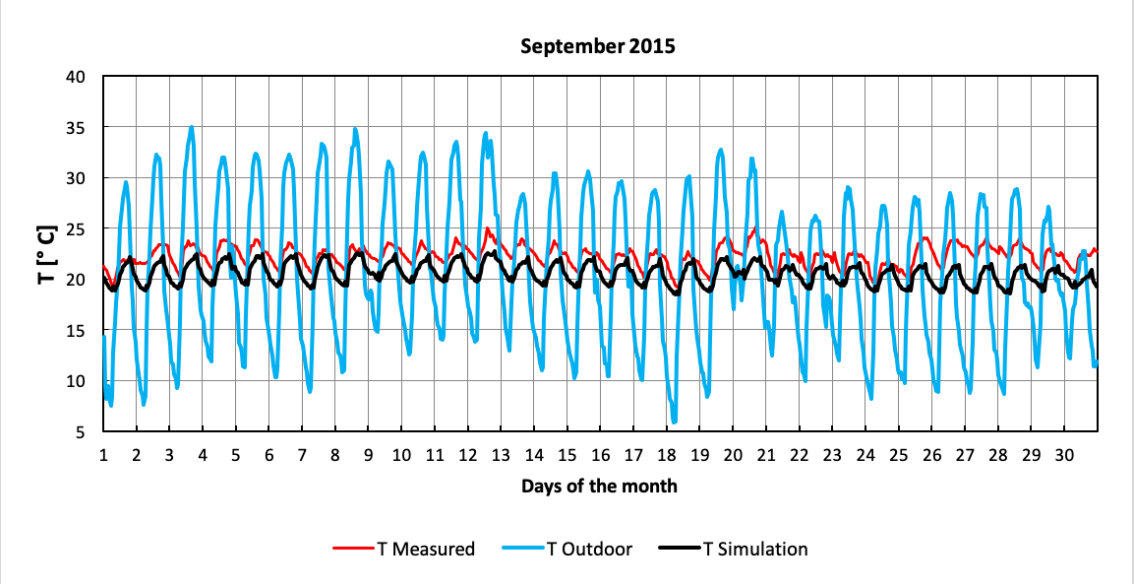

Figure A 11. Measured, simulated interior and outdoor temperatures versus day of the month graph, September 2015

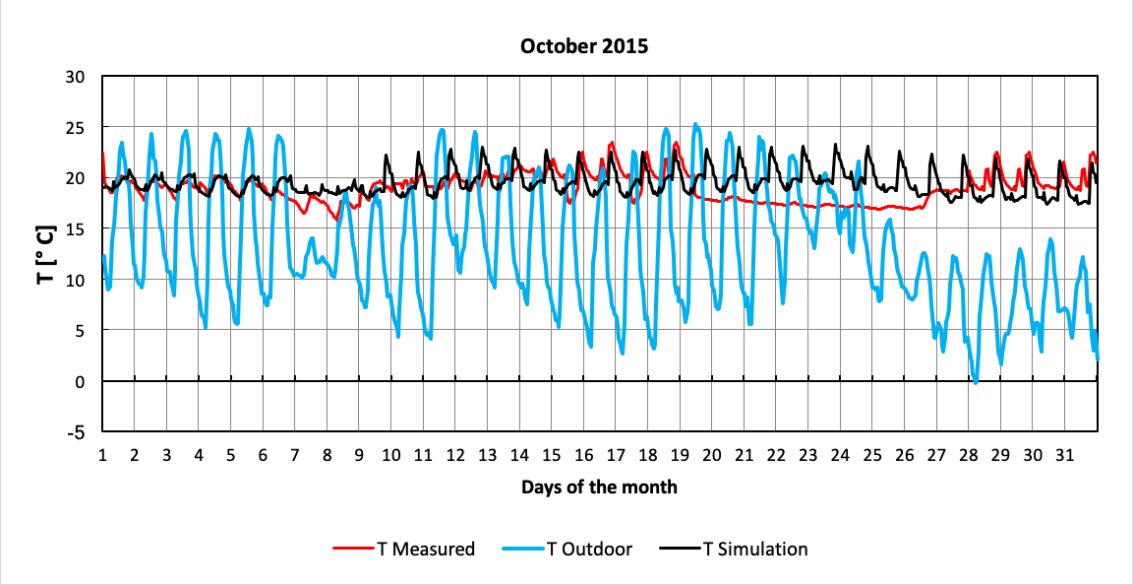

Figure A 12. Measured, simulated interior and outdoor temperatures versus day of the month graph, October 2015

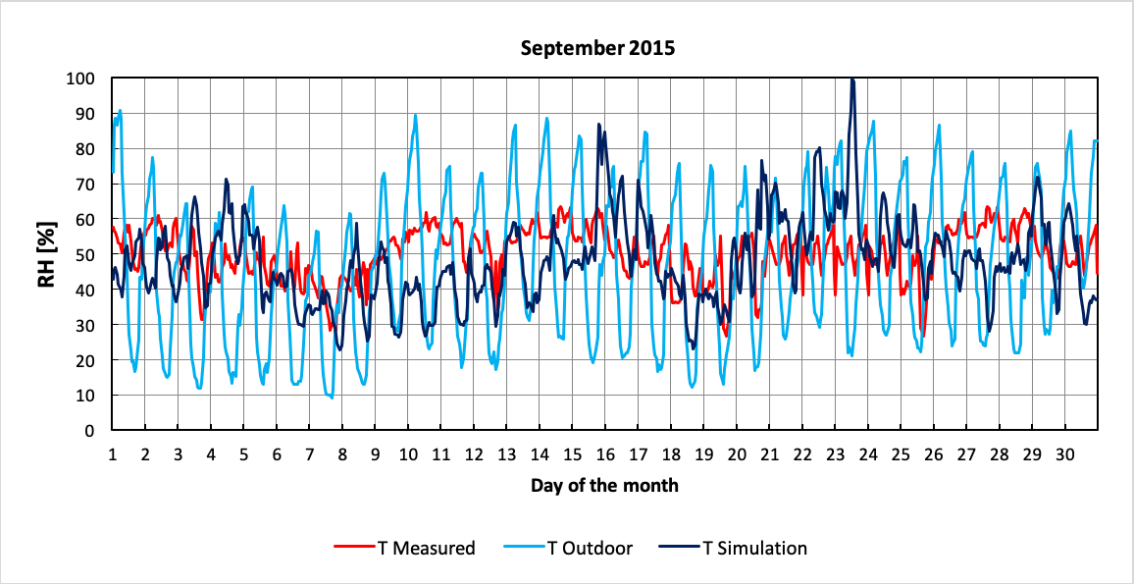

Figure A 13. Measured, simulated interior and outdoor relative humidity versus day of the month graph, September 2015

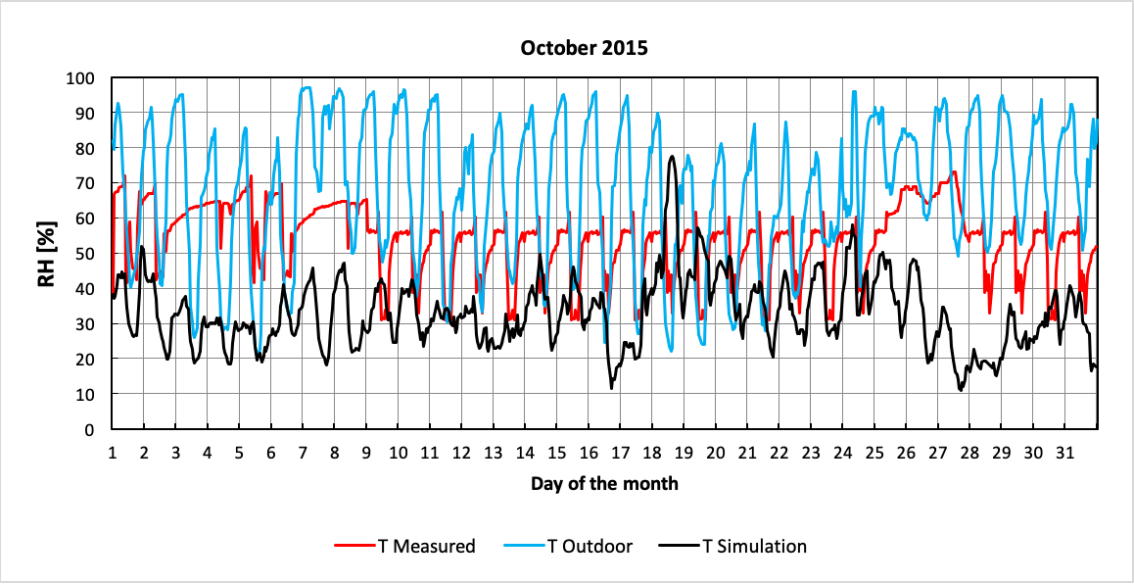

Figure A 14. Measured, simulated interior and outdoor relative humidity versus day of the month graph, October 2015

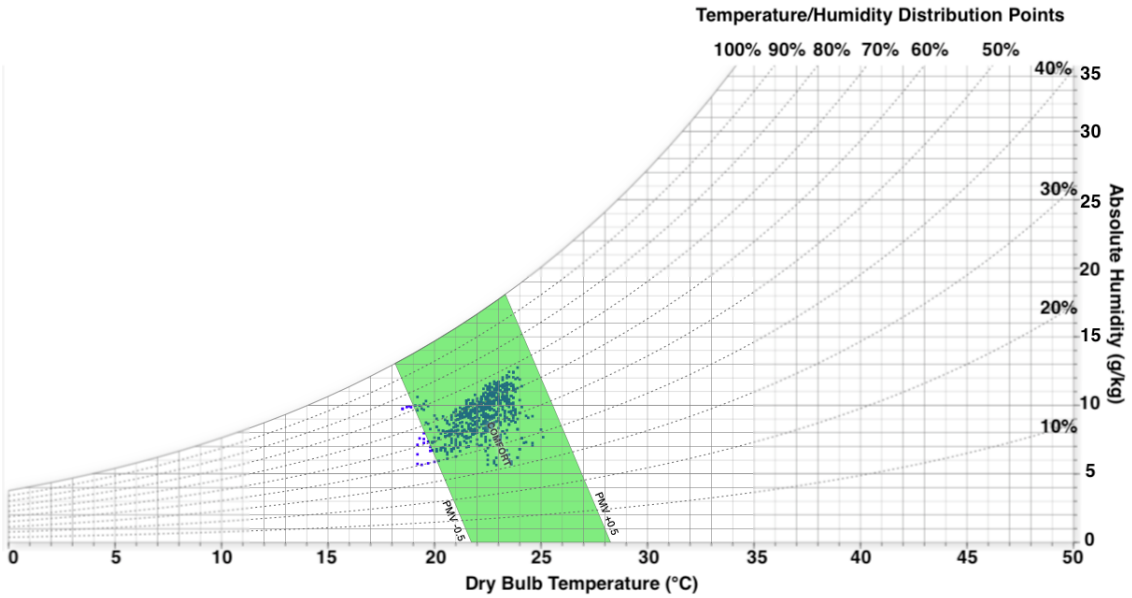

Figure A 15. Hourly temperature, humidity distribution on psychrometric chart, September 2015 [33], (Source: [43])

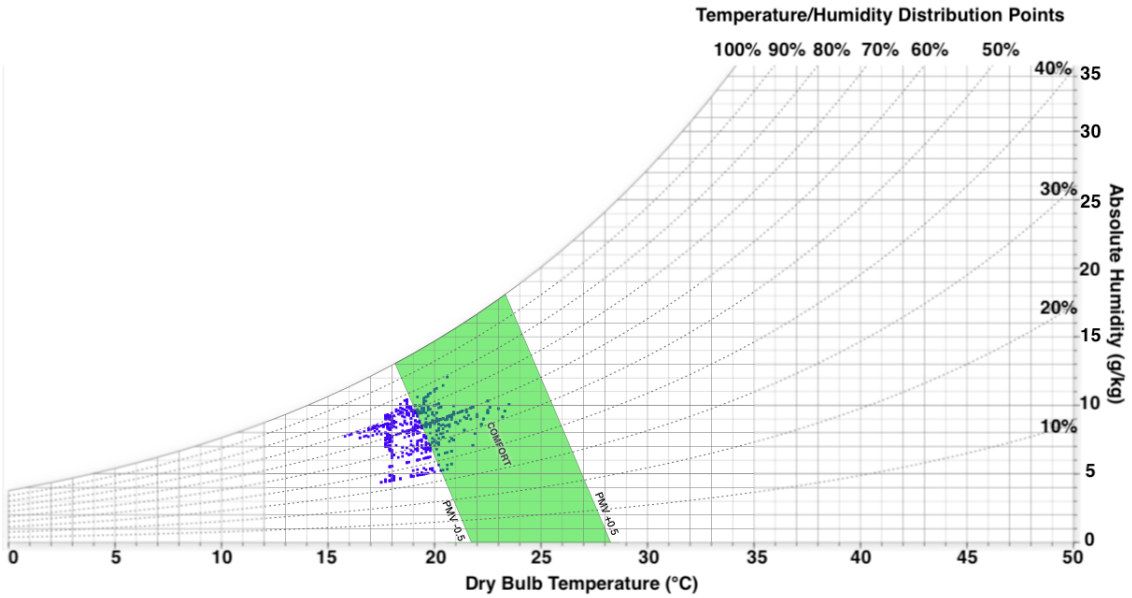

Figure A 16. Hourly temperature, humidity distribution on psychrometric chart, October 2015 [33], (Source: [43])

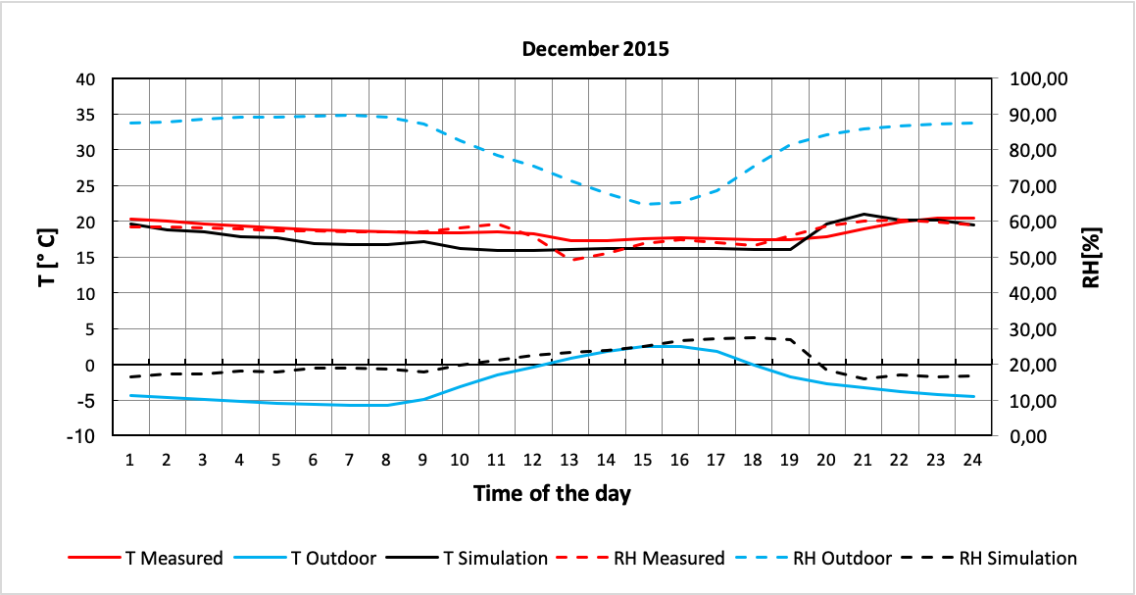

Figure A 17. Daily average of December 2015 [32]

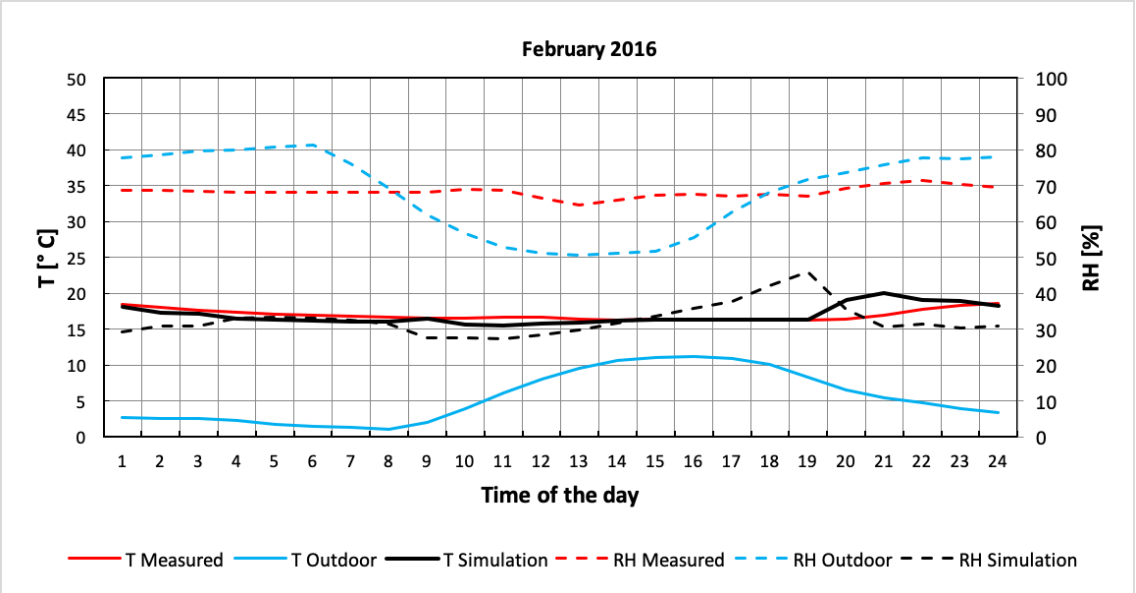

Figure A 18. Daily average of February 2016 [32]

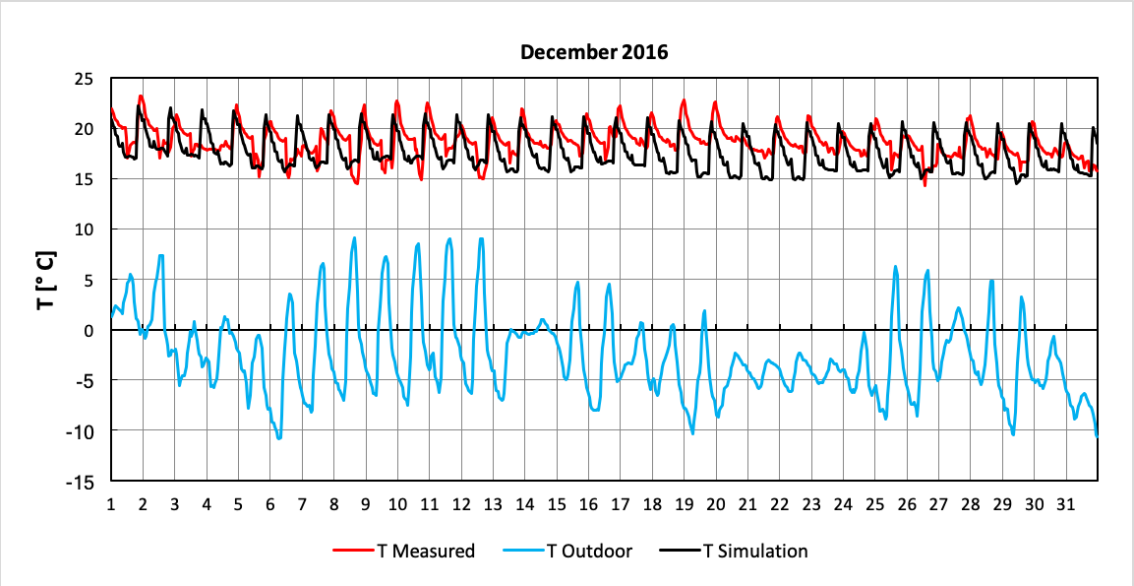

Figure A 19. Measured, simulated interior and outdoor temperatures versus day of the month graph, December 2015

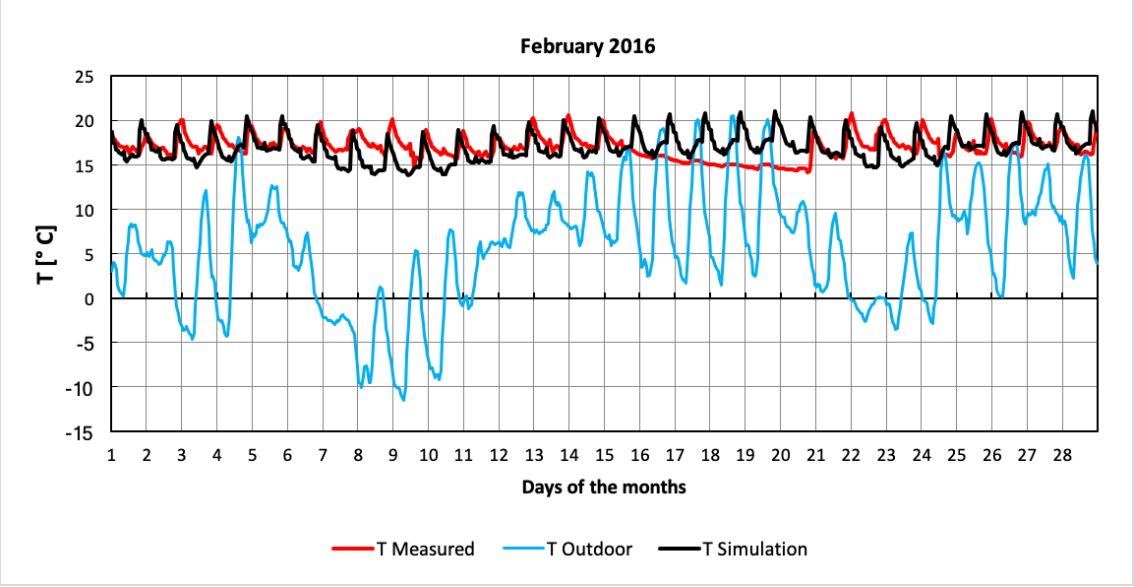

Figure A 20. Measured, simulated interior and outdoor temperatures versus day of the month graph, February 2016

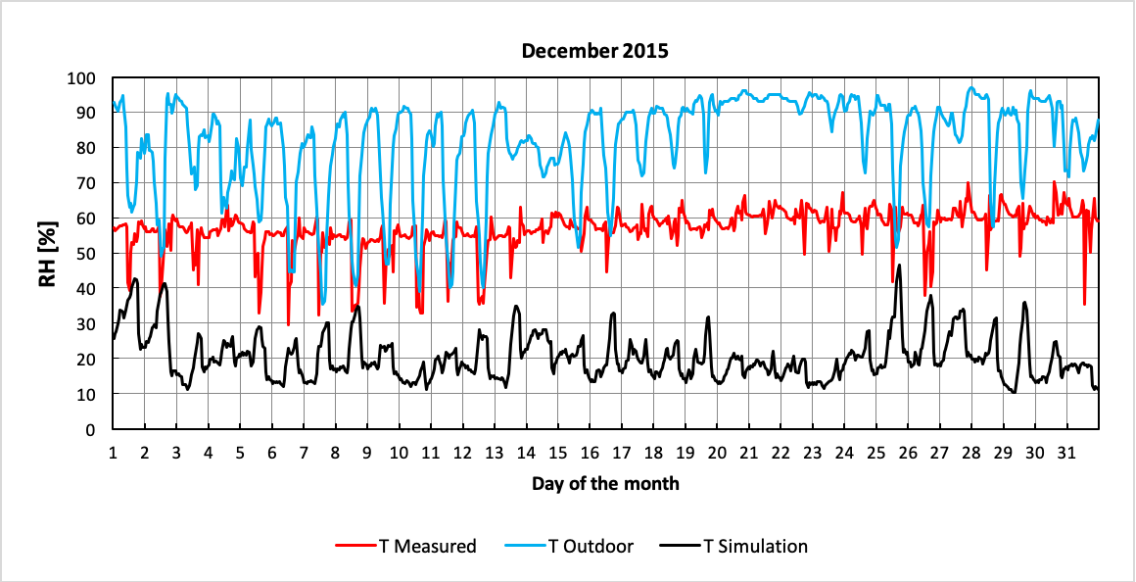

Figure A 21. Measured, simulated interior and outdoor relative humidity versus day of the month graph, December 2015

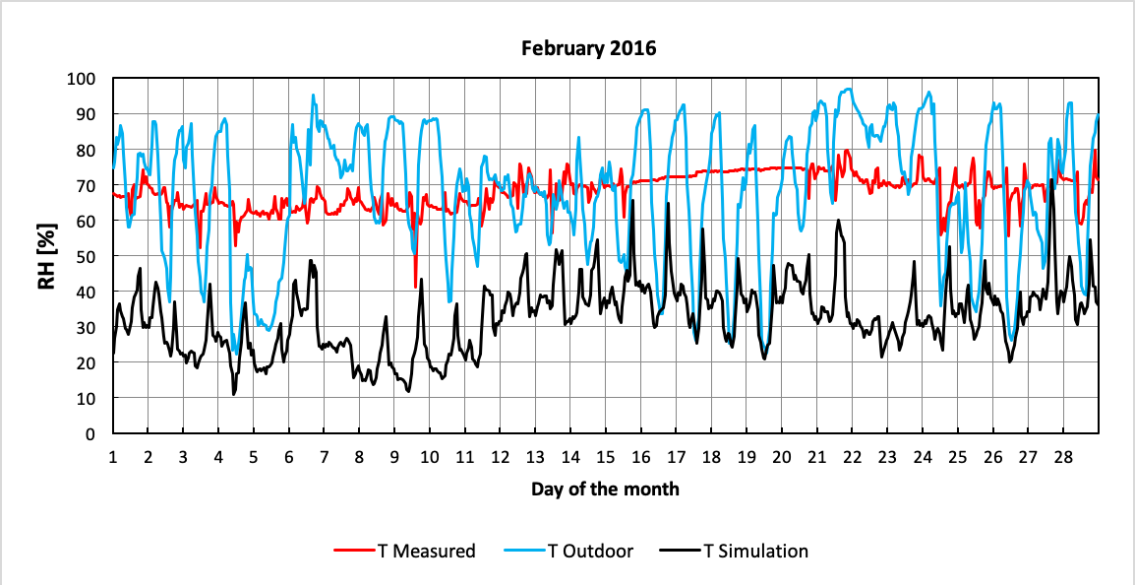

Figure A 22. Measured, simulated interior and outdoor relative humidity versus day of the month graph, February 2016

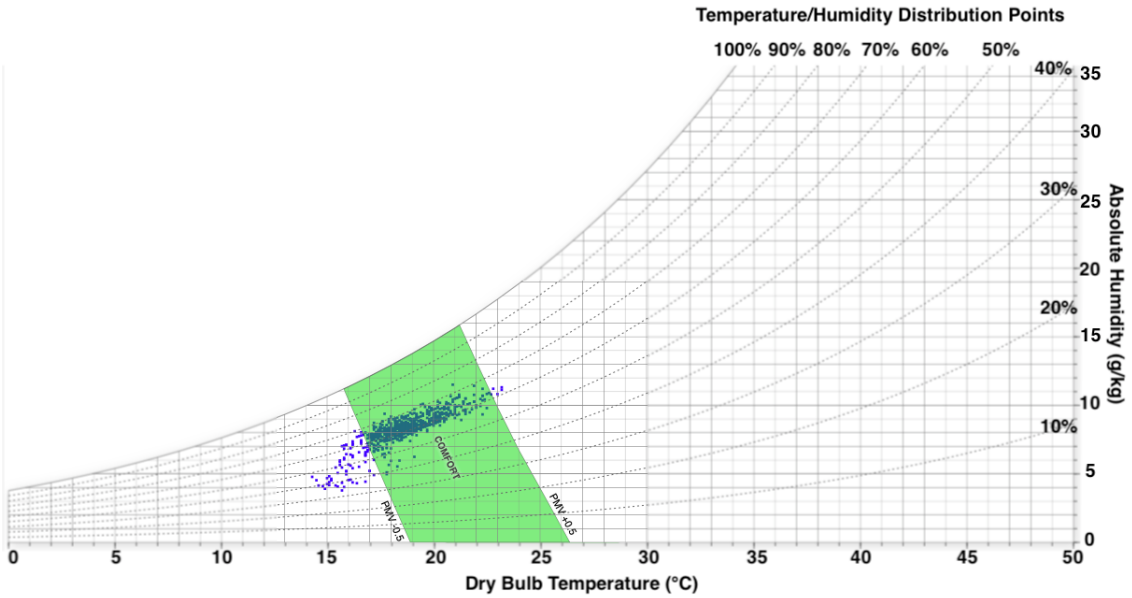

Figure A 23. Hourly temperature, humidity distribution on psychrometric chart, December 2015 [33], (Source: [43])

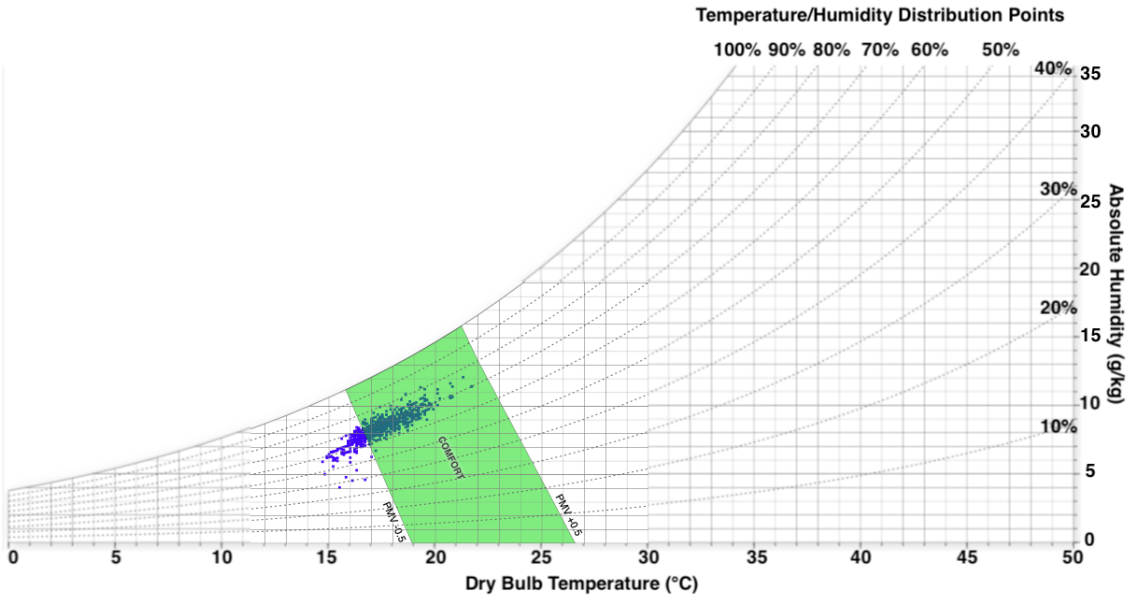

Figure A 24. Hourly temperature, humidity distribution on psychrometric chart, February 2016 [33], (Source: [43])

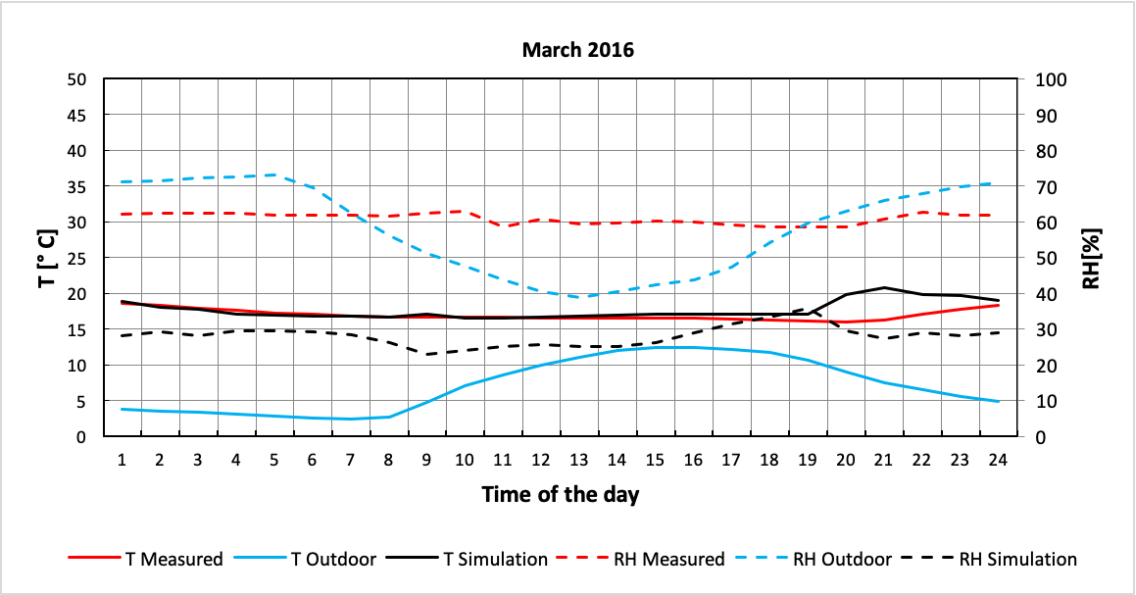

Figure A 25. Daily average of March 2016 [32]

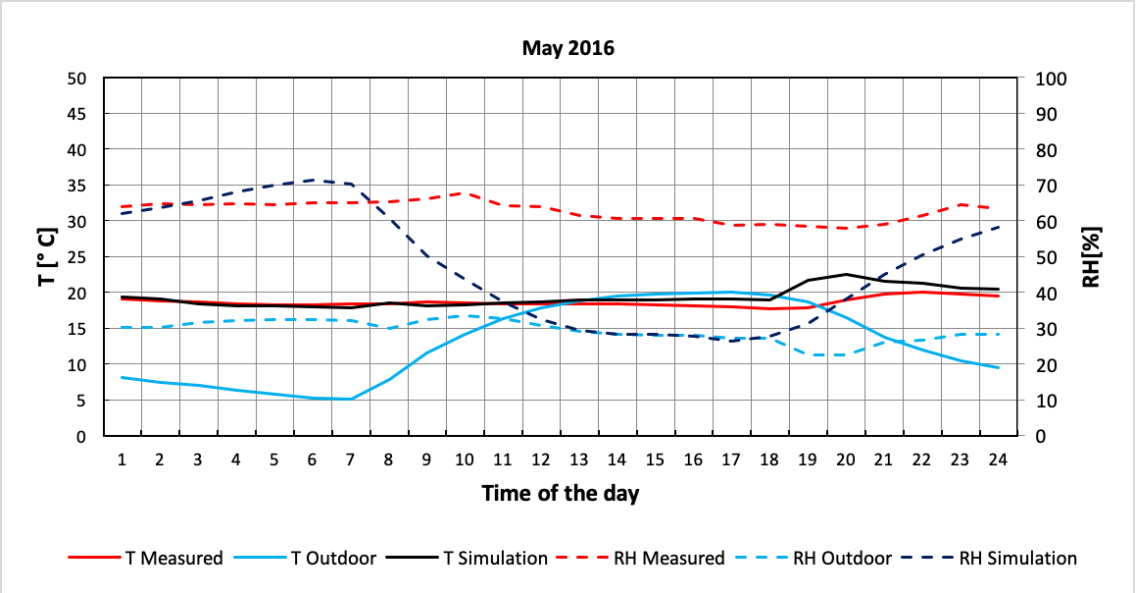

Figure A 26. Daily average of May 2016 [32]

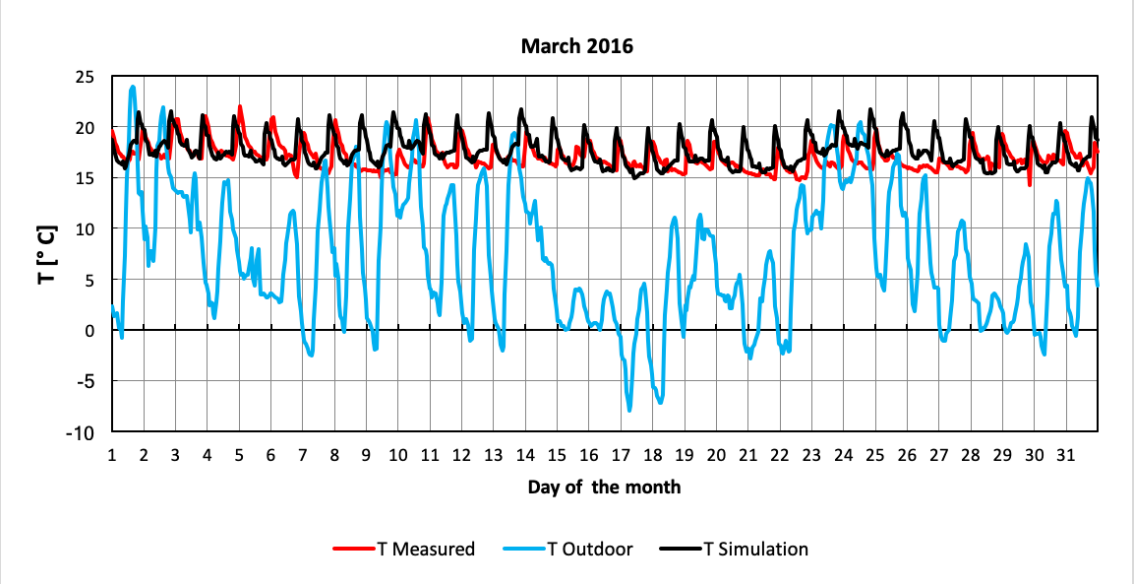

Figure A 27. Measured, simulated interior and outdoor temperatures versus day of the month graph, March 2016

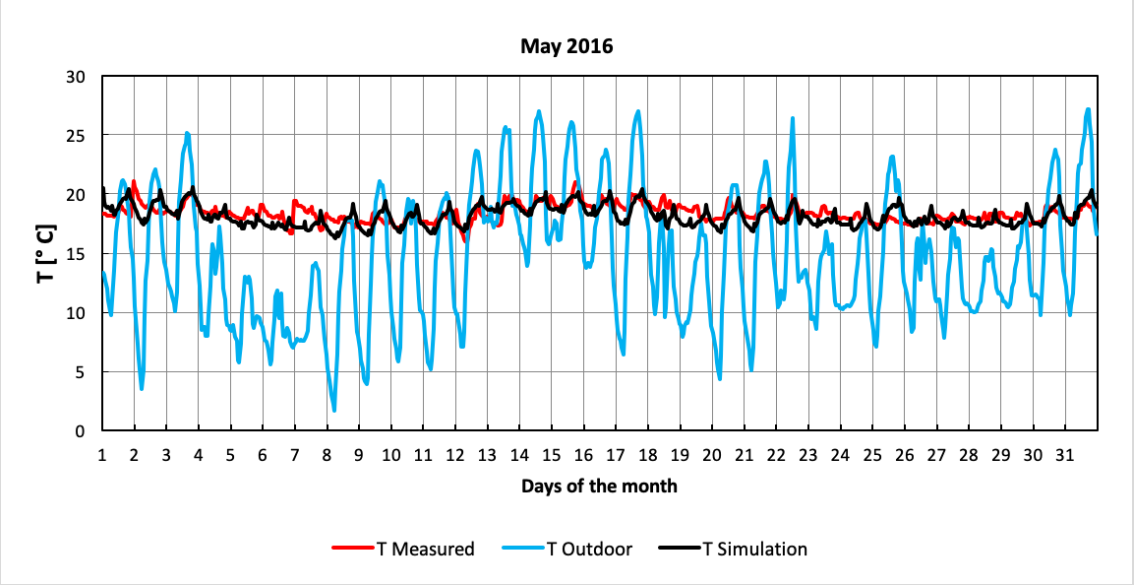

Figure A 28. Measured, simulated interior and outdoor temperatures versus day of the month graph, May 2016

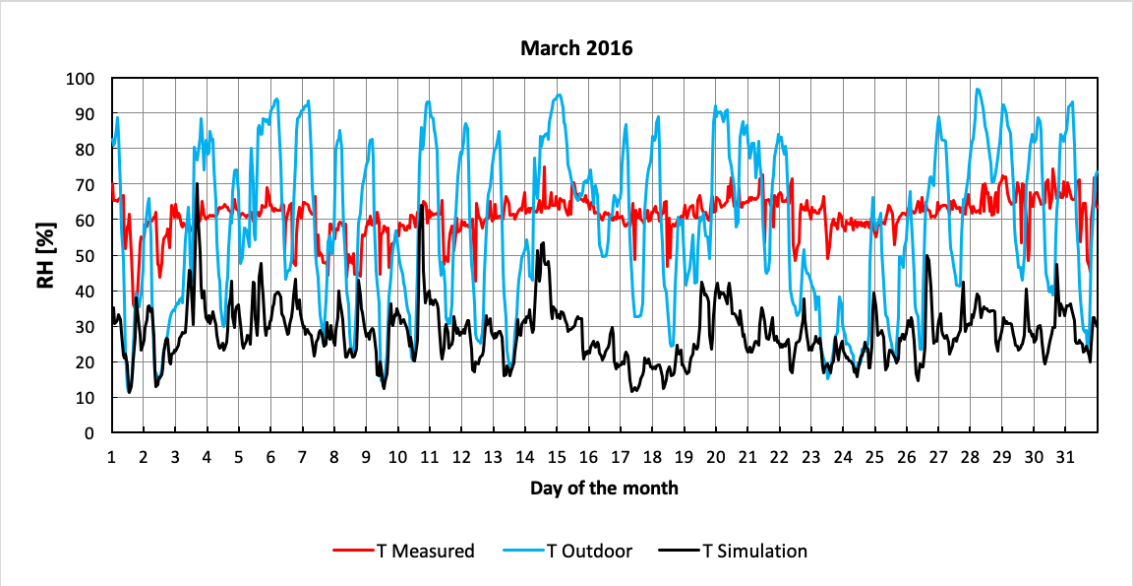

Figure A 29. Measured, simulated interior and outdoor relative humidity versus day of the month graph, March 2016

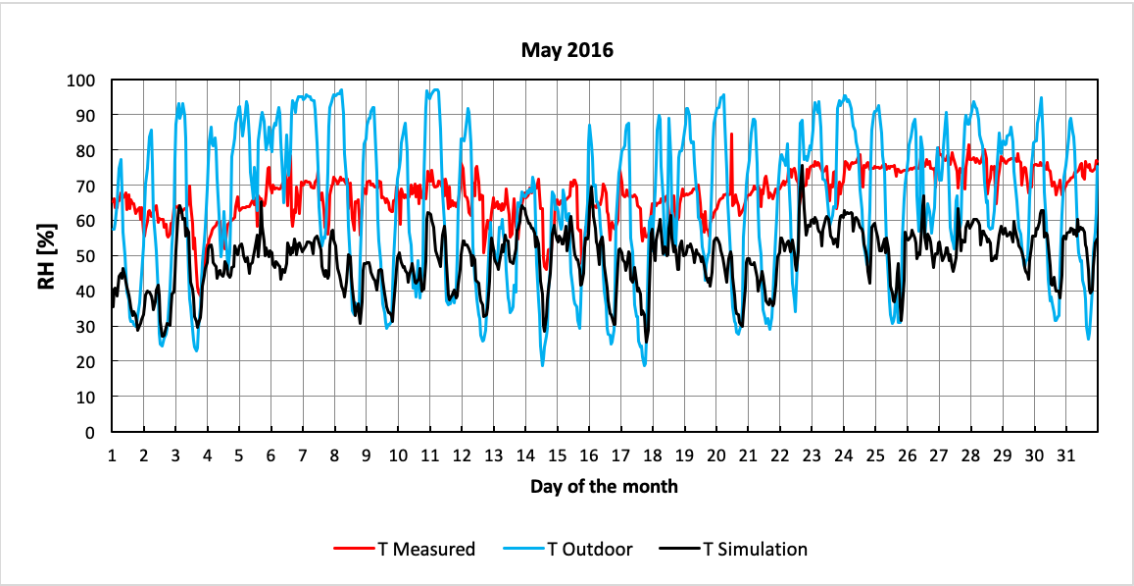

Figure A 30. Measured, simulated interior and outdoor relative humidity versus day of the month graph, May 2016

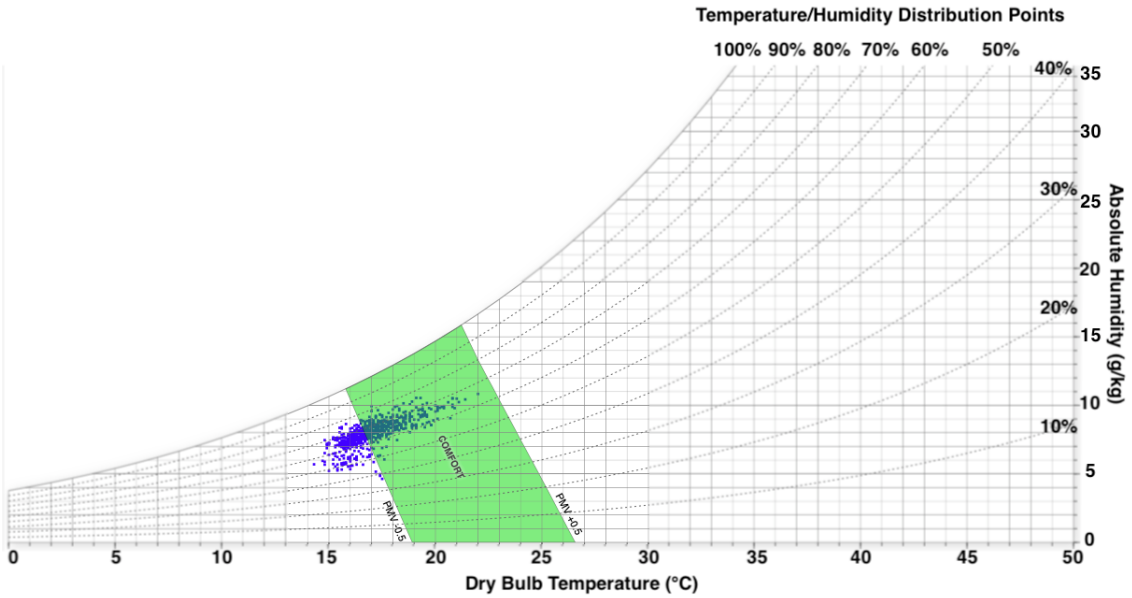

Figure A 31. Hourly temperature, humidity distribution on psychrometric chart, March 2016 [33], (Source: [43])

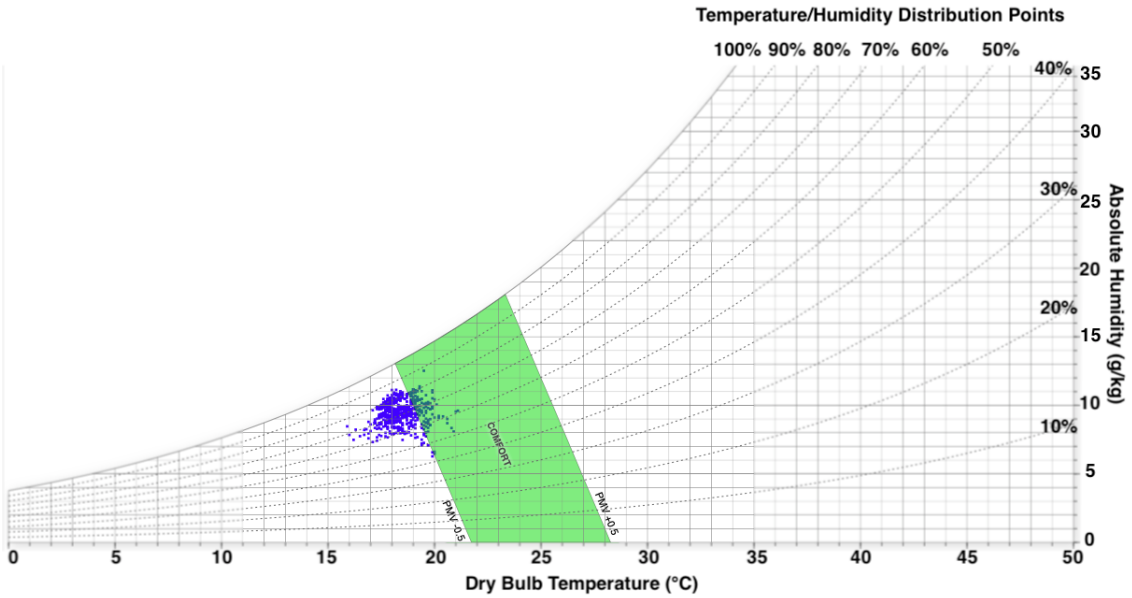

Figure A 32. Hourly temperature, humidity distribution on psychrometric chart, May 2016 [33], (Source: [43])